DELFT UNIVERSITY OF TECHNOLOGY

REPORT 03-16

LITERTURE STUDY: NUMERICAL METHODS FOR SOLVING STEFAN PROBLEMS

E.JAVIERRE-PÉREZ[1]

ISSN 1389-6520

Reports of the Department of Applied Mathematical Analysis

Delft 2003

[1]Supported by the Dutch Technology Foundation (STW).

Literature Study:
Numerical Methods for solving Stefan problems

E. Javierre-Pérez[2]

[2]Supported by the Dutch Technology Foundation (STW).

Contents

List of Figures

List of Tables

Chapter 1

Introduction

In this work a study of the dissolution and growth of dispersoids in Aluminium alloys has been carried out. This problem is a so-called Stefan problem (or moving boundary problem). Its particularity is that a portion of the boundary of the domain changes with time. This feature obliges us to consider advanced techniques for its numerical solution. This is the purpose of the project and the direction of the literature study presented in this report.

In the first part of this report the theoretical aspects of the particle dissolution/growth problem are studied, see chapters 2 and 3. The derivation of the problem is presented and some generalizations are considered. During the whole report we will mostly consider binary alloys, but the multicomponent problem is also studied and presented in these chapters. The similarity solutions for special geometries are analyzed and presented. The morphological stability of the growth is also studied, and the effect of the curvature on the interface movement (given by the Gibbs-Thomson effect) is revealed as an important condition.

After this, the numerical solution of the problem is considered. For this purpose several numerical methods are studied. All the numerical methods in this paper are presented for the one-dimensional problem, due to its easy understanding. Furthermore some numerical experiments were done for this problem. We present a list of numerical methods for Stefan problems, in chapters 4, 5, 6 and 7, applied to our problem. Subsequently, numerical experiments were done for the methods that were considered applicable for future research (higher dimensions). These numerical experiments are presented in chapter 8.

Chapter 2

The Stefan problem. Derivation and properties

2.1 Introduction

Problems in which the solution of a differential equation has to satisfy certain conditions on the boundary are called boundary-value problems. In other cases, however, the boundary is an unknown function of time, which has to be determined with the solution of the differential equation. In these cases we need two boundary conditions: one to determine the position of the moving boundary and the second to complete the solution of the differential equation. This kind of problems are called Stefan problems, with reference to the work of J. Stefan who was interested (around 1890) in the melting of the polar ice cap. Many more phenomena can be described by a Stefan problem (for instance the freezing of food or the decrease of oxygen in a muscle in the vicinity of a clotted bloodvessel). The only difference between the various Stefan problems are the governing equations, further the idea of the model is the same. Our aim in this paper is to give a detailed study about a specific Stefan problem: the diffusion process and the dissolution and growth of dispersoids in Aluminium alloys.

In this problem we have a particle (with fixed composition) in an Aluminium cell. We denote by $\Omega_X(T) \subset \mathbb{R}^n$ (with $n \in \{1,2,3\}$) the domain of the Aluminium matrix at time T, whose boundaries are denoted by $S(T)$ the moving interface between the particle and the Aluminium matrix, and Γ the outer fixed boundary of the cell. The transport of chemical elements from/to the Aluminium matrix is described by the diffusion equation

$$\frac{\partial C}{\partial T}(X,T) = \nabla \cdot \Big(D(X,T) \nabla C(X,T) \Big), \quad \forall X \in \Omega_X(T), T \in [0, T_{end}],$$

where $C(X,T)$ and $D(X,T)$ are the unknown concentration (in $\frac{mol}{m^3}$ or $\frac{kg}{m^3}$) and the given diffusivity (in $\frac{m^2}{s}$) at the point $X \in \Omega_X(T)$ at time T. It is assumed implicitly in this equation that C is a continuous function with continuous derivatives with respect to time and space, as well that $D(X,T)\nabla C(X,T)$ is a continuous function and differentiable with respect to space.

In the general case we will assume the particle and the cell to have the same geometry, and that the diffusivity is constant in the whole domain. Under these hypotheses, we distinguish between three geometries: the planar, the cylindrical and the spherical. Hence, the diffusion equation can be expressed by:

$$\frac{\partial C}{\partial T}(X,T) = \frac{D}{X^a} \frac{\partial}{\partial X} (X^a \frac{\partial C}{\partial X}(X,T)), \quad \forall X \in \Omega_X(T), T \in [0, T_{end}],$$

where the parameter a describes the geometry of the problem: $a = 0$ planar, $a = 1$ cylindrical and $a = 2$ spherical.

2.2 The one-dimensional one-phase Stefan problem

Consider for instance an Al_2Cu particle in an $Al - Cu$ alloy at a given temperature. We are interested in the dissolution process of the particle. We consider the one-dimensional problem, and denote by T the time. We can describe the domain at time T as in Figure 2.1,

Figure 2.1: The domain for the one-dimensional problem

where $\Omega_S(T)$ denotes the particle domain, $\Omega_X(T)$ denotes the Aluminium matrix domain, which are determined by $S(T)$ the position of the moving interface between the particle and the Aluminium matrix. The outer boundaries of the whole of domain are 0 and L (which are fixed in time). Therefore L is the length of the whole domain (including the particle domain and the Aluminium matrix domain).

We denote the concentration of Cu in the domain point X at time T by $C(X,T)$. Hence, the dissolution process in the Aluminium matrix is ruled by Fick's Second Law:

$$\frac{\partial C}{\partial T}(X,T) = D\frac{\partial^2 C}{\partial X^2}(X,T) \quad \forall X \in \Omega_X(T),\ T \in (0, T_{end}], \tag{2.1}$$

where D is the diffusion coefficient (in m^2/s), and it is assumed to be constant. Further, T_{end} is an arbitrary positive number. As initial condition in the matrix domain we use

$$C(X,0) = c_0, \quad X \in \Omega_X(0), \tag{2.2}$$

where $\Omega_X(0)$ the initial Aluminium domain is known (that is, the initial position of the moving boundary $S(0) = S_0$ is known). We also know the concentration of Cu at the particle

$$C(X,T) = c_{part}, \quad X \in \Omega_S(T),\ T \in [0, T_{end}]. \tag{2.3}$$

We suppose that there is no flux of Cu from the Aluminium matrix through the outer boundary L, hence

$$\frac{\partial C}{\partial X}(L,T) = 0, \quad T \in [0, T_{end}]. \tag{2.4}$$

Further, we assume local thermodynamic equilibrium at the interface, this implies that the concentration at the interface is determined from the $Al - Cu$ phase diagram, hence

$$C(S(T),T) = c_{sol}, \quad T \in (0, T_{end}]. \tag{2.5}$$

It is proved in [1], among others, that if the boundary $S(T)$ is fixed in time, that there exists a unique smooth solution for the problem given by equations (2.1)-(2.5). Note that if $S(T)$ is fixed, the solution $C(X,T)$ does not satisfy mass-conservation. In the following an expression for the movement of the interface is derived based on mass-conservation per unit area. We consider the position of the interface at two successive times T and $T + \Delta T$, and we consider the case that the function S is increasing, as in Figure 2.2.

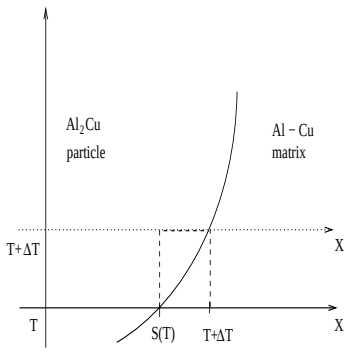

Figure 2.2: Mass balance through the interface

The increment of mass (in the particle) due to the movement of the interface and the condition (2.3) is

$$c_{part}(S(T+\Delta T)-S(T)),$$

and the mass due to the flux of Cu atoms through the interface together with the condition (2.5) is

$$c_{sol}(S(T+\Delta T)-S(T))+D\frac{\partial C}{\partial X}(S(T),T)\Delta T+\mathcal{O}\big((\Delta T)^2\big),$$

where $D\frac{\partial C}{\partial X}$ denotes the flux of Cu through the interface. Obviously these two quantities must be equal. Then dividing by ΔT and taking the limit as $\Delta T \to 0$ we obtain

$$(c_{part}-c_{sol})\frac{dS}{dT}(T)=D\frac{\partial C}{\partial X}(S(T),T),\quad T\in[0,T_{end}]. \tag{2.6}$$

This condition determines the movement of the interface and it is called the Stefan condition. The equations (2.1)-(2.6) describe the one-dimensional Stefan problem for the dissolution process. Existence and uniqueness of a one-dimensional Stefan problem established for instance in [2]. More information about Stefan problems can be found in [3]. About the Stefan condition we can make two remarks:

1. It is necessary that $c_{part} \neq c_{sol}$ to prevent an undetermined interface velocity;

2. If $c_{sol} = c_0$, we get no movement of the interface, and the initial distribution of the concentration is the solution of the diffusion equation (2.1);

3. If we integrate the diffusion equation in both variables X and T we get the integral formulation for the Stefan condition,

$$\int_0^L \big[C(X,T)-C(X,0)\big]dX=-(c_{part}-c_{sol})\big(S(T)-S(0)\big).$$

   This formula implies that the function S is continuous, whereas that equation (2.6) requires that S has continuous time derivative.

2.3 Conserving solutions

The mass of the whole system (particle and Aluminium matrix) at a certain time T (denoted by $m_{sys}(T)$) can be calculated easily by

$$m_{sys}(T) = \int_{\Omega_S(T)\cup\Omega_X(T)} C(X,T)dX \ = c_{part}S(T) + \int_{S(T)}^{L} C(X,T)dX, \tag{2.7}$$

where $\Omega_S(T)$ denotes the particle domain T and $\Omega_X(T)$ denotes the Aluminium matrix domain both at time T (see Figure 2.1). It is clear that, the solution of the Stefan problem should be such that no material is destroyed or created in time, hence:

$$m_{sys}(T) \ = \ m_{sys}(0) \ = \ c_{part}S(0) + c_0(1 - S(0)), \quad \forall T \in [0, T_{end}],$$

according to equations (2.2) and (2.3). If the solution of the Stefan problem satisfies this condition, then it is called a *conserving solution*. The Stefan problem (2.1)-(2.6) is called *well-posed* if its solution is a conserving solution.

Remark: Differentiation of equation (2.7) with respect to time gives the Stefan condition for the moving boundary again.

2.4 Maximum principle for the Stefan problem

The well-posedness condition for a Stefan problem is based on the maximum principle for parabolic equations [4]. Because of this importance, it is formulated here for the problem given by (2.1)-(2.6). Let be $E = \{(X,T) \ : \ X \in \Omega_X(T), \ T \in (0, T_{end}]\}$, $S_T = \{(S(T),T) \ : \ T \in (0, T_{end}]\}$, $\Gamma_1 = \{(X,0) \ : \ X \in \Omega_X(0)\}$ and $\Gamma_2 = \{(L,T) \ : \ T \in (0, T_{end}]\}$ (see Figure 2.3).

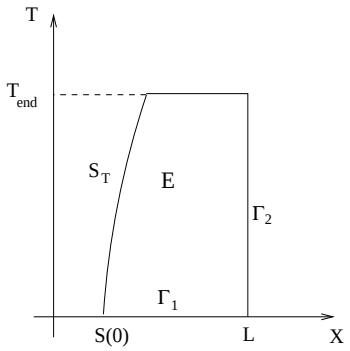

Figure 2.3: Evolution of the domain with time

Proposition 2.4.1 (Maximum Principle) *If $C(X,T)$ satisfies the weak inequality*

$$D\frac{\partial^2 C}{\partial X^2}(X,T) - \frac{\partial C}{\partial T}(X,T) \geq 0,$$

in the region E, then the maximum of C with respect to X and T must occur on one of the three sides S_T, Γ_1 or Γ_2. Furthermore, if this maximum is reached in a point $P(X_0,T_0)$ on S_T or on Γ_2 and $\frac{\partial}{\partial \nu}$ denotes the outer normal derivate from $\Omega_X(T)$, then we have that $\frac{\partial C}{\partial \nu}(X_0,T_0) > 0$.

We can also apply this principle to the local minimum of $C(X,T)$, reversing the inequality. But in this case, if the local minimum is reached in $P(X_0,T_0)$ on S_T or on Γ_2 then we have

that $\frac{\partial C}{\partial \nu}(X_0, T_0) < 0$. The above maximum principle (Proposition 2.4.1) is proved in Protter and Weinberger [4], Chapter 3, page 159 and following.

Consequence 1 *The Stefan problem, given by equations (2.1)-(2.6) has no conserving solution iff*

$$(c_{part} - c_0)(c_{part} - c_{sol}) \leq 0 \ ,$$

with $c_{part}, c_{sol}, c_0 \in \mathbb{R}_0^+$ *and* $c_{part} \neq c_0$.

Proof: It can be found in [5] (pages 251 and 252). ■

Consequence 2 *The maximum (and the minimum) of* C *can not be reached on* Γ_2.

Proof: This would imply that $\frac{\partial C}{\partial X}(L, T) > 0$ ($\frac{\partial C}{\partial X}(L, T) < 0$ for the case of the minimum) for all $T \in (0, T_{end}]$, which is inconsistent with (2.4). ■

Consequence 3 *If we have a well-posed problem, then the interface moves monotonously.*

Proof: Assume that $(c_{part} - c_0)(c_{part} - c_{sol}) > 0$. On the other hand, we are in one of the following two cases:

1. $c_0 > c_{sol}$. This implies (by the maximum principle) that the minimum of C is reached on S_T, and therefore that $\frac{\partial C}{\partial X}(S(T), T) > 0$. Hence, if $c_{part} > c_{sol}$ (and therefore $c_{part} > c_0$) it follows that $\frac{dS}{dT}(T) > 0$. If $c_{part} < c_{sol}$ (and therefore $c_{part} < c_0$) it follows that $\frac{dS}{dT}(T) < 0$.

2. $c_0 < c_{sol}$, which implies that the maximum of C is reached on S_T, and hence $\frac{\partial C}{\partial X}(S(T), T) < 0$. Repeating the last procedure it follows that if $c_{part} > c_{sol}$ then $\frac{dS}{dT}(T) < 0$ and if $c_{part} < c_{sol}$ then $\frac{dS}{dT}(T) > 0$. ■

Summing up the last consequence, if $(c_{part} - c_{sol})(c_0 - c_{sol}) > 0$ we will obtain that the particle grows ($\frac{dS}{dT}(T) > 0$) and if $(c_{part} - c_{sol})(c_0 - c_{sol}) < 0$ the particle will dissolve ($\frac{dS}{dT}(T) < 0$). See figures 2.4, 2.5 as examples.

2.5 Existence and uniqueness of solution

It is proved in [1] that the system described by (2.1)-(2.5) has a unique solution for a given fixed boundary S. The existence and uniqueness of solution for a one-dimensional Stefan problem has been widely studied in the existing literature. Evans proved in [6] the existence of solution of a Stefan problem equivalent to (2.1)-(2.6). Later, Douglas proved the uniqueness of the solution in [7]. Vuik [2] proved existence and uniqueness of solution for a more general class of Stefan problems, in which the domain is infinite and the Stefan condition is described by the use of a multifunction and a functional. It allows that the smoothness conditions imposed in this problem are weaker that in the initial Stefan problem. In [8] (in Chapter 8) the variational formulation for the Stefan problem is presented and a penalty method is used to study the existence and uniqueness of solution for that equivalent problem. Also in [9] the variational inequality formulation for the Stefan problem was analyzed and numerically solved in [10].

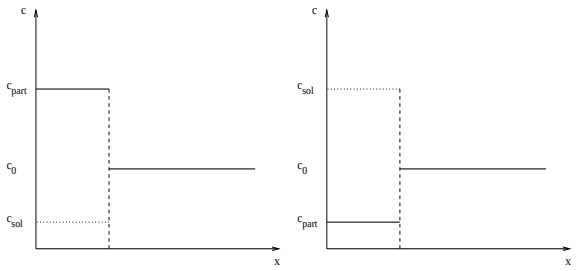

Figure 2.4: Initial concentration distribution for growth.

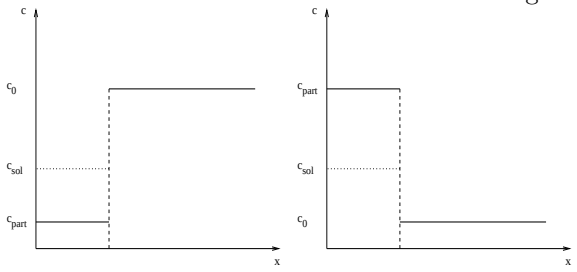

Figure 2.5: Initial concentration distribution for dissolution.

2.6 Similarity solutions

Analytical solutions are only available for a few problems. Most of them are for the one-dimensional problem and infinite or semi-finite domain, with simple initial conditions and constant diffusivity D. These solutions are functions of $(X - S(0))/T^{1/2}$ as is proved in [11], and are called similarity solutions. Next, the similarity solutions for each particular geometry will be deduced. The diffusion in the Aluminium matrix is ruled by

$$\frac{\partial C}{\partial T}(X,T) = \frac{D}{X^a}\frac{\partial}{\partial X}(X^a \frac{\partial C}{\partial X}(X,T)), \tag{2.8}$$

with $a = 0, 1, 2$ for planar, cylindrical and spherical geometry.

2.6.1 Planar geometry

Let consider the equation (2.8) with $a = 0$ in a infinite domain ($\Omega_S(T) = \{X \in \mathbb{R} \mid X < S(T)\ \}$, $\Omega_X(T) = \{X \in \mathbb{R} \mid S(T) < X\ \}$) together with the conditions derived in Section 2.2. Let be $\mu = \frac{X - S(0)}{2\sqrt{DT}}$ a new variable and define the function $g(\mu) := C(X,T)$. Using the chain rule we find

$$\frac{\partial C}{\partial T}(X,T) = -\frac{\mu}{2T}g'(\mu),$$

$$\frac{\partial C}{\partial X}(X,T) = \frac{1}{2\sqrt{DT}}g'(\mu),$$

$$\frac{\partial^2 C}{\partial X^2}(X,T) = \frac{1}{4DT}g''(\mu),$$

and replacing them into (2.8) it follows that g must satisfy the second order equation

$$-2\mu g'(\mu) = g''(\mu).$$

Integrating this equation we find $g(\mu) = A\,\mathrm{erfc}(\mu) + B$ where A and B are constants to be determined from the initial and boundary conditions of the problem. From (2.2) we got that $B = c_0$. A is determined from the interface concentration (2.5) which leads to

$$c_0 + A\,\mathrm{erfc}\left(\frac{S(T)-S(0)}{2(DT)^{1/2}}\right) = c_{sol}, \quad \forall T \in [0, T_{end}],$$

which only can be satisfied if $S(T) = S(0) + 2k\sqrt{DT}$, where k is a constant. This implies that $A = \dfrac{c_{sol} - c_0}{\mathrm{erfc}(k)}$. Finally, k is determined from the Stefan condition (2.6):

$$(c_{part} - c_{sol})k = -\frac{c_{sol} - c_0}{\sqrt{\pi}} \frac{e^{-k^2}}{\mathrm{erfc}(k)}.$$

2.6.2 Cylindrical geometry

Here we repeat the procedure used for planar geometry. The main difference is that we must assume $S(0) = 0$ to find an analytical expression for S and C. Then, after the change of variables we find the relation

$$-\big(2\mu + \frac{1}{\mu}\big)g'(\mu) = g''(\mu),$$

that after integration leads to

$$g'(\mu) = C_1 \frac{1}{\mu} e^{-\mu^2},$$

where C_1 is constant. To solve this equation we propose the change of variable $\mu^2 = y$ and integration, then we find that

$$g(\mu) = A\,\mathrm{Ei}(\mu^2) + B,$$

where A and B are integration constants (A might be different than the used in the previous integration), and Ei denotes the exponential integral function. This function is defined as

$$Ei(x) := -\int_{-x}^{\infty} \frac{e^{-t}}{t} dt = \int_{-\infty}^{x} \frac{e^{t}}{t} dt \quad \text{if } x > 0,$$

and more information about this function can be found in Chapter 5 of [12]. The initial concentration establishes that $B = c_0$, whereas the concentration at the interface (2.5) imposes that

$$c_{sol} = A\,\mathrm{Ei}\left(\big(\frac{S(T)}{2\sqrt{DT}}\big)^2\right) + c_0,$$

that can only become true if $S(T) = 2k\sqrt{DT}$. In this case, A is given by

$$A = \frac{c_{sol} - c_0}{\mathrm{Ei}(k^2)}.$$

Finally, k is obtained from the Stefan condition (2.6)

$$(c_{part} - c_{sol})\sqrt{\frac{D}{T}} = D\frac{1}{2\sqrt{DT}} \frac{-A}{k} e^{-k^2},$$

or after simplification

$$k = -\frac{c_{sol} - c_0}{c_{part} - c_{sol}} \frac{e^{-k^2}}{2\,\mathrm{Ei}(k^2)}.$$

2.6.3 Spherical geometry

Again we assume that $S(0) = 0$ and we use the same procedure to get an analytical solution as for the planar case. In this case, the differential equation for g is

$$g''(\mu) = -2\left(\mu + \frac{1}{\mu}\right)g'(\mu),$$

that by sequential integration leads to

$$g(\mu) = A\left[\frac{1}{\mu}\exp(-\mu^2) - \sqrt{\pi}\,\mathrm{erfc}(\mu)\right] + B,$$

where A and B are constants to be determined by the initial and boundary conditions. From (2.2) we got that $B = c_0$. Interfacial condition (2.5) leads to

$$A\left[\frac{2\sqrt{DT}}{S(T)}\exp\Big(-\big(\frac{S(T)}{2\sqrt{DT}}\big)^2\Big) - \sqrt{\pi}\,\mathrm{erfc}\,\big(\frac{S(T)}{2\sqrt{DT}}\big)\right] + c_0 = c_{sol}, \quad \forall T \in [0, T_{end}],$$

which only can be satisfied if $S(T) = 2k\sqrt{DT}$, where k is a constant. Hence,

$$A = \frac{c_{sol} - c_0}{\frac{1}{k}e^{-k^2} - \sqrt{\pi}\,\mathrm{erfc}(k)},$$

and k is determined from the Stefan condition (2.6):

$$(c_{part} - c_{sol})k\sqrt{\frac{D}{T}} = \frac{D}{2\sqrt{DT}}\frac{-A}{k^2}e^{-k^2},$$

which once A is substituted and the simplifications are done results

$$(c_{part} - c_{sol})k^3 = -\frac{c_{sol} - c_0}{\frac{1}{k}e^{-k^2} - \sqrt{\pi}\,\mathrm{erfc}(k)}\frac{e^{-k^2}}{2}.$$

2.7 Generalizations

The preceding problem is the standard Stefan problem for the diffusion process, but it can be generalized in various ways. First of all, we will present the non-dimensional formulation for the problem introduced before. After that we will present the formulation of the problem in two and three spatial dimensions, since it will be our focus in the near future. We will also present the Gibbs-Thomson effect for the displacement of the interface, that has a crucial importance in the two and three dimensional problems as we will present in Chapter 3. Finally, non-linear parameters in the formulation, the inverse Stefan problem and the implicit Stefan problem will be explained.

2.7.1 Non-dimensional forms

The variables and the parameters used until now denote quantities expressed in physical units, e.g. S position in meters, T time in seconds, ... One technique is to present the Stefan problems with non-dimensional variables. This is achieved by making a change of variables. The new variables for the dissolution problem are:

$$x = \frac{X}{L},\ t = \frac{D}{L^2}T,\ c = \frac{C}{c_{part}},\ s = \frac{S}{L}, \tag{2.9}$$

where we have assume the diffusivity D constant. If the diffusivity is a function of X and T then we should use a particular value of this in the last change of variables, as for instance its maximum

value, its minimum or its average value. In this case we would obtain a different problem from the one we get if the diffusivity is constant, but it would not be difficult to work this out. Next, using the chain rule we get the relations:

$$\frac{\partial C}{\partial T} = c_{part}\frac{D}{L^2}\frac{\partial c}{\partial t}, \quad \frac{\partial C}{\partial X} = \frac{c_{part}}{L}\frac{\partial c}{\partial x},$$

$$\frac{\partial^2 C}{\partial X^2} = \frac{c_{part}}{L^2}\frac{\partial^2 c}{\partial x^2}, \quad \frac{\partial S}{\partial T} = \frac{D}{L}\frac{\partial s}{\partial t}.$$

Using these relations, our scaled problem becomes

$$\frac{\partial c}{\partial t}(x,t) = \frac{\partial^2 c}{\partial x^2}(x,t)\ ,\ x \in \Omega(t)\ ,\ t \in (0, t_{end}], \tag{2.10}$$

$$c(x,0) = \frac{c_0}{c_{part}}\ ,\ x \in \Omega(0), \tag{2.11}$$

$$c(x,t) = 1\ ,\ x \in \Omega_s(t),\ t \in [0, t_{end}], \tag{2.12}$$

$$c(s(t),t) = \frac{c_{sol}}{c_{part}}\ ,\ t \in [0, t_{end}], \tag{2.13}$$

$$\frac{\partial c}{\partial x}(1,t) = 0\ ,\ t \in [0, t_{end}], \tag{2.14}$$

$$\frac{ds}{dt}(t) = \lambda\frac{\partial c}{\partial x}(s(t),t)\ ,\ t \in [0, t_{end}], \tag{2.15}$$

with

$$\lambda = \frac{c_{part}}{c_{part} - c_{sol}},$$

where $\Omega(t)$ and $\Omega_s(t)$ are the corresponding domains to $\Omega_X(T)$ and $\Omega_S(T)$ in the original problem due to the change of variables, and $t_{end} = \frac{D}{L^2}T_{end}$.

2.7.2 Two and three space dimensions

We can extend the problem introduced in the Section 2.2 for more spatial dimensions. We will formulate the Stefan problem for the two-dimensional problem only. Obviously the formulation of the three-dimensional problem is completely analogous. We consider a domain as sketched in Figure 2.6.

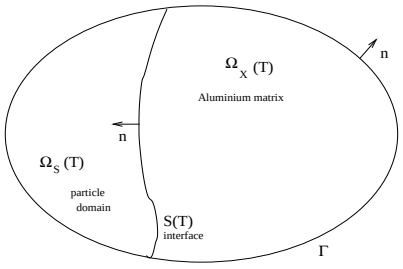

Figure 2.6: The domain of the two-dimensional problem.

The domain filled with Aluminium is denoted by $\Omega_X(T)$. The boundary of this domain consists

of the interface between the particle and the Aluminium matrix $S(T)$, and the outer boundary Γ which is fixed in time except the two points of intersection with $S(T)$. In the Aluminium-rich phase $\Omega_X(T)$ the Cu concentration $C(X,Y,T)$ satisfies the diffusion equation given by the Fick's Second Law:

$$\frac{\partial C(X,Y,T)}{\partial T} = D\Delta C(X,Y,T), \quad (X,Y) \in \Omega_X(T),\ T \in (0,T_{end}].$$

The initial concentration of Cu at the Aluminium matrix is

$$C(X,Y,0) = c_0(X,Y), \quad (X,Y) \in \Omega_X(0),$$

where $\Omega_X(0)$ is known, and the concentration of Cu at the Al_2Cu particle is assumed to be constant and equal to c_{part} for the entire particle domain. We assume no flux through the outer boundary, so

$$\frac{\partial C(X,Y,T)}{\partial n} = 0, \quad (X,Y) \in \Gamma,\ T \in [0,T_{end}],$$

where n is the unit normal vector at the boundary pointing outward with respect to $\Omega_X(T)$. At the interface we assume that the concentration of Cu satisfied

$$C(X,Y,T) = c_{sol}, \quad (X,Y) \in S(T),\ T \in [0,T_{end}].$$

To determine the concentration at the interface we follow the same argument as for the one-dimensional problem,

$$(c_{part} - c_{sol})v_n(X,Y,T) = D\frac{\partial C(X,Y,T)}{\partial n}, \quad (X,Y) \in S(T),\ T \in (0,T_{end}].$$

where v_n denotes the normal velocity of the interface. For a more detailed derivation of the mass balance, we refer to [5], Chapter 5.

2.7.3 Interface reactions and Gibbs-Thomson effect

One special case not considered until now is the case that the concentration of Cu on the interface is not given explicitly. That is, if $C(S(T),T) = \lim_{X \to S(T)+} C(X,T)$ for all $T \in [0,T_{end}]$. In this case the corresponding Stefan problem needs one extra condition to determine $C(S(T),T)$. The mass balance through the interface is still valid:

$$(c_{part} - C(S(T),T))\frac{dS}{dT}(T) = D\frac{\partial C}{\partial X}(S(T),T), \quad T \in [0,T_{end}], \tag{2.16}$$

and the extra condition we need is obtained by incorporation of the reactions at the interface. Therefore, supposing a first order reaction at the interface we get:

$$K(C^{sol}(T) - C(S(T),T)) = D\frac{\partial C}{\partial X}(S(T),T) + C(S(T),T)\frac{dS}{dT}(T), \quad T \in [0,T_{end}], \tag{2.17}$$

which is derived in more detail in [13]. This Robin condition replaces the Dirichlet condition at the interface, which holds for local equilibrium. $K = V_m K_1$ (with V_m the molar volume of the Aluminium matrix and K_1 is the atomic transfer coefficient of the interface) is a measure of the rate of the interface reaction (m/s). For K large the problem is diffusion controlled (note that $K \to \infty$ implies $C(S(T),T) \to C^{sol}(T)$), whereas for K small the problem is reaction controlled.

$C^{sol}(T)$ is the maximal solubility of Cu at the interface. Due to capillarity effects if the interface is a smooth curve or surface in space, it turns out that the maximum solubility is a function of

the local curvature curvature of the interface. This relation is called the Gibbs-Thomson effect and we can find more details about it in [14]:

$$C^{sol}(T) = C^{sol}_{\infty} exp(\vartheta\kappa(T)), \tag{2.18}$$

where C^{sol}_{∞} is the maximal solubility at the planar interface and $\vartheta = \frac{2\gamma V^p_m}{R\mathcal{T}C^{pm}}$ in which γ is the specific interfacial free energy of the interface, V^p_m is the molar volume of the particle, R is the universal gas constant, $\mathcal{T}$ the absolute temperature, C^{pm} is the mole fraction of Cu in the particle and $\kappa(T)$ denotes the local curvature of the interface. It can be useful to remember some properties of the curvature of a curve:

1. A circle of radius r has curvature $\kappa = \frac{1}{r}$ in all its points;
2. The curvature of a straight line is zero;
3. For a curve given by the parameterization $(x, y(x))$ the curvature is
$$\frac{|y''(x)|}{(1 + (y'(x))^2)^{\frac{3}{2}}};$$
4. The sign of the curvature is important to determine the direction of the movement of the interface. So we use the following convention: positive curvature for a concave interface toward the particle, and negative in other way (see Figure 2.7)

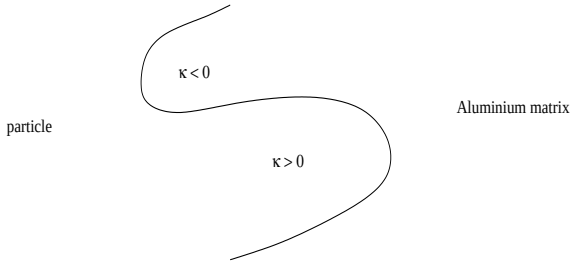

Figure 2.7: Determination of the sign of the curvature.

If we denote by v the velocity of the moving boundary $\frac{dS(T)}{dT}$ and we substract (2.16) from (2.17), then, we get

$$K(C^{sol}(T) - C(S(T), T)) = c_{part}v.$$

From the above expression it follows that

$$C(S(T), T) = \frac{c_{part}}{K}v + C^{sol}(T),$$

and after combination with equation (2.18), this gives

$$C(S(T), T) = \frac{c_{part}}{K}v + C^{sol}_{\infty} exp(\vartheta\kappa(T)). \tag{2.19}$$

2.7.4 Non-linear parameters

As we mentioned before the diffusion coefficient D can be a function of the concentration, position and time $D(C, X, T)$. In this general case the diffusion equation yields

$$\frac{\partial C}{\partial T}(X, T) = \frac{\partial}{\partial X}(D(C, X, T)\frac{\partial C}{\partial X}(X, T)), \quad X \in \Omega_X(T),\ T \in (0, T_{end}].$$

In the same way, the concentration at the interface can be a function of time $c_{sol}(T)$, the initial concentration c_0 can be a function of the position $c_0(X)$ and in place of no flux through the outer boundary M we can have a determined flux of Cu given by a function of the concentration, the position and the time:

$$\frac{\partial C}{\partial X}(L,T) = \phi(C,X,T), \quad T \in [0, T_{end}].$$

We also can have a source $q(C,X,T)$ of Cu at the interface, then the movement of the interface would be given by

$$(c_{part} - c_{sol})\frac{dS}{dT}(T) = D\frac{\partial C}{\partial X}(X,T) + q(C,X,T), \quad X = S(T),\ T \in [0, T_{end}].$$

2.7.5 Inverse Stefan problem

An inverse Stefan problem is one in which the motion of the interface S is known and some other boundary condition has to be determined. For instance, we may be interested in determining the flux f through the outer boundary of the Aluminium matrix given by

$$\frac{\partial C}{\partial X}(L,T) = f(T), \quad \forall T \in [0, T_{end}],$$

which causes the prescribed movement of the interface S, or the concentration at the interface $C(S(T),T)$ that induces the movement S. In [3] (Section 3.6.3) we can find an iterative procedure for solving the inward solidification of a cylinder in which the rate of movement of the interface is constrained to be constant. A solution of an inverse Stefan problem is, of course, the solution of a Stefan problem, and may provide an indirect method to solve Stefan problems or know some properties of the solution.

2.7.6 Implicit Stefan problems

As far as we have seen until here, the Stefan condition connects the velocity of the interface with the dependent variable C, see (2.6). In our particular case, the velocity of the interface is related with the gradient of concentration $\frac{\partial C}{\partial X}$ on the interface. However, some problems exist in which such an explicit relation does not occur. These problems are the so-called *implicit Stefan problems*. An example would be the problem (2.10)-(2.14) with the condition

$$\frac{\partial c}{\partial x}(s(t),t) = q(t), \quad t \in [0, t_{end}], \tag{2.20}$$

instead of (2.15). Schatz [15] introduced the transformations $w = \frac{\partial c}{\partial x}$ or $w = \frac{\partial c}{\partial t}$ to express an implicit Stefan problem in an explicit form. As an application of this idea we repeat here the procedure for the last problem, given by (2.10)-(2.14) and (2.20). The transformation $w = \frac{\partial c}{\partial x}$ gives, assuming that all the used derivatives of c are continuous:

$$\frac{\partial w}{\partial t}(x,t) = \frac{\partial^2 w}{\partial x^2}(x,t)\ ,\ x \in \Omega(t)\ ,\ t \in (0, t_{end}],$$

$$w(x,0) = 0\ ,\ x \in \Omega(0),$$

$$w(s(t),t) = q(t)\ ,\ t \in [0, t_{end}],$$

$$w(1,t) = 0\ ,\ t \in [0, t_{end}],$$

$$-q(t)\frac{ds}{dt}(t) = \frac{\partial w}{\partial x}(s(t),t)\ ,\ t \in [0, t_{end}],$$

which is an explicit Stefan problem analogous to the presented one in this report. In other cases it can be suitable to use the other transformation. For more information we refer to [3] (Section 1.3.10) and [15].

2.8 Vector-valued Stefan problem

Instead of considering only one chemical element in our domain, we can consider $n+1$ chemical species denoted by $Sp_1, \ldots, Sp_{n+1}$. We suppose that the concentrations of $Sp_i,\ i \in \{1, \ldots, n\}$ are small with respect to the concentration of Sp_{n+1}. The concentration of these species at point X of the matrix at time T are denoted by $C_i(X,T)$ (mol/m^3), $i \in \{1, \ldots, n\}$. We consider a planar domain, then the diffusion problem is reduced to a one-dimensional problem that we will explain next. We are going to introduce the formulation in the most complete way, and we will comment on the simplifications that follow. The Sp_{n+1}-rich matrix domain at time T is denoted by $\Omega_X(T) = \{X \in \mathbb{R} \mid 0 \leq S(T) < X < L\ \}$.

The dissolution at the Sp_{n+1}-rich matrix is ruled by the multi-component version of the Fick's Second Law:

$$\frac{\partial C_i}{\partial T}(X,T) = \sum_{j=1}^{n} D_{ij}\frac{\partial^2 C_j}{\partial X^2}(X,T), \quad X \in \Omega_X(T),\ T \in (0, T_{end}],\ i \in \{1, \ldots, n\}, \tag{2.21}$$

where D_{ij} is the diffusion coefficient of the species Sp_i corresponding to the species Sp_j in the Aluminium matrix (supposed to have a constant composition). The derivation of these equations can be found [16]. We can formulate these equations in a vectorial way:

$$\frac{\partial \vec{C}}{\partial T}(X,T) = \mathbb{D}\frac{\partial^2 \vec{C}}{\partial X^2}(X,T), \quad X \in \Omega_X(T),\ T \in (0, T_{end}],\ i \in \{1, \ldots, n\},$$

where $\vec{C}(X,T)$ is the column vector whose components are $C_i(X,T),\ i \in \{1, \ldots, n\}$ and $\mathbb{D}$ is the diffusion matrix given by:

$$\mathbb{D} = \begin{pmatrix} D_{11} & \ldots & D_{1n} \\ \vdots & \ddots & \vdots \\ D_{n1} & \ldots & D_{nn} \end{pmatrix}.$$

If we assume each species to diffuse independently of the others, $D_{ij} = 0$ for $i \neq j$ then the diffusion matrix is diagonal. The terms in (2.21) resulting from coefficients D_{ij} when $i \neq j$ are referred to as cross-diffusion terms. The initial concentrations of the components in the Sp_{n+1}-rich phase are given by

$$C_i(X,0) = C_i^0(X), \quad X \in \Omega_X(0),\ i \in \{1, \ldots, n\}, \tag{2.22}$$

or with vectorial notation

$$\vec{C}(X,0) = \vec{C_0}(X), \quad X \in \Omega_X(0),$$

where $\Omega_X(0)$ has to be known, that is $S(0) = S_0$ is given. We assume the whole metal is divided into periodical cells with symmetrical and differentiable initial concentrations. Then, when $\mathbb{D}$ is not singular it follows for a boundary, $X = L$, not being an interface, that

$$\frac{\partial C_i}{\partial X}(L,T)=0, \quad T\in[0,T_{end}],\ i\in\{1,\dots,n\}, \tag{2.23}$$

this implies that there is no flux through the outer boundary

$$D\frac{\partial \vec{C}}{\partial X}(L,T)=0, \quad T\in[0,T_{end}].$$

If we denote the concentration at the interface by

$$C_i(S(T),T)=:C_i^{sol}, \quad T\in[0,T_{end}],\ i\in\{1,\dots,n\}, \tag{2.24}$$

then there still are $n+1$ unknown quantities: $S(T)$ and the interface concentration for each chemical specie C_i^{sol}. Therefore we need $n+1$ equations to have a well posed problem. To determine the concentration at the interface we use the stoichiometry of the particle. If it is $(Sp_1)_{m_1}(Sp_2)_{m_2}(\dots)(Sp_n)_{m_n}$, where $m_1, m_2, \dots$ are the stoichiometric constants, then we have the following hyperbolic relationship for the interfacial concentrations:

$$(C_1^{sol})^{m_1}(C_2^{sol})^{m_2}(\dots)(C_n^{sol})^{m_n}=\mathcal{K}, \tag{2.25}$$

where $\mathcal{K}$ is a constant which depends on the temperature of the system. We can see more details about this relation in [16] and [17]. And finally, to determine the movement of the interface we follow a mass balance (with detail in [16]) and get

$$(C_i^{part}-C_i^{sol})\frac{dS}{dT}(T)=\sum_{j=1}^{n}D_{ij}\frac{\partial C_j}{\partial X}(S(T),T), \quad T\in[0,T_{end}],\ i\in\{1,\dots,n\}. \tag{2.26}$$

The problem described by the equations (2.21)-(2.26) falls within the class of Stefan-problems (diffusion with a moving boundary). Since we consider the dissolution of several chemical components it is referred to as a vector-valued Stefan problem. The unknowns in this problem are: the movement of the boundary $S(T)$, the concentration of each chemical specie at the interface C_i^{sol} and the concentration of each chemical specie at the Sp_{n+1}-rich matrix $C_i(X,T)$. Note that, using the equation (2.26) with two different chemical species Sp_i and Sp_k (with $i\neq k$) it follows that

$$\sum_{j=1}^{n}\frac{D_{ij}}{C_i^{part}-C_i^{sol}}\frac{\partial C_j}{\partial X}(S(T),T)=\sum_{j=1}^{n}\frac{D_{kj}}{C_k^{part}-C_k^{sol}}\frac{\partial C_j}{\partial X}(S(T),T), \quad T\in[0,T_{end}].$$

As we did for the one-component Stefan problem, we can determine which multi-component Stefan problems give a conserving solution (i.e. a solution that does not create or destroy mass). In [17] the multi-component Stefan problem is studied in detail, with the hypothesis of $D_{ij}=0$ if $i\neq j$. This yields a diagonal matrix $\mathbb{D}$. The situation $D_{ij}\neq 0$ for $i\neq j$ is studied in [18].

Chapter 3

Morphological stability in the diffusion process

3.1 Morphological stability of a growing particle

We consider the diffusion-controlled growth of a spherical particle, with solute concentration c_{part}, in an infinite supersaturated alloy with initial solute concentration c_0. Let c_f be the equilibrium concentration (i.e. the solubility) from the thermodynamic phase diagram, then we assume

$$\left|\frac{c_0 - c_{sol}}{c_{part} - c_{sol}}\right| \lesssim \left|\frac{c_0 - c_f}{c_{part} - c_f}\right| \ll 1. \tag{3.1}$$

Here c_{sol} denotes the equilibrium concentration for a general (curved) interface. This condition produces that the velocity of the interface at a given instant of time is small enough to get a smooth movement. We study the stability of growth, therefore we introduce a small perturbation in the particle shape given by

$$r(\theta, \varphi, t) = R(t) + \delta(t) Y_{lm}(\theta, \varphi) \tag{3.2}$$

where the function r denotes the perturbed interface position (i.e. the distance from a point of the perturbed interface to the center of the particle). R is a function of time which denotes the sphere radius in the case of no perturbation, δ is a function of time with small values so that powers higher than one may be neglected and $Y_{lm}(\theta, \varphi)$ denotes the spherical harmonic function. The parameters l and m are integers such that $0 \leq m \leq l$. This function is the solution of the angular part of the Laplace equation and for more information we refer to the Appendix, section 10.3. We have chosen this kind of perturbation following [19], and because an arbitrary infinitesimal perturbation may be resolved into a harmonic spectrum by standard methods. In [20] the authors study different kinds of perturbations for different geometries (planar, cylindrical and spherical). In [21], Chapter 4, the authors give a brief conceptual explanation about the solidification process, the appearance of instabilities and their consequences (sidebranches, grooves, ...).

Since diffusion happens much faster than the movement of the boundary, at each instant of time our problem is equivalent to solve the Laplace equation holding the boundary fixed. The boundary conditions we need for the Laplace equation are the concentration in the infinite domain, given by $\lim_{r\to\infty} c(r, \theta, \varphi) = c_0$, and the concentration at the interface given by Eq. (3.2). The solution is

$$c(r, \theta, \varphi) = \frac{A_{lm}}{r} + \frac{B_{lm}}{r^{l+1}} \delta Y_{lm}(\theta, \varphi) + c_0 \tag{3.3}$$

where A_{lm} and B_{lm} are constants to be determined from the boundary conditions in the interface.

We remark here for clarity that δY_{lm} represents a multiplication of δ with Y_{lm}. In the Appendix, section 10.3, it is explained how to get this solution. Here r does not represent the perturbed interface position given by Eq. (3.2) but the radial co-ordinate of any point in the solvent matrix.

In the study of the growing stability we can also deal with geometric aspects of the problem (for instance, the curvature). To illustrate it we can realize two parallel studies of the stability. In one we choose the concentration at the interface constant (as we have for a planar interface), rejecting the influence of the curvature. In the other we study the stability for general interfaces where the Gibbs-Thomson effect (also called the capillarity effect) establish the importance of the curvature for the concentration at the interface.

3.1.1 Constant interface concentration

In this case, we assume the concentration of solute at the interface to be constant and to be equal to c_f, where c_f is the maximal solute solubility. Evaluating the concentration (3.3) at the interface given by (3.2) we get

$$c_f = \frac{A_{lm}}{R+\delta Y_{lm}} + \frac{B_{lm}}{(R+\delta Y_{lm})^{l+1}}\delta Y_{lm} + c_0$$

and using the Taylor expansion for those quotients and deleting higher order terms we get

$$c_f = \frac{A_{lm}}{R} + \big(\frac{B_{lm}}{R^{l+1}} - \frac{A_{lm}}{R^2}\big)\delta Y_{lm} + c_0, \tag{3.4}$$

from which follows (equating powers of δY_{lm}) that the constants A_{lm} and B_{lm} are

$$A_{lm} = (c_f - c_0)R,$$

$$B_{lm} = (c_f - c_0)R^l.$$

On other hand, for this problem the velocity of the interface is given by the equation

$$v = \frac{dR}{dt} + \frac{d\delta}{dt}Y_{lm} = \frac{D}{c_{part} - c_f}\frac{\partial c}{\partial r} \tag{3.5}$$

where D denotes the diffusion coefficient of the solute and the normal derivative $\frac{\partial c}{\partial r}$ is evaluated on the interface (Eq. (3.2)) and yields from differentiation of Eq. (3.3)

$$\frac{\partial c}{\partial r} = -\frac{(c_f - c_0)R}{(R+\delta Y_{lm})^2} - (l+1)\frac{(c_f - c_0)R^l}{(R+\delta Y_{lm})^{l+2}}\delta Y_{lm}$$

and if we use the Taylor expansion we get

$$\begin{aligned}\frac{\partial c}{\partial r} &= -\frac{c_f - c_0}{R}\big(1 - 2\frac{\delta Y_{lm}}{R}\big) - (l+1)\frac{c_f - c_0}{R^2}\big(1 - (l+2)\frac{\delta Y_{lm}}{R}\big)\delta Y_{lm} \\ &= -\frac{c_f - c_0}{R} + 2\frac{c_f - c_0}{R^2}\delta Y_{lm} - (l+1)\frac{c_f - c_0}{R^2}\delta Y_{lm} \\ &= \frac{c_0 - c_f}{R} + \frac{c_0 - c_f}{R^2}(l-1)\delta Y_{lm},\end{aligned} \tag{3.6}$$

where powers of δY_{lm} higher than one have been neglected. Finally, introducing this value into equation (3.5) we get

$$\frac{dR}{dt} + \frac{d\delta}{dt}Y_{lm} = \frac{D}{c_{part} - c_f}\big[\frac{c_0 - c_f}{R} + \frac{c_0 - c_f}{R^2}(l-1)\delta Y_{lm}\big].$$

From this equation if we separate terms with and without Y_{lm} we get the velocity for the radius of the unperturbed sphere

$$\frac{dR}{dt} = \frac{D}{c_{part} - c_f} \frac{c_0 - c_f}{R},$$

and the relation give us that the behavior of our perturbation is

$$\frac{d\delta}{dt} = \frac{D}{c_{part} - c_f} \frac{c_0 - c_f}{R^2}(l-1)\delta. \tag{3.7}$$

Next, we analyze the sign of the term $\frac{\dot{\delta}}{\delta}$ that determines the behavior of the perturbation. The result is presented in Table 3.1

	Growth ($\frac{c_0-c_f}{c_{part}-c_f} > 0$)	Dissolution ($\frac{c_0-c_f}{c_{part}-c_f} < 0$)
$l > 1$	$\frac{\dot{\delta}}{\delta} > 0$	$\frac{\dot{\delta}}{\delta} < 0$
$l = 1$	$\frac{\dot{\delta}}{\delta} = 0$	$\frac{\dot{\delta}}{\delta} = 0$
$l = 0$	$\frac{\dot{\delta}}{\delta} < 0$	$\frac{\dot{\delta}}{\delta} > 0$

Table 3.1: Behavior of the perturbation for the case of planar interface.

Then, we see that if the particle is growing, all the sinusoidal perturbations corresponding to values $l > 1$ will increase, and hence we conclude that the interface is unstable. For the case $l = 1$ we obtain no growth of the perturbation and after a long-time the perturbation will be the same as initially, that is

$$r(\theta, \varphi, t) = R(t) + \delta_0 Y_{1m}(\theta, \varphi),$$

where $\delta_0 = \delta(0)$ denotes the initial amplitude of our perturbation, and $m = 0, 1$. If $l = 0$ we should remark that $Y_{00}(\theta, \varphi) = \frac{1}{2\sqrt{\pi}}$ (see Appendix, sections 10.2 and 10.3 for details) and hence the perturbation that we obtain is another sphere with a larger radius (assuming $\delta > 0$)

$$r(\theta, \varphi, t) = R(t) + \frac{1}{2\sqrt{\pi}}\delta(t)$$

In this case, when the particle is growing, the perturbation decreases and hence, for this particular mode, the interface is said stable. The conclusion of this analysis is that, if we introduce a perturbation in the interface position when the particle is growing, that we can express as

$$r(\theta, \varphi, t) = R(t) + \sum_{l=0}^{\infty} \sum_{m=0}^{l} \delta_{lm}(t) Y_{lm}(\theta, \varphi),$$

then we will obtain that the sinusoidal modes for $l > 1$ will grow, and therefore fingers and sidebranches will appear at the interface. The behavior of the perturbation when the particle is dissolving is easily established from Table 3.1, repeating what we have done above.

3.1.2 General interface: Capillarity effect

In this section we will consider the effect of capillarity on the interface concentration. This effect is established through the Gibbs-Thompson equation

$$c_{sol} = c_f exp(2\Gamma_D \kappa) = c_f exp(\Gamma_D \tilde{\kappa}), \tag{3.8}$$

where $\Gamma_D = \frac{\gamma\Omega}{R_g T}$ is the capillarity constant in which γ is the interfacial free energy, Ω is the increment of precipitate molar volume, R_g the gas constant and T the absolute temperature. κ is the mean curvature of the interface points (chosen positive for a concave interface toward the particle, see Figure 2.7), and $\tilde{\kappa}$ is two times the mean curvature, that is the sum of the principal curvatures. To find more information about mean curvature we refer to the Appendix, section 10.1. For our problem we only need to know that $\tilde{\kappa}$ is given by the equation

$$\tilde{\kappa}(\theta,\varphi) = \frac{2}{R}[1 - \frac{\delta Y_{lm}}{R}] + l(l+1)\frac{\delta Y_{lm}}{R^2} \tag{3.9}$$

and if we use first power truncation for the Taylor expansion of the interface concentration together with Eq. (3.9) we get

$$\begin{aligned} c_{sol}(\theta,\varphi) &= c_f[1 + \Gamma_D \tilde{\kappa}(\theta,\varphi)] \\ &= c_f\left[1 + \Gamma_D\big(\frac{2}{R}[1 - \frac{\delta Y_{lm}(\theta,\varphi)}{R}] + l(l+1)\frac{\delta Y_{lm}(\theta,\varphi)}{R^2}\big)\right] \\ &= c_f\big[1 + \frac{2\Gamma_D}{R} + (l-1)(l+2)\frac{\Gamma_D}{R^2}\delta Y_{lm}(\theta,\varphi)\big]. \end{aligned} \tag{3.10}$$

Now, we have to repeat all the steps followed for the planar interface concentration to determine the explicit expression for the concentration in the matrix and finally to get the equation for the growth of the perturbation. To determine the concentration (that is, to determine A_{lm} and B_{lm}) we combine (3.3) together with (3.10) and we get

$$\frac{A_{lm}}{R + \delta Y_{lm}} + \frac{B_{lm}}{(R + \delta Y_{lm})^{l+1}} + c_0 = c_f\big[1 + \frac{2\Gamma_D}{R} + (l-1)(l+2)\frac{\Gamma_D}{R^2}\delta Y_{lm}(\theta,\varphi)\big]$$

and using the Taylor expansion for those ratios to first order in δ we find

$$\frac{A_{lm}}{R} + \big(\frac{B_{lm}}{R^{l+1}} - \frac{A_{lm}}{R^2}\big)\delta Y_{lm} + c_0 = c_f[1 + \frac{2\Gamma_D}{R}] + c_f(l-1)(l+2)\frac{\Gamma_D}{R^2}\delta Y_{lm}. \tag{3.11}$$

Therefore the constants we are looking for are

$$A_{lm} = (c_f - c_0)R + 2c_f\Gamma_D,$$

$$B_{lm} = (c_f - c_0)R^l + c_f\Gamma_D R^{l-1} l(l+1),$$

and after substitution into Eq. (3.3) the solute concentration in the points of the matrix is given by

$$c(r,\theta,\varphi) = \frac{(c_f - c_0)R + 2c_f\Gamma_D}{r} + \frac{(c_f - c_0)R^l + c_f\Gamma_D R^{l-1} l(l+1)}{r^{l+1}}\delta Y_{lm} + c_0. \tag{3.12}$$

To determine the velocity of the interface the first we have to do is to evaluate the normal derivate $\frac{\partial c}{\partial r}$ at the interface (which is given by Eq. (3.2))

$$\begin{aligned}\frac{\partial c}{\partial r} &= -\frac{(c_f - c_0)R + 2c_f\Gamma_D}{(R+\delta Y_{lm})^2} - \\ &- (l+1)\frac{(c_f - c_0)R^l + c_f\Gamma_D R^{l-1}l(l+1)}{(R+\delta Y_{lm})^{l+2}}\delta Y_{lm} = \\ &= -\frac{(c_f - c_0)R + 2c_f\Gamma_D}{R^2}(1 - 2\frac{\delta Y_{lm}}{R}) - \\ &- (l+1)\frac{(c_f - c_0)R^l + c_f\Gamma_D R^{l-1}l(l+1)}{R^{l+2}}\delta Y_{lm} \end{aligned} \tag{3.13}$$

where the last equation is obtained by neglecting powers of δ higher than one. If we denote $c_R = c_f(1 + \frac{2\Gamma_D}{R})$ then the last equation yields

$$\frac{\partial c}{\partial r} = \frac{c_0 - c_R}{R} + \Big((l-1)\frac{c_0 - c_f}{R^2} - \frac{c_f\Gamma_D}{R^3}[l(l+1)^2 - 4]\Big)\delta Y_{lm}. \tag{3.14}$$

The other factor that appears in the velocity formula is

$$\frac{D}{c_{part} - c_{sol}},$$

where if we combine this with Eq. (3.10) and subsequently linearise, then we get

$$\begin{aligned}\frac{D}{c_{part} - c_{sol}} &= \frac{D}{c_{part} - c_R - c_f(l-1)(l+2)\Gamma_D\frac{\delta Y_{lm}}{R^2}} = \\ &= \frac{D}{c_{part} - c_R}\Big[1 + \frac{c_f(l-1)(l+2)\Gamma_D}{c_{part} - c_R}\frac{\delta Y_{lm}}{R^2}\Big]. \end{aligned} \tag{3.15}$$

Finally combining equations (3.15) and (3.14) gives

$$\begin{aligned} v = \frac{D}{c_{part} - c_{sol}}\frac{\partial c}{\partial r} &= \frac{D}{c_{part} - c_R}\Big[1 + \frac{c_f(l-1)(l+2)\Gamma_D}{c_{part} - c_R}\frac{\delta Y_{lm}}{R^2}\Big]\cdot \\ &\cdot \Big[\frac{c_0 - c_R}{R} + \Big((l-1)\frac{c_0 - c_f}{R^2} - \frac{c_f\Gamma_D}{R^3}[l(l+1)^2 - 4]\Big)\delta Y_{lm}\Big] = \\ &= \frac{D}{c_{part} - c_R}\Big[\frac{c_0 - c_R}{R} + \Big(\frac{c_0 - c_R}{R}\frac{c_f(l-1)(l+2)\Gamma_D}{(c_{part} - c_R)R^2} + \\ &+ (l-1)\frac{c_0 - c_f}{R^2} - \frac{c_f\Gamma_D}{R^3}(l-1)(l^2 + 3l + 4)\Big)\delta Y_{lm}\Big]. \end{aligned} \tag{3.16}$$

In the final step we neglected the quadratic term of δY_{lm}. Rearranging the terms in this equation we find

$$\begin{aligned} v = \frac{D}{c_{part} - c_R}\Big[&\frac{c_0 - c_R}{R} + \Big((l-1)\frac{c_0 - c_f}{R^2} + \\ &+ \frac{(l-1)c_f\Gamma_D}{R^3}\big((l+2)\frac{c_0 - c_R}{c_{part} - c_R} - (l^2 + 3l + 4)\big)\Big)\delta Y_{lm}\Big], \end{aligned} \tag{3.17}$$

and since we assume in condition (3.1) that the term $\frac{c_0 - c_R}{c_{part} - c_R}$ is sufficiently small to be neglected, the velocity for the interface is approximated by

$$v = \frac{D}{c_{part} - c_R}\Big[\frac{c_0 - c_R}{R} + \Big((l-1)\frac{c_0 - c_f}{R^2} - \\ - \frac{(l-1)c_f\Gamma_D}{R^3}(l^2 + 3l + 4)\Big)\delta Y_{lm}\Big]. \tag{3.18}$$

Repeating the procedure that we did in the previous section (that is, equating terms with and without δY_{lm}) we find the following equation for the behavior of the perturbation

$$\begin{aligned}\frac{d\delta}{dt} &= \frac{D(l-1)}{c_{part} - c_R}\Big[\frac{c_0 - c_f}{R^2} - \frac{c_f\Gamma_D}{R^3}(l^2 + 3l + 4)\Big]\delta = \\ &= \frac{c_f D(l-1)}{(c_{part} - c_R)R^2}\Big[\frac{c_0 - c_f}{c_f} - \frac{\Gamma_D}{R}(l^2 + 3l + 4)\Big]\delta = \\ &= \frac{D(l-1)}{(c_{part} - c_R)R}\Big[G - \frac{c_f\Gamma_D}{R^2}(l+1)(l+2)\Big]\delta,\end{aligned} \tag{3.19}$$

where $G = (c_0 - c_R)/R$ is the normal concentration gradient at the interface of the undisturbed sphere (see Eq. (3.3) with $\delta = 0$). Note if we have $l = 1$ we get the same result as in the previous case (the perturbation keeps constant). Further, if $\Gamma_D = 0$ then the result is identical to Eq. (3.7). Through Eq. (3.19) we can analyze the behavior of the perturbation, that is if it grows or decays. This behavior is determined by the sign of

$$(c_{part} - c_R) \cdot \Big[\frac{c_0 - c_f}{c_f} - \frac{\Gamma_D}{R}(l^2 + 3l + 4)\Big]. \tag{3.20}$$

If it is positive means the perturbation grows and if it is negative then the perturbation decays. We have to remark that this sign depends on the radius R (the radius of growing of the unperturbed sphere), which is a function of time, therefore the behavior of the perturbation can change with time. We also note that the Eq. (3.20) depends on l, that is the nature of the perturbation depends on the spherical harmonic function we use (as we should expect, but that dependence only appears through one of its two parameters). Moreover, if we assume that $c_{part} > c_R$ and a given l, we find a critical value of the sphere radius

$$R_c(l) = \frac{c_f\Gamma_D}{c_0 - c_f}(l^2 + 3l + 4) = \frac{1}{2}(l^2 + 3l + 4)R^*, \tag{3.21}$$

where $R^* = \frac{2c_f\Gamma_D}{c_0 - c_f}$ (is the critical nucleation radius if $c_R = c_0$). Therefore if we assume that $c_0 - c_f > 0$ we find that above this critical radius $R_c(l)$ the perturbation grows and the sphere turns unstable and below this value the perturbation decays and we not have any stability problems. If $c_0 - c_f < 0$ then the behavior is the contrary.

From equation (3.19) we can also analyze the value l_M of l that produces the maximum rate of growth for the perturbation. It can be obtained by differentiating the coefficient of δ in that equation with respect to l, which produces

$$\frac{c_0 - c_f}{c_f} - \frac{\Gamma_D}{R}(3l^2 + 4l + 1), \tag{3.22}$$

whose roots are

$$l^{(1)} = -\frac{2}{3} + \sqrt{\frac{1}{9} + \frac{(c_0 - c_f)R}{3c_f\Gamma_D}},$$

$$l^{(2)} = -\frac{2}{3} - \sqrt{\frac{1}{9} + \frac{(c_0 - c_f)R}{3c_f\Gamma_D}}.$$

The second root $l^{(2)}$ is quickly refused because it corresponds to a negative number. Moreover, l should take positive integer values, therefore the value l_M should be the integer closest to $l^{(1)}$ and which produces the larger value of the rate given in Eq. (3.22). In [19] the authors bring that value near by

$$\sqrt{\frac{(c_0 - c_f)R}{3c_f\Gamma_D}}.$$

Since the perturbations corresponding to l_M grow most rapidly, it is clear to expect these perturbations tend to produce a dimpled condition in the spherical surface on a scale $\lambda_M = (2\pi R)/l_M$ easier than other perturbations.

3.1.3 Small-scale stability of nonspherical forms: planar approximation

Suppose we have a nonspherical surface such that we can do a partition of it into zones Q (as few as possible) so that the principal radii of curvature R_1 and R_2 are (approximately) uniform. That is, each zone Q is (approximately) a part of a sphere. Hence the concentration gradient G can be considered constant. In this section we study the stability of the zones Q with respect to undulations of small wavelengths λ compared with the minimum of R_1, R_2 and L (L denotes the amplitude of the undulation). That means we only consider waves in Q that can be considered as lying on an infinite plane on which the initial gradient is G. Their behavior determines the small-scale stability of Q. Those small wavelengths correspond to large $l = 2\pi R/\lambda$, and if we use the notation $w = 2\pi/\lambda = l/R$ for the frequency of the perturbation, the equation that determines the behavior of the instability (3.19) yields with $\frac{l\pm1}{R} \approx w$ and $\frac{l+2}{R} \approx w$ that

$$\frac{d\delta}{dt} = \frac{Dw}{c_{part} - c_R}\big[G - c_f\Gamma_D w^2\big]\delta. \tag{3.23}$$

With that equation we can search the frequencies that determine the growing or decaying of the perturbation. This behavior is determined by

$$w_0 = \sqrt{\frac{G}{c_f\Gamma_D}}, \tag{3.24}$$

and if $\lambda > \lambda_0 = 2\pi/w_0$, the perturbation will grow. Otherwise, it will decay. The maximum growing rate of the perturbation is got by differentiating (3.23) with respect to w and is

$$w_M = \sqrt{\frac{G}{3c_f\Gamma_D}} = \frac{w_0}{\sqrt{3}}. \tag{3.25}$$

3.2 Solidification case

In this section we study the stability of a solid sphere growing in an originally uniformly supercooled melt. The difference with the previous problem is that the heat can flow inside and outside of the sphere (and in the precipitate growth problem diffusion only takes place outside of the sphere). Because of that reason the velocity of the interface is given by

$$v = -\frac{1}{L_v}\big[k_s(\frac{\partial T}{\partial n})_s + k_l(\frac{\partial T}{\partial n})_l\big], \tag{3.26}$$

where L_v is the latent heat of freezing per unit volume, k_s and k_l are the thermal conductivities of the solid and the liquid phases, $(\partial T/\partial n)_S$ is the temperature derivative at the interface along the normal pointing toward the solid and $(\partial T/\partial n)_S$ is the same derivative with the normal pointing toward the liquid. In the same way as in the precipitate growth we can approximate the temperature at the interface by

$$T = T_f - T_f \Gamma_T \tilde{\kappa}, \tag{3.27}$$

where $\Gamma_T = \gamma/L_v$ is the capillary constant for this problem, T_f is the interface temperature when we consider a flat interface (that is when we consider the curvature $\kappa \to 0$) and $\tilde{\kappa}$ is the sum of the two principal curvatures (i.e. two times the mean curvature), supposed positive for a concave interface toward the solid. As we did before, we impose

$$\big|C_v \frac{T_f - T_0}{L_v}\big| \ll 1$$

to have a problem in which the interface does not move fast. C_v is the specific heat per unit volume of the liquid and T_0 is the initial temperature outside of the sphere. In this problem we have to solve the Laplace equation in both domains (inside and outside of the sphere). The general solutions are:

- outside of the sphere:

$$T_1(r,\theta,\varphi) = \frac{A_{lm}^{(1)}}{r} + \frac{B_{lm}^{(1)}}{r^{l+1}} \delta Y_{lm}(\theta,\varphi) + T_0, \tag{3.28}$$

- inside of the sphere:

$$T_2(r,\theta,\varphi) = A_{lm}^{(2)} + B_{lm}^{(2)} r^l \delta Y_{lm}(\theta,\varphi) \tag{3.29}$$

where the constants $A_{lm}^{(1)}, B_{lm}^{(1)}, A_{lm}^{(2)}, B_{lm}^{(2)}$ are obtained from the temperature at the interface.

3.2.1 Constant interface temperature

If we try to apply the procedure for the case of a constant interface concentration (where we assume that the interface temperature is the same as for a planar interface) in the precipitate growing to the solidification case, we find that the equation for the temperature outside of the sphere is similar to the corresponding equation for the concentration, that is

$$T_1(r,\theta,\varphi) = \frac{(T_f - T_0)R}{r} + \frac{(T_f - T_0)R^l}{r^{l+1}} \delta Y_{lm}(\theta,\varphi) + T_0, \tag{3.30}$$

and if we seek the solution for the temperature inside of the sphere such that it would be T_f at the interface and bounded when $r \to 0$, then the solution we get is $T_2(r,\theta,\varphi) = T_f$, i.e. the temperature is constant. Therefore the equation for the velocity will be

$$v = -\frac{k_l}{L_v}\frac{\partial T_1}{\partial r} = \frac{k_l}{L_v}\big[\frac{T_0 - T_f}{R} + \frac{T_0 - T_f}{R^2}(l-1)\delta Y_{lm}\big] \tag{3.31}$$

from which we see that the behavior of the perturbation is given by

$$\frac{d\delta}{dt} = \frac{k_l}{L_v}(l-1)\frac{T_0 - T_f}{R^2}\delta, \tag{3.32}$$

that is always positive except for the case $l = 1$. This means we always get growing of the perturbation (that is, unstable interface) except when $l = 1$, in which case the perturbation remains constant during the whole process as we saw in the precipitate case.

3.2.2 General interface: Capillarity effect

In this case the temperature at the interface is given by Eq. (3.27) and $\tilde{\kappa}$ is given by Eq. (3.9). Therefore, the temperature at the interface yields

$$T = T_f[1 - \frac{2\Gamma_T}{R}] - (l-1)(l+2)\frac{T_f\Gamma_T}{R^2}\delta Y_{lm}. \tag{3.33}$$

Using this relation and linearization for the temperature outside and inside of the sphere, given by Eq. (3.28) and (3.29), then we get

$$\begin{aligned} T_1(r,\theta,\varphi) = &\frac{(T_f - T_0)R - 2\Gamma_T T_f}{r} + \\ &+ \frac{(T_f - T_0)R^l - l(l+1)T_f\Gamma_T R^{l-1}}{r^{l+1}}\delta Y_{lm}(\theta,\varphi) + T_0, \end{aligned} \tag{3.34}$$

for the temperature outside of the sphere, and

$$T_2(r,\theta,\varphi) = T_f\big[1 - \frac{2\Gamma_T}{R}\big] + \frac{(l-1)(l+2)T_f\Gamma_T}{R^{l+2}}r^l\delta Y_{lm}(\theta,\varphi), \tag{3.35}$$

for the temperature inside of the sphere. Now, evaluating the radial derivative in the Eq. (3.26) we find:

$$\big(\frac{\partial T}{\partial r}\big)_s = -\frac{\partial T_2}{\partial r}\big|_{interface} = l\frac{T_f\Gamma_T(l-1)(l+2)}{R^3}\delta Y_{lm},$$

$$\begin{aligned} \big(\frac{\partial T}{\partial r}\big)_l = \frac{\partial T_1}{\partial r}\big|_{interface} = &-\frac{(T_f - T_0)R - 2T_f\Gamma_T}{R^2} - \\ &- (l-1)\big[\frac{T_f - T_0}{R^2} - \frac{T_f\Gamma_T}{R^3}[(l+1)(l+2)+2]\big]\delta Y_{lm}, \end{aligned}$$

and therefore the interface velocity is given by

$$\begin{aligned} v = \frac{dR}{dt} + \frac{d\delta}{dt}Y_{lm}(\theta,\varphi) = \\ = -\frac{1}{L_v}\Bigg[k_s l\frac{T_f\Gamma_T(l-1)(l+2)}{R^3}\delta Y_{lm} - k_l\Bigg(\frac{(T_f - T_0)R - 2T_f\Gamma_T}{R^2} + \\ + (l-1)\big\{\frac{T_f - T_0}{R^2} - \frac{T_f\Gamma_T}{R^3}[(l+1)(l+2)+2]\delta Y_{lm}\big\}\Bigg)\Bigg]. \end{aligned}$$

Finally, after separating on terms with and without Y_{lm} the equation for the behavior of the perturbation is

$$\frac{d\delta}{dt} = \frac{T_f(l-1)k_l}{L_v R^2}\Bigg[\frac{T_f - T_0}{T_f} - \frac{\Gamma_T}{R}\Bigg((l+1)(l+2) + 2 + l(l+2)\frac{k_s}{k_l}\Bigg)\Bigg]\delta \tag{3.36}$$

and hence stability is determined by the sign of

$$\frac{T_f - T_0}{T_f} - \frac{\Gamma_T}{R}\Bigg((l+1)(l+2) + 2 + l(l+2)\frac{k_s}{k_l}\Bigg). \tag{3.37}$$

Note that if $k_s = 0$ then we get the same formula as in the precipitate case (Eq. (3.20)). If the sign of (3.37) is positive the perturbation grows and if it is negative the perturbation decays. Note further, that if $\Gamma_T = 0$ then Eq. (3.36) and (3.32) are equivalent.

Chapter 4

Survey of some numerical methods

We make a first classification of the numerical methods for solving the Stefan problem (2.1-2.6) into two categories: front-tracking methods and implicit methods. Front-tracking methods in which the position of the interface is computed at each time step, and implicit methods which do not deal explicitly with the position of the interface, but it is updated by some alternative way. Thereafter some examples of them will be given.

4.1 Front-Tracking Methods

4.1.1 Fixed finite-difference grid

The space domain is discretized in a uniform grid with nodes $x_i = (i-1)\Delta x$, and finite differences are used to discretize the equations. The spatial separation Δx is related with the total number of grid nodes $N+1$ by $1 = (N+1)\Delta x$. Moreover, the position of the interface will usually be located between two consecutive nodes x_i and x_{i+1}, see Figure 4.1.

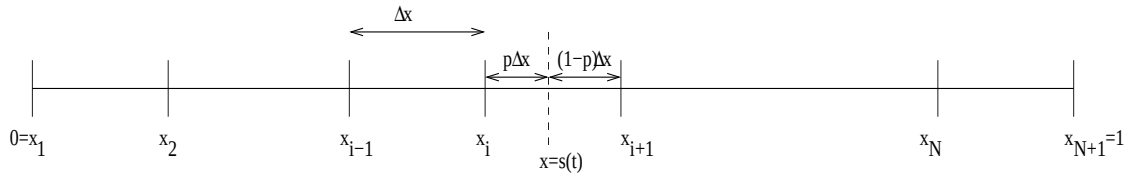

Figure 4.1: Fixed grid

In this situation, diffusion equation (2.10) is discretized by

$$\frac{c_j^{n+1} - c_j^n}{\Delta t} = \frac{c_{j-1}^n - 2c_j^n + c_{j+1}^n}{(\Delta x)^2}, \quad \forall j : i+2 \leq j \leq N. \tag{4.1}$$

Equation (2.14) implies that

$$\frac{c_{N+1}^{n+1} - c_N^{n+1}}{\Delta x} = 0, \tag{4.2}$$

and inside the particle the concentration is given by (2.12)

$$c_j^{n+1} = 1, \quad \forall j : 1 \leq j \leq i. \tag{4.3}$$

Hence, the only critical point of this method arises in the vicinity of the interface, where the distance between the interface and the two neighboring nodes is unequal. For these nodes we can use an interpolation formula to solve the diffusion equation (2.10) and the movement of the

interface (2.15). For instance, if we use a Lagrange interpolation formula with three nodes a_1, a_2 and a_3, we can approximate the function $f(x)$ by the second degree polynomial

$$Pf(x) = f(a_1)\frac{(x-a_2)(x-a_3)}{(a_1-a_2)(a_1-a_3)} + f(a_2)\frac{(x-a_1)(x-a_3)}{(a_2-a_1)(a_1-a_3)} + f(a_3)\frac{(x-a_1)(x-a_2)}{(a_3-a_1)(a_3-a_2)}.$$

Hence, if we assume that $p\Delta x$ is the distance between the interface and x_i, and hence $(1-p)\Delta x$ the distance between x_{i+1} and the interface (see Figure 4.1), we can adapt the latest formula to discretize (2.10) in the node x_{i+1}:

$$\frac{c_{i+1}^{n+1} - c_{i+1}^n}{\Delta t} = \frac{2}{(\Delta x)^2}\left[\frac{c_{sol}}{c_{part}}\frac{1}{(1-p)(2-p)} - \frac{c_{i+1}^n}{1-p} + \frac{c_{i+2}^n}{2-p}\right], \tag{4.4}$$

and (2.15):

$$\frac{s^{n+1} - s^n}{\Delta t} = \frac{\lambda}{\Delta x}\left[-\frac{c_{sol}}{c_{part}}\left(\frac{1}{1-p} + \frac{1}{2-p}\right) + c_{i+1}^n\frac{2-p}{1-p} - c_{i+2}^n\frac{1-p}{2-p}\right], \tag{4.5}$$

where Forward Euler method has been used for time discretizations, but any other discretization could be used. In [22] more finite difference schemes for partial differential equations can be found. It has to be noted that Fordward Euler is conditionally stable, and $\frac{\Delta t}{(\Delta x)^2} \leq \frac{1}{2}$ should be provided to guarantee stability. Furthermore, when the interface is very close to the node x_{j+1}, that is when the distance $(1-p)\Delta x \to 0$ the presented method shows instabilities, because of the divisions by a very small number in the interpolation polynomial. In that case, we propose to repeat the procedure but choosing as interpolation nodes the interface position, x_{j+2} and x_{j+3}.

Therefore, the numerical solution of (2.10)-(2.15) can be summarized as follow: starting from known values of all variables at time $t^n = n\Delta t$,

1. calculate c_j^{n+1} for $0 \leq j \leq i$ from (4.3),
2. calculate c_j^{n+1} for $i+2 \leq j \leq N$ from (4.1),
3. calculate c_{i+1}^{n+1} from (4.4),
4. calculate the new position of the interface s^{n+1} from (4.5),
5. calculate the index i such that $x_i \leq s^{n+1} < x_{i+1}$, and back to step 1.

Due to the construction of this method, we must be carefull with the selected grid because of the concentration of the nearest node at the interface is calculated under the assumption that the interface does not cross more than one cell by time step. That is, if the position of the interface at time t^n, i.e. $s(t^n)$, lies between the grid nodes x_i and x_{i+1}, then $s(t^{n+1})$ must lie between x_{i-1} and x_i, x_i and x_{i+1} or x_{i+1} and x_{i+2}. This poses an extra requirement on the time stepping.

4.1.2 Variable time stepping

The spirit of this method is to determine the time step such that the position of the interface coincides with a node of the fixed spatial grid. Next, this idea will be reproduced for the problem (2.10)-(2.15). Let be $x_i = i\Delta x$ (for $i = 0, \ldots, N$) the nodes of a uniform grid and $\Delta t^n = t^{n+1} - t^n$. Let assume that $s(t^n) = x_i$ and that the boundary position is increasing in x. Hence, we have to find Δt^n such that $s(t^{n+1}) = x_{i+1}$. Thus, at time t^{n+1} the diffusion equation (2.10) leads to

$$\frac{c_j^{n+1} - c_j^n}{\Delta t^n} = \frac{c_{j-1}^{n+1} - 2c_j^{n+1} + c_{j+1}^{n+1}}{(\Delta x)^2},$$

for all the grid nodes x_j such that $s(t^{n+1}) < j < N$, that is $i+1 < j < N$. For x_N we have that $c_N^{n+1} - c_{N-1}^{n+1} = 0$ due to (2.14). For the nodes inside the particle at time t^{n+1}, that is the x_j such that $0 \leq j \leq i$, equation (2.12) implies that $c_j^{n+1} = 1$, and for the interface (2.13) leads to $c_{i+1}^{n+1} = \frac{c_{sol}}{c_{part}}$. Finally, Stefan condition (2.15) implies that

$$\frac{s(t^{n+1}) - s(t^n)}{\Delta t^n} = \lambda \frac{c_{i+2}^{n+1} - c_{sol}/c_{part}}{\Delta x}. \tag{4.6}$$

Therefore, the algorithm would be as follows:

1. let $\Delta t_{(0)}^n > 0$ be chosen arbitrarily. Do $r = 0$.

2. Calculate the concentration distribution at time $t_{(r)}^{n+1} = t^n + \Delta t_{(r)}^n$ as explained above.

3. Use (4.6) to check the validity of the time step:

$$res(r) := \Delta t_{(r)}^n - \frac{(\Delta x)^2}{\lambda\big(c_{i+2}^{n+1} - c_{sol}/c_{part}\big)},$$

   and if $|res(r)|$ is larger than a given tolerance then use $\Delta t_{(r+1)}^{n+1} = \Delta t_{(r)}^{n+1} + res(r)$ and go to 2. Otherwise, do $t^{n+1} = t^n + \Delta t_{(r)}^{n+1}$.

Nonetheless, this method has an important drawback: it is not easily applicable to higher dimensions. For more information about this method we refer to [3], Chapter 4.

4.1.3 Method of lines

As is well known, the method of lines is thought to use a space discretization to obtain a set of coupled initial value problems, which are solved using the usual procedures for this kind of problems, see for instance [23]. An interesting feature of this method is that, for fixed domain problems, we can observe the solution in a set of points. However, this becomes a problem when we have a moving boundary problem and we use a fixed space discretization. In this case, we can interpret the method of lines other way round, doing first a time discretization and obtaining an ordinary differential problem in space. This last is the procedure presented here and for more detail we refer to [3].

Hence, at time $t = t_n$ the equations (2.10)-(2.15) can be approximated by the system

$$c''(x) - \frac{c(x) - \tilde{c}(x)}{\Delta t} = 0, \quad s < x < 1, \tag{4.7}$$

$$c'(1) = 0, \tag{4.8}$$

$$c(s) = \frac{c_{sol}}{c_{part}}, \tag{4.9}$$

$$\frac{s - s_{n-1}}{\Delta t} - \lambda c'(s) = 0, \tag{4.10}$$

where s and $c(x)$ denote the position of the moving interface and the concentration at time t_n and $\tilde{c}$ denotes the concentration at time t_{n-1}, or its linear extension beyond the interface if necessary. That is, in the case of a decreasing interface position it would happen that $s(t_n) < s(t_{n-1})$, and in this case we have

$$\tilde{c}(x) = \tilde{c}(s_{n-1}) + (x - s_{n-1})\tilde{c}'(s_{n-1}), \quad x < s_{n-1}.$$

Hence, the method of lines requires to find the interface positions at successive times t_n and the solution of the second-order ordinary differential equations (4.7)-(4.10). For linear equations and conditions on the fixed boundaries we might use Riccati transformations [3] at time t_n and introduce the functions $\phi(x) = c'(x)$, $R(x)$ and $z(x)$ related by $\phi(x) = R(x)c(x) + z(x)$ and being the solutions to the initial value problems

$$\frac{dR}{dx}(x) = \frac{1}{\Delta t} - R^2(x), \quad R(1) = 0,$$

$$\frac{dz}{dx}(x) = R(x)z(x) - \frac{\tilde{c}(x)}{\Delta t}, \quad z(1) = 0.$$

The position of the interface s at time t_n given by (4.10) is the root of the equation

$$\frac{s - s_{n-1}}{\Delta t} - \lambda\big[R(s)\frac{c_{sol}}{c_{part}} + z(s)\big] = 0.$$

Once the position of the interface $s = s(t_n)$ is known, the function $c(x)$ is obtained by integration of

$$\frac{dc}{dx}(x) = R(x)c(x) + z(x), \quad s < x < 1,$$

with the boundary condition

$$c(s) = \frac{c_{sol}}{c_{part}}.$$

4.1.4 Front-fixing methods

In this type of methods the position of the interface is fixed by a suitable choice of new space variables. In our case, the transformation should be

$$\xi = \frac{x - s(t)}{1 - s(t)}, \tag{4.11}$$

that transforms the diffusion domain $(s(t), 1)$ into $(0, 1)$, and makes the interface position to correspond with $\xi = 0$ for all time t. Of course, the interface position should not be equal to 1. However, this is not an exclusive condition for the problem (2.10)-(2.15) since under general hypothesis this will never happen. Then, using the chain rule for the new function $\tilde{c}(\xi, t) = c(x, t)$ we have

$$\frac{\partial c}{\partial x} = \frac{\partial \tilde{c}}{\partial \xi}\frac{\partial \xi}{\partial x} = \frac{1}{1 - s(t)}\frac{\partial \tilde{c}}{\partial \xi},$$

$$\frac{\partial^2 c}{\partial x^2} = \frac{1}{(1 - s(t))^2}\frac{\partial^2 \tilde{c}}{\partial \xi^2},$$

$$\frac{\partial c}{\partial t} = \frac{\partial \tilde{c}}{\partial \xi}\frac{\partial \xi}{\partial t} + \frac{\partial \tilde{c}}{\partial t} = \frac{ds}{dt}\frac{x - 1}{(1 - s)^2}\frac{\partial \tilde{c}}{\partial \xi} + \frac{\partial \tilde{c}}{\partial t},$$

which transform the diffusion equation (2.10) into

$$\frac{\partial^2 \tilde{c}}{\partial \xi^2}(\xi, t) = (1 - s(t))^2\frac{\partial \tilde{c}}{\partial t} + (1 - \xi)(s(t) - 1)\frac{ds}{dt}(t)\frac{\partial \tilde{c}}{\partial \xi}(\xi, t), \quad 0 < \xi < 1,\ t \in (0, t_{end}). \tag{4.12}$$

Analogous, the Stefan condition (2.15) becomes

$$\frac{ds}{dt}(t) = \lambda \frac{1}{1-s(t)} \frac{\partial \tilde{c}}{\partial \xi}(0,t), \quad t \in (0, t_{end}). \tag{4.13}$$

The rest of boundary conditions are easily attainable. Thus, (2.13) transforms to

$$\tilde{c}(0,t) = \frac{c_{sol}}{c_{part}}, \ t \in (0, t_{end}), \tag{4.14}$$

and (2.14) to

$$\frac{\partial \tilde{c}}{\partial \xi}(1,t) = 0, \ t \in (0, t_{end}). \tag{4.15}$$

Therefore, discretizations of (4.12)-(4.15) will lead to numerical solutions of the diffusion problem. Moreover, front-fixing methods can be easily generalized to two and three dimensions for simple geometries, since curved-shaped regions can be transformed to rectangular or cubic domains through differentiable functions. However, it might become difficult for complex geometries.

4.2 Implicit Methods

4.2.1 Enthalpy Method

The enthalpy method is tightly related to thermodynamical concepts for the temperature and hence this method will be presented for the solidification (or melting) of a certain material within the domain $[0,1]$. The equations that model this two-phase Stefan problem are

$$\left| \begin{array}{ll} \dfrac{\partial T}{\partial t}(x,t) = K \dfrac{\partial^2 T}{\partial x^2}(x,t) & \text{if } x \in \Omega_1(t) \cup \Omega_2(t),\ t \in [0, t_{end}] \\ \dfrac{\partial T}{\partial x}(x,t) = 0 & \text{if } x = \{0,1\},\ t \in [0, t_{end}] \\ T(x,0) = T_0(x) & x \in [0,1] \\ T(s(t),t) = T_e & t \in [0, t_{end}] \\ s(0) = s_0 & \\ -\rho L \dfrac{ds}{dt}(t) = \left[K \vec{\nabla} T \cdot \vec{n}\right]_1^2 & x = s(t),\ t \in [0, t_{end}] \end{array} \right. \tag{4.16}$$

where T represents the temperature, K the thermal diffusivity, s the position of the interface separating the two phases Ω_i $i = 1, 2$ and $\vec{n}$ is the normal vector. Further, ρ is the density of the material, L is the latent heat and T_e is the melting temperature. Let us introduce the enthalpy function $H(T)$, which is the total heat content (that is, the sum of the specific heat and the latent heat required for a phase change)

$$H(T) = \int_{T_0}^{T} \left\{ c_{spm}(\theta)\rho(\theta) + L\rho(\theta)\delta(\theta) \right\} d\theta = \left\{ \begin{array}{ll} c_{spm}\rho T + L\rho & \text{if } x \in \Omega_2 \\ c_{spm}\rho T & \text{if } x \in \Omega_1 \end{array} \right. \tag{4.17}$$

where we have assumed that $c_{spm}(\theta)$, $\rho(\theta)$ and $\rho(\theta)$ are constants, and T_0 is a fixed temperature ($T_0 < T_e$), where we have chosen it to be the absolute zero. See Figure 4.2.

We can reformulate the problem (4.16) as

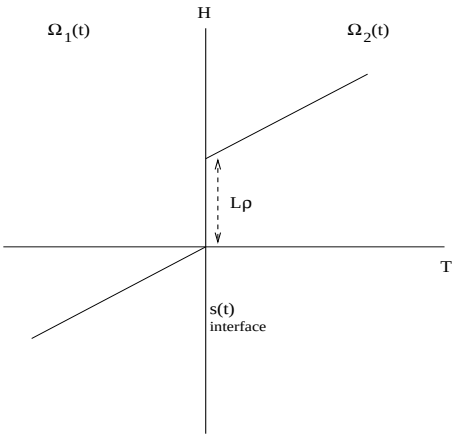

Figure 4.2: Enthalpy function.

$$\left|\begin{array}{ll} \dfrac{\partial H}{\partial t}(x,t) = K\dfrac{\partial^2 T}{\partial x^2}(x,t) & \text{if } x \in \Omega_1(t) \cup \Omega_2(t),\ t \in [0, t_{end}] \\ \dfrac{\partial T}{\partial x}(x,t) = 0 & \text{if } x = 0, 1,\ t \in [0, t_{end}] \\ T(x,0) = T_0(x) & x \in [0,1] \\ s(0) = s_0, & \end{array}\right. \tag{4.18}$$

which should be interpreted in a weak formulation sense since H is a step function. It is reported in [24, 25] that a unique weak solution exists for (4.18). For more information about this derivation and this method we refer to [3, 25, 26]. The numerical solution of this problem can be tackled with different procedures. As an example, in [3] an explicit finite-difference scheme is presented, in which for each time step the enthalpy function is calculated first and the temperature is obtained by relation (4.17).

4.2.2 Variational Inequalities

To formulate Stefan problems in terms of certain inequalities is another possibility. In these cases the expressions refer to a fixed domain and the explicit use of the Stefan condition is avoided. Some references in this field are [3, 8, 24]. Stefan problems are expressed as parabolic variational inequalities with general form

$$(u_t, v - u) + a(u, v - u) \geq (f, v - u),$$

to be satisfied for all the test functions v in a certain set, and a a bilinear and continuous from.

In the present work, we consider the non-dimensional formulation of diffusion process described by equations (2.10)-(2.15), and the nomenclature used in Section 2.7.1. We define $D_{t_{end}} := (0,1) \times (0, t_{end})$. Let be $\hat{c}(x,t) = c(x,t) - 1$, for $(x,t) \in D_{t_{end}}$. This new variable transforms the problem to

$$\frac{\partial \hat{c}}{\partial t}(x,t) = \frac{\partial^2 \hat{c}}{\partial x^2}(x,t)\ ,\ x \in \Omega(t)\ ,\ t \in (0, t_{end}], \tag{4.19}$$

$$\hat{c}(x,0) = \frac{c_0 - c_{part}}{c_{part}}\ ,\ x \in \Omega(0), \tag{4.20}$$

$$\hat{c}(x,t) = 0 \ , \ x \in \Omega_s(t), \ t \in [0, t_{end}], \tag{4.21}$$

$$\hat{c}(s(t),t) = \frac{c_{sol} - c_{part}}{c_{part}} \ , \ t \in [0, t_{end}], \tag{4.22}$$

$$\frac{\partial \hat{c}}{\partial x}(1,t) = 0 \ , \ t \in [0, t_{end}], \tag{4.23}$$

$$\frac{ds}{dt}(t) = \lambda \frac{\partial \hat{c}}{\partial x}(s(t),t) \ , \ t \in [0, t_{end}], \tag{4.24}$$

where λ is the same that in Section 2.7.1. With this change of variables we obtain that the concentration inside the particle is zero. However, the derivation of the variational inequalities formulation also requires that the concentration on the interface is zero. For this propose we introduce the next function:

$$\tilde{c}(x,t) = \begin{cases} 0 & \text{if } x \in \Omega_s(t) \ , \ t \in [0, t_{end}], \\ \hat{c}(x,t) - \dfrac{c_{sol} - c_{part}}{c_{part}} & \text{if } x \in \{s(t)\} \cup \Omega(t) \ , \ t \in [0, t_{end}]. \end{cases}$$

This function $\tilde{c}$ is the solution of the next problem:

$$\begin{cases} \dfrac{\partial \tilde{c}}{\partial t} = \dfrac{\partial^2 \tilde{c}}{\partial x^2} \ , \ x \in \Omega(t) \ , \ t \in (0, t_{end}], \\ \tilde{c}(s(t),t) = 0 \ , \ t \in [0, t_{end}], \\ \dfrac{\partial \tilde{c}}{\partial x}(1,t) = 0 \ , \ t \in [0, t_{end}], \\ \dfrac{ds}{dt}(t) = \lambda \dfrac{\partial \tilde{c}}{\partial x}(s(t),t) \ , \ t \in [0, t_{end}], \end{cases} \tag{4.25}$$

and also solves the differential equation

$$\frac{\partial \tilde{c}}{\partial t}(x,t) - \frac{\partial^2 \tilde{c}}{\partial x^2}(x,t) = \frac{1}{\lambda} \frac{\partial \chi_{\Omega(t)}}{\partial t}(x,t), \quad (x,t) \in D_{t_{end}}$$

in a distributional sense, where $\chi_{\Omega(t)}$ is the characteristic function over the domain $\Omega(t)$ (that is, it is equal to 1 in the Aluminium-matrix $\Omega(t)$ and 0 in the rest of the domain $D_{t_{end}} \setminus \Omega(t)$). Likewise, let us regroup the initial conditions in only one function

$$\tilde{c}_0(x) = \begin{cases} 0 & \text{if } x \in \Omega_s(0) \\ 0 & \text{if } x = s(0) \\ \dfrac{c_0 - c_{sol}}{c_{part}} & \text{if } x \in \Omega(0). \end{cases}$$

Let us introduce a new variable

$$u(x,t) = \int_0^t \tilde{c}(x,\tau) d\tau, \quad (x,t) \in \bar{D}_{t_{end}}. \tag{4.26}$$

Then, differentiating u both in time and space we have

$$\frac{\partial u}{\partial t}(x,t) = \tilde{c}(x,t),$$

$$\frac{\partial u}{\partial x}(x,t) = \int_0^t \frac{\partial \tilde{c}}{\partial x}(x,\tau)d\tau,$$

$$\frac{\partial^2 u}{\partial x^2}(x,t) = \int_0^t \frac{\partial^2 \tilde{c}}{\partial x^2}(x,\tau)d\tau = \int_0^t \big[\frac{\partial \tilde{c}}{\partial \tau}(x,\tau) - \frac{1}{\lambda}\frac{\partial \chi_{\Omega(\tau)}}{\partial \tau}(x,\tau)\big]d\tau = \tilde{c}(x,t) - \tilde{c}(x,0) - \frac{1}{\lambda}\big[\chi_{\Omega(t)} - \chi_{\Omega(0)}\big].$$

Hence, regrouping terms we find that

$$\frac{\partial u}{\partial t}(x,t) - \frac{\partial^2 u}{\partial x^2}(x,t) - \tilde{c}_0(x) + \frac{1}{\lambda}\chi_{\Omega(0)}(x,0) = \frac{1}{\lambda}\chi_{\Omega(t)}(x,t), \quad \forall (x,t) \in D_{t_{end}},$$

or equivalently

$$\frac{\partial u}{\partial t}(x,t) - \frac{\partial^2 u}{\partial x^2}(x,t) - f(x) = \frac{1}{\lambda}\bigg(\chi_{\Omega(t)}(x,t) - 1\bigg), \quad \forall (x,t) \in D_{t_{end}},$$

where $f(x) = \tilde{c}_0(x) - \frac{1}{\lambda}\big(\chi_{\Omega(0)}(x,0) - 1\big)$ is not a function of time. Therefore, it follows that the variable u solves the differential problem

$$\left|\begin{array}{ll} \dfrac{\partial u}{\partial t} - \dfrac{\partial^2 u}{\partial x^2} - f \leq 0 & \text{in } D_{t_{end}} \\ u \geq 0 & \text{in } D_{t_{end}} \\ \big(\dfrac{\partial u}{\partial t} - \dfrac{\partial^2 u}{\partial x^2} - f\big)u = 0 & \text{in } D_{t_{end}} \\ \dfrac{\partial u}{\partial x}(x,t) = 0 & x \in \{0,1\},\ t \in (0, t_{end}) \\ u(x,0) = 0, & x \in (0,1). \end{array}\right. \tag{4.27}$$

Summing up the done until here, we have that if $\tilde{c}$ is a solution of (4.25) then u defined by (4.26) is a solution of (4.27). The moving interface is the interface separating the regions $\{(x,t) \in D_{t_{end}} \mid u(x,t) > 0\}$ and $\{(x,t) \in D_{t_{end}} \mid u(x,t) = 0\}$. However, we can not gain the problem (4.25) from (4.27) because of the boundary conditions. On the other hand, we know that both problems have unique solution, and hence we can conclude that these solutions have to be the same. Therefore, solving (4.25) is equivalent to solving (4.27).

Next, we consider the discretization of the problem (4.27). Using a fixed grid as in Section 4.1.1 (see Figure 4.1), we use a fully implicit scheme in time to discretize the first equation of (4.27)

$$\frac{u_i^{n+1} - u_i^n}{\Delta t} - \frac{u_{i-1}^{n+1} - 2u_i^{n+1} + u_{i+1}^{n+1}}{(\Delta x)^2} - f_i \leq 0,$$

which is valid for the grid nodes x_i such that $i = 1, \ldots, N-1$, and f_i denotes $f(x_i)$. Boundary conditions produce

$$\frac{u_1^{n+1} - u_0^{n+1}}{\Delta x} = 0,$$

$$\frac{u_N^{n+1} - u_{N-1}^{n+1}}{\Delta x} = 0.$$

In a vectorial form, last discretization is $A\mathbf{u} - \mathbf{b} \leq 0$ where A is the usual tridiagonal matrix, $\mathbf{u}$ denotes the unknown variable dependent u at time t^{n+1} and $\mathbf{b}$ is a vector related with the values of u in the previous time t^n. Then, problem (4.27) is equivalent to find the vector $\mathbf{u}$ that solves

$$
\begin{aligned}
&A\mathbf{u} - \mathbf{b} \leq 0,\\
&\mathbf{u} \geq 0,\\
&(A\mathbf{u} - \mathbf{b})\mathbf{u}^T = 0,
\end{aligned}
$$

for each time step. This is a quadratic programming problem (also called a linear complementary problem) and several methods exist for its numerical solution, for instance the successive over-relaxation method as presented in [10].

The variational formulation for our problem is easily derived from the differential inequalities (4.27). Integrating over the space domain we find

$$
\begin{aligned}
\int_0^1 \big(\frac{\partial u}{\partial t} - \frac{\partial^2 u}{\partial x^2} - f\big)(v-u)dx &= \int_0^1 \frac{\partial u}{\partial t}(v-u)dx - \int_0^1 \frac{\partial^2 u}{\partial x^2}(v-u)dx - \int_0^1 f(v-u)dx = \\
&= \int_0^1 \frac{\partial u}{\partial t}(v-u)dx + \int_0^1 \frac{\partial u}{\partial x}\frac{\partial}{\partial x}(v-u)dx - \big[\frac{\partial u}{\partial x}(v-u)\big]_0^1 - \int_0^1 f(v-u)dx = \\
&= \int_0^1 \frac{\partial u}{\partial t}(v-u)dx + \int_0^1 \frac{\partial u}{\partial x}\frac{\partial}{\partial x}(v-u)dx - \int_0^1 f(v-u)dx,
\end{aligned}
$$

where we have used integration by parts and the boundary conditions of (4.27). From the last relation we find that

$$
\begin{aligned}
&\int_0^1 \frac{\partial u}{\partial t}(v-u)dx + \int_0^1 \frac{\partial u}{\partial x}\frac{\partial}{\partial x}(v-u)dx = \\
&\quad = \int_0^1 f(v-u)dx + \int_0^1 \big(\frac{\partial u}{\partial t} - \frac{\partial^2 u}{\partial x^2} - f\big)vdx - \int_0^1 \big(\frac{\partial u}{\partial t} - \frac{\partial^2 u}{\partial x^2} - f\big)udx \leq \\
&\quad \leq \int_0^1 f(v-u)dx
\end{aligned}
$$

where the test functions $v \in \mathbb{K} := \{w \in H^1((0,1)) \mid w \geq 0\}$, which is a convex subspace of $H^1(0,1)$, and the third condition of problem (4.27) has been used. Hence, problem (4.27) is equivalent to solve

$$
\left|
\begin{array}{l}
\text{Find } u \in \mathbb{K} \text{ with } u(x,0) = 0, \text{ such that}\\
(u_t, v-u) + a(u, v-u) \leq (f, v-u), \qquad \forall v \in \mathbb{K},
\end{array}
\right. \tag{4.28}
$$

where $a(u,v) := \displaystyle\int_0^1 \frac{\partial u}{\partial x}\frac{\partial v}{\partial x}dx$ and f is the introduced before. This is an obstacle problem. More information about this kind of problems can be found in [27].

Chapter 5

Moving Grid Method

5.1 Introduction

The Moving Grid Method (MGM) is one of the so-called front-tracking methods. The main idea is to adjust the grid such that at all times the same number of gridnodes are in the diffusive phase. Hence, the grid has to be updated each time step because of the motion of the interface. This method has been deeply studied in the current literature. In [28] the moving grid method is compared with a fixed domain discretization for the melting problem. In [29] it is used together with finite elements for two dimensional problems, whereas in [30] it is presented for the one dimensional problem with finite differences. Other references are [3, 5, 26, 31] for binary problems and [32, 33, 34] for multi-component problems. For more dimensional cases the topology of the grid may become worse and then remeshing may be necessary. This is done in [29] for instance.

We will use this method for solving the Stefan problem (2.10)-(2.15) with finite difference discretizations. We consider a equidistant space grid with $M + 1$ nodes as in Figure 5.1. Hence, the first grid node will be the interface between the particle and the Aluminium-matrix.

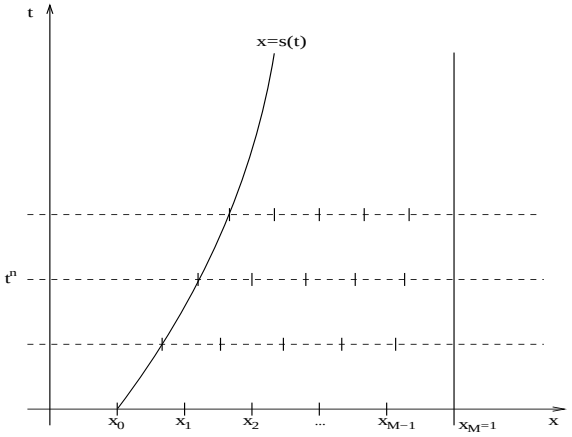

Figure 5.1: Moving grid

5.2 Numerical solution

If we discretize (2.10) with Implicit Euler in time and central differences in space we obtain

$$\frac{c_i^{n+1} - c_i^n}{\Delta t} = \frac{c_{i-1}^{n+1} - 2c_i^{n+1} + c_{i+1}^{n+1}}{(\Delta x)^2}, \tag{5.1}$$

for the nodes x_i such that $1 \leq i \leq M-1$. The problem of this discretization is that the values c_i^n should be the concentrations at time t^n but in the nodes of the grid at time t^{n+1}, or the other way around values c_i^{n+1} are the concentrations at time t^{n+1} but in the grid nodes of time t^n. Hence if we decide to apply the last discretization [30], we must interpolate the result of (5.1) to the new grid. We call this method Interpolative Moving Grid. Another way to handle this method is to consider a correction of the displacement [5, 29]. In this case we compute the time-derivative of the concentration based on the old and the new nodes, that is

$$\frac{Dc}{Dt}(x(t), t) = \frac{\partial c}{\partial t} + \frac{dx}{dt}(t)\frac{\partial c}{\partial t}, \tag{5.2}$$

where $x(t)$ denotes the position of a general node of the grid at time t, and $\frac{dx}{dt}$ the velocity of the grid. Then, considering this material derivative the diffusion equation (2.10) becomes

$$\frac{Dc}{Dt} - \frac{dx}{dt}\frac{\partial c}{\partial x} = \frac{\partial^2 c}{\partial x^2}. \tag{5.3}$$

We call this method Corrective Moving Grid. This will also be presented below. Henceforth, we will use the notation $c_i^{n+1}(x^n)$ to refer to the concentration at time t^{n+1} of the node x_i of the grid at time t^n. We must also point out that the space step Δx varies with time because of the updating of the grid. Hence, we will use $\Delta x(x^n)$ to refer to the space interval in the grid at time t^n.

Remark: There is only a slight difference between the so-called Interpolative MG and Corrective MG, because the system of equations to solve are similar but distinct. This is the reason of presenting both here.

5.2.1 Interpolative Moving Grid

We can apply two different schemes in the so-called Interpolative Moving Grid Method. The difference between them is the moment we do interpolation. That is, in the first scheme the diffusion equation is solved in the mesh at time t^n, subsequently the movement of the interface is calculated as well as the new mesh, and finally the interpolation of the concentration at time t^{n+1} is done. However, an alternative scheme arises if we first calculate the movement of the interface and therefore the mesh at time t^{n+1} with the concentration at time t^n, subsequently we interpolate the concentration at time t^n to the mesh nodes at time t^{n+1} and finally we solve the diffusion equation with the interpolated concentration values. Next, we are going to present both schemes in detail.

Scheme 1

Let us assume that we know the concentration and the grid at time t^n. Then, the concentration at time t^{n+1} but in the grid x^n is given by the diffusion equation (2.10), which is discretized using Implicit Euler for time and central differences for space, yielding

$$\frac{c_i^{n+1}(x^n) - c_i^n(x^n)}{\Delta t} = \frac{c_{i-1}^{n+1}(x^n) - 2c_i^{n+1}(x^n) + c_{i+1}^{n+1}(x^n)}{\left(\Delta x(x^n)\right)^2}, \quad 1 \leq i \leq M-1. \tag{5.4}$$

Further, the Neumann condition (2.14) is discretized by

$$\frac{c_M^{n+1}(x^n) - c_{M-1}^{n+1}(x^n)}{\Delta x(x^n)} = 0. \tag{5.5}$$

Finally, the interface condition (2.13) establishes that

$$c_0^{n+1}(x^n) = \frac{c_{sol}}{c_{part}}. \tag{5.6}$$

The system of equations formed by (5.4)-(5.6) can be expressed in a compact form as $\mathbf{A}\mathbf{c}^{n+1}(x^n) = \mathbf{b}$, where $\mathbf{A}$ is a strictly diagonal dominant matrix given by

$$\begin{pmatrix} 1 & 0 & 0 & \cdots & 0 \\ -\alpha & 1+2\alpha & -\alpha & \cdots & 0 \\ \vdots & \ddots & \ddots & \ddots & \vdots \\ 0 & \cdots & -\alpha & 1+2\alpha & -\alpha \\ 0 & \cdots & 0 & -1 & 1 \end{pmatrix},$$

where $\alpha = \dfrac{\Delta t}{\left(\Delta x(x^n)\right)^2}$ and the vector $\mathbf{b}$ is

$$\begin{pmatrix} \frac{c_{sol}}{c_{part}} \\ c_1^n(x^n) \\ \vdots \\ c_{M-1}^n(x^n) \\ 0 \end{pmatrix}.$$

The solution of this system of equations can be done by an iterative method (Gauss Jacobi, SOR) or by direct solution using the LU decomposition. Tridiagonal Thomas solver is another possibility. Once we have solved this system, next we calculate the position of the interface at time t^{n+1} using (2.15)

$$s^{n+1} = s^n + \lambda \Delta t \frac{c_2^{n+1}(x^n) - \frac{c_{sol}}{c_{part}}}{\Delta x(x^n)}, \tag{5.7}$$

and with it the grid at time t^{n+1}

$$x_i(x^{n+1}) = s^{n+1} + i\Delta x(x^{n+1}), \tag{5.8}$$

where $\Delta x(x^{n+1}) = \dfrac{1 - s^{n+1}}{M}$. Hence, the remainder is to interpolate the concentration at the new grid. It is done by Taylor expansion:

$$c_i^{n+1}(x^{n+1}) = c_i^{n+1}(x^n) + \frac{c_{i+1}^{n+1}(x^n) - c_{i-1}^{n+1}(x^n)}{2\Delta x(x^n)}\left(x_i^{n+1} - x_i^n\right), \quad 1 \le i \le M-1, \tag{5.9}$$

where the term $\dfrac{c_{i+1}^{n+1}(x^n) - c_{i-1}^{n+1}(x^n)}{2\Delta x(x^n)}$ is used to approximate the spatial derivative of the concentration in the node of interest. $c_0^{n+1}(x^{n+1}) = \dfrac{c_{sol}}{c_{part}}$ because of (2.13) and $c_M^{n+1}(x^{n+1}) = c_M^{n+1}(x^n)$ since the last node does not change its position, interpolation is not necessary.

We must note that equation (5.7) underestimates the velocity of the interface. We can correct this drawback introducing a ghost point inside the particle domain, on the left of the node x_0. Then the concentration at this ghost point will be ruled by the diffusion equation applied on the interface

$$0 = \frac{c_0^{n+1}(x^n) - c_0^n(x^n)}{\Delta t} = \frac{c_{-1}^{n+1}(x^n) - 2c_0^{n+1}(x^n) + c_1^1(x^n)}{\left(\Delta x(x^n)\right)^2},$$

and using (5.6) we obtain the concentration at the ghost point

$$c_{-1}^{n+1}(x^n) = 2\frac{c_{sol}}{c_{part}} - c_1^{n+1}(x^n).$$

Hence, using central differences in (2.15) we obtain

$$\frac{s^{n+1} - s^n}{\Delta t} = \lambda \frac{\frac{c_{sol}}{c_{part}} - c_{-1}^{n+1}(x^n)}{2\Delta x(x^n)} = \lambda \frac{c_1^{n+1}(x^n) - \frac{c_{sol}}{c_{part}}}{2\Delta x(x^n)},$$

which overestimates the velocity of the interface, but however this last estimation is more accurate ($\mathcal{O}((\Delta x(x^n))^2)$) than the previous one (5.7) ($\mathcal{O}(\Delta x(x^n))$), see [30].

Scheme 2

Let assume $c^n(x^n)$ the concentration at time t^n in the nodes of the grid distribution at time t^n known. Then we can approximate the position of the interface at time t^{n+1} by

$$s^{n+1} = s^n + \lambda \Delta t \frac{c_1^n(x^n) - \frac{c_{sol}}{c_{part}}}{2\Delta x(x^n)},$$

where we have used the ghost point procedure to approximate the partial derivative with respect to x of the concentration at the interface. The grid distribution at time t^{n+1} is obtained as explained in the above scheme and therefore not repeated here. Once that we know the grid $x(t^{n+1})$ at time t^{n+1} we can interpolate the concentration to these nodes as we did for Scheme 1:

$$c_i^n(x^{n+1}) = c_i^n(x^n) + \frac{c_{i+1}^n(x^n) - c_{i-1}^n(x^n)}{2\Delta x(x^n)}\left(x_i^{n+1} - x_i^n\right), \quad 1 \le i \le M-1, \tag{5.10}$$

$c_0^n(x^{n+1}) = \frac{c_{sol}}{c_{part}}$ and $c_M^n(x^{n+1}) = c_M^n(x^n)$ as we explained before. After that, we have to solve diffusion equation (2.10) in the new grid x^{n+1}. If we use Implicit Euler in time and central differences in space to discretize (2.10) as above, we get

$$\frac{c_i^{n+1}(x^{n+1}) - c_i^n(x^{n+1})}{\Delta t} = \frac{c_{i-1}^{n+1}(x^{n+1}) - 2c_i^{n+1}(x^{n+1}) + c_{i+1}^{n+1}(x^{n+1})}{\left(\Delta x(x^{n+1})\right)^2}, \quad 1 \le i \le M-1. \tag{5.11}$$

with the boundary conditions

$$c_0^{n+1}(x^{n+1}) = \frac{c_{sol}}{c_{part}}, \tag{5.12}$$

$$\frac{c_M^{n+1}(x^{n+1}) - c_{M-1}^{n+1}(x^{n+1})}{\Delta x(x^{n+1})} = 0. \tag{5.13}$$

The result is a linear system of equations, which matrix is similar to the presented in Scheme 1 with the unique difference that now $\alpha = \frac{\Delta t}{\left(\Delta x(x^{n+1})\right)^2}$, and in the right hand side $\mathbf{b}$ we have to replace $c_i^n(x^n)$ for $c_i^n(x^{n+1})$ $(i = 1, \dots M-1)$.

5.2.2 Corrective Moving Grid

Let us consider the material derivative of concentration (5.3) and consider the Implicit Euler discretization in time and central differences for spatial discretization

$$\frac{c_i^{n+1}(x^{n+1}) - c_i^n(x^n)}{\Delta t} - \frac{x_i^{n+1} - x_i^n}{\Delta t}\frac{c_{i+1}^n(x^n) - c_{i-1}^n(x^n)}{2\Delta x(x^n)} = \\ = \frac{c_{i-1}^{n+1}(x^{n+1}) - 2c_i^{n+1}(x^{n+1}) + c_{i+1}^{n+1}(x^{n+1})}{\left(\Delta x(x^{n+1})\right)^2}, \tag{5.14}$$

for $i = 1, \ldots, M-1$. Note that the convective term has been discretized explicitly. The boundary conditions imply that

$$\frac{c_M^{n+1}(x^{n+1}) - c_{M-1}^{n+1}(x^{n+1})}{\Delta x(x^{n+1})} = 0, \tag{5.15}$$

$$c_0^{n+1}(x^{n+1}) = \frac{c_{sol}}{c_{part}}. \tag{5.16}$$

The main point we should note is that we need to know the interface position and the grid at time t^{n+1} before going to solve (5.14). Hence equation (2.15) has to be discretized explicitly

$$s^{n+1} = s^n + \Delta t \lambda \frac{c_1^n(x^n) - \frac{c_{sol}}{c_{part}}}{\Delta x(x^n)}, \tag{5.17}$$

otherwise we will obtain a non-linear system of equations from (5.14)-(5.16). The grid at time t^{n+1} is defined as in (5.8).

Difference between IMG and CMG

Let us consider a general node x_i inside the domain of the Aluminium matrix, that is $1 \leq i \leq M-1$, and substitute (5.9) into (5.4), then we obtain

$$\frac{c_i^{n+1}(x^{n+1}) - c_i^n(x^n)}{\Delta t} - \frac{x_i^{n+1} - x_i^n}{\Delta t}\frac{c_{i+1}^{n+1}(x^n) - c_{i-1}^{n+1}(x^n)}{2\Delta x(x^n)} = \\ = \frac{c_{i-1}^{n+1}(x^n) - 2c_i^{n+1}(x^n) + c_{i+1}^{n+1}(x^n)}{\left(\Delta x(x^n)\right)^2}. \tag{5.18}$$

In we compare (5.18) with (5.14) we realize that the left hand side coincides, but however the right hand side is not the same. The difference is that the concentration is considered in different nodes (i.e. the nodes of the grid at time t^n in (5.18) and the nodes of the grid at time t^{n+1} in (5.14)), hence the resulting system of equations is not the same and not the same solutions should be expected although the difference is small. However, this difference disappears if we use Scheme 2. If we substitute (5.10) into (5.14), then we obtain

$$\frac{c_i^{n+1}(x^{n+1}) - c_i^n(x^n)}{\Delta t} - \frac{x_i^{n+1} - x_i^n}{\Delta t}\frac{c_{i+1}^n(x^n) - c_{i-1}^n(x^n)}{2\Delta x(x^n)} = \\ = \frac{c_{i-1}^{n+1}(x^{n+1}) - 2c_i^{n+1}(x^{n+1}) + c_{i+1}^{n+1}(x^{n+1})}{\left(\Delta x(x^{n+1})\right)^2},$$

that is exactly the same formula than for the Corrective Moving Grid Method.

If we consider the applicability of the moving grid method for $2D/3D$ problems we have to consider that the grid should be generated each time step, which requires an extra cost in computational time. This might be improved generating the grid after a certain number of time steps (that is, we might think that our old grid is good enough to the new time step and then only rebuild the grid when a considerable movement of the interface has happened). Moreover, in the interpolative moving grid we have to interpolate the concentration to the new grid nodes, and this becomes especially laborious for $3D$ problems. And finally the explicit treatment of the interface obliges us to consider elaborate procedures when topological changes (such as breaking or merging of interfaces) occur, which are captured in a natural way in the implicit methods.

Chapter 6

Level Set Method

6.1 Introduction

In this Chapter we present the Level Set Method for problems with one spatial dimension. Contrary to the Moving Grid Method (MGM), the Level Set Method (LSM) uses an implicit representation for the interface, captured as the zero level set of a continuous function. The advantage of this implicit treatment for the moving interface over the explicit approach in the MGM is that topological changes (such as merging or breaking of interfaces) are handled in a simple way. Moreover, the LSM is readily implemented for both two and three spatial dimensions. However, a drawback of LSM is that there may be a considerable loss of mass.

In the current literature we can find much information about the level set method. As far as we know the paper by Osher and Sethian [35] presents the first study about LSM. Since then, this method has been applied to numerous problems. The book of Sethian [36] gives an introduction to LSM, both from theoretical and numerical point of view, which together with [37] give efficient computational techniques for building approximate solutions. In [38] the LSM for solving Stefan problems is presented, for a solidification problem. In [39] the reinitialization process for the level set function is introduced. The problem of not conserving mass has recently been removed with the aid of massless marker particles, dealt in [40]. Another technique is the so-called Mass-Conserving Level-Set Method (MCLSM) of van der Pijl, Segal and Vuik [41] where the level set function is corrected each time step to achieve mass conservation.

In the present paper finite difference schemes are used to discretize the differential equations. Finite elements can also be used for LSM, for more information we refer to [36, 42, 43]. One problem that arises when we use the level set method is that the so-called transport-equations (i.e. hyperbolic equations) appear. Working numerically with these equations is always delicate. The books of LeVeque [44, 45] are good compilations of different techniques for numerical solution of these problems. High order numerical schemes can also be found in [36, 44, 46].

6.2 Description of the method

In the present paper we describe the Level Set Method for the non-dimensional formulation of the diffusion process described by (2.10)-(2.15). The main idea of this method is to introduce a new function that parameterizes the domain, and such that it captures the interface as its zero level set. Hereafter in this chapter, this function will be called the level set function, and is denoted by ϕ. Hence, the interface can be represented as

$$\Gamma(t) = \{\ x \in [0,1] \mid \phi(x,t) = 0\}. \tag{6.1}$$

Initially, ϕ is set equal to the signed distance function from the interface, such that ϕ is positive inside the particle and negative outside,

$$\phi(x,0) = \begin{cases} +d & \text{if } 0 \leq x < s(0) \\ 0 & \text{if } x = s(0) \\ -d & \text{if } s(0) < x \leq 1 \end{cases}, \tag{6.2}$$

where d is the distance from the interface to the point x (that is, $d = |x - s(0)|$). In order to satisfy the condition (6.1) we have to move the zero level set of ϕ exactly as the interface moves. In general, for the points at the interface we should have

$$\phi(s(t),t) = 0, \quad \forall t \geq 0. \tag{6.3}$$

If we take the total time derivative in the last equation we find

$$\phi_t(s(t),t) + \frac{ds}{dt}(t)\phi_x(s(t),t) = 0, \quad \forall t \geq 0, \tag{6.4}$$

where the subscripts t and x denote partial differentiation in time and space respectively. The last equation is only valid at the interface. However, using a function v that is a continuous extension of the interface velocity onto the whole domain [0,1], we extend the equation of motion for ϕ to

$$\phi_t(x,t) + v(x,t)\phi_x(x,t) = 0. \tag{6.5}$$

This equation describes the time evolution of the level set function ϕ in such a way that the zero level set of ϕ is always identified with the moving interface. In the next section we will deal with a continuous extension of the velocity v.

6.2.1 Extension of the velocity off the interface

The front velocity is given in equation (2.15). We cannot extend this equation onto the whole domain because the concentration is not continuous at the interface position. However, this drawback is easily overcome if we consider the advection equation

$$v_{\tau_{ext}} + S(\phi\phi_x)v_x = 0, \tag{6.6}$$

where S denotes the sign function and τ_{ext} is a fictitious time, with the boundary condition

$$v(x_I,0) = \frac{ds}{dt}(t), \tag{6.7}$$

where x_I is used for denoting the interface position at time t, that is $x_I = s(t)$, and the right side of equation (6.7) is given by the equation (2.15). Without loss of generality we can set the velocity equal to zero initially for the whole domain gridpoints. With this equation we extend the interface velocity in the proper upwind direction, which can be seen by inspection of $S(\phi\phi_x)$ at both sides of the interface. Further, through (6.6) we do not change the value of v at the interface since the sign function is zero on the interface. This procedure has been used for more dimensional problems, in which advection equation is solved in different coordinate directions, see [26, 38]. However, in [47] the velocity is considered constant and equal to the interface velocity through lines in the normal direction starting in the interface. Another alternative might be to consider

$$v(x,t) = \frac{1}{1+|\phi(x,t)|}\frac{ds}{dt}(t),$$

which supplies an easy and computationally cheap way to extend the velocity when the velocity of the interface and the level set function are known. The drawback of this last extension is the difficulty of generalize to more dimensional problems. In the LSM it is important to move the

interface with the correct velocity and to maintain ϕ a distance function (that will be presented below). Hence, it does not seem important how the velocity is extended onto the whole domain and any of the presented methods should not present differences. Nonetheless, we choose here to use the advection equation.

6.2.2 Reinitialization of ϕ

The problem that arises, when a solution of the equation (6.4) is computed, is that the resulting level set function can cease to be an exact distance function ($||\nabla\phi|| = |\frac{\partial\phi}{\partial x}| \neq 1$) even after one time step. However, maintaining ϕ as a distance function is essential in the level set method to capture the interface position properly. One way to avoid this numerical difficulty is to reinitialize ϕ such that it remains a signed distance function at each time-step. The reinitialization of the level set function has to conserve the contour $\phi = 0$ and reset ϕ at all points close to the front. Further, it is proved that by the use of reinitialization the numerical treatment of the problem (and in particular of the mass conservation) is improved, see [39].

The most extended procedure (see [26, 36, 39, 47]) is to solve the problem

$$\begin{cases} \phi_\tau = S(\phi_0)(1 - |\nabla\phi|) \\ \phi(x,0) = \phi_0(x) \ \text{ at } \tau = 0, \end{cases}$$

where τ represents again a fictitious time, and ϕ_0 is a function whose zero level set is the interface. Solving this problem to steady state, the zero level set of the solution ϕ_{lim} is the same as that of the function ϕ_0 and moreover, away from the interface ϕ_{lim} is such as will converge to $|\nabla\phi| = 1$, i.e. it is a distance function. The more ϕ is close to a distance function, the faster the convergence to steady state is. It is observed from numerical experiments that convergence takes place in a few time-steps.

However, according to [48] the above reinitialization procedure is such that a considerable amount of mass is lost in time. This is due to the numerical approximation of the initial level set function ϕ_0, that can produce errors in the location of the interface. Hence, in the cited work the authors use the following procedure to reinitialize ϕ:

$$\begin{cases} \phi_\tau + (A_0 - A(\tau))(-P + \kappa)|\nabla\phi| = 0 \\ \phi(x,0) = \phi_0(x) \ \text{ at } \tau = 0, \end{cases}$$

where A_0 is the total mass for the initial condition $\phi_0(x)$ (before the reinitialization) and $A(\tau)$ is the mass corresponding to the level set function $\phi(x,\tau)$ during the reinitialization process. P is a positive constant, and κ is the curvature of the interface, that can be obtained from the level set function by $\kappa = \nabla \cdot \left(\frac{\nabla\phi}{|\nabla\phi|}\right)$.

6.3 Discretization

In all of our computations we take a grid in the interval $[0,1]$ of size Δx. The total number of gridpoints will be $M+1$ where $M = 1/\Delta x$. The time step for this discretization is Δt. We will use the notation c_i^n, ϕ_i^n and v_i^n to denote the concentration, level set function and velocity in the gridpoint $x_i = (i-1)\Delta x$ at time $t^n = n\Delta t$, where $i = 1, \ldots, M+1$.

6.3.1 Discretization of the diffusion equation

We solve equation (2.10) together with (2.12) to update the concentration at the next time. Therefore, the first thing we have to do is to determine the position of the interface with respect to the gridpoints. That is, to determine the two nodes x_j and x_{j+1} such that $x_j \leq s(t^{n+1}) < x_{j+1}$, see Figure 6.1. This is easy to determine by analyzing the sign of the function ϕ in the corresponding

time t^{n+1}.

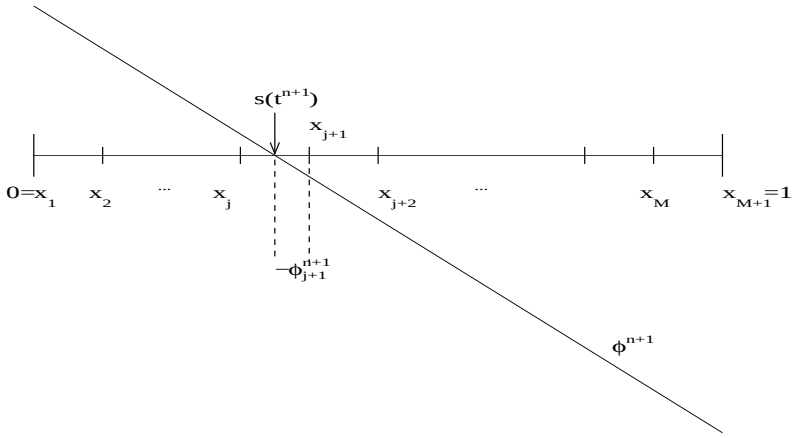

Figure 6.1: Grid and level set function at time t^n

Once we have found these nodes we have $c_i^{n+1} = 1$ for $i = 1, \ldots, j$, and for the rest of the gridnodes we solve the diffusion equation (2.10). This has to be done by taking care of the points near the interface.

For the time discretization we will use the implicit Euler scheme, and for space discretizations away from the interface (that is, for $i \geq j + 2$) we use a central difference scheme, that is

$$\frac{c_i^{n+1} - c_i^n}{\Delta t} = \frac{c_{i-1}^{n+1} - 2c_i^{n+1} + c_{i+1}^{n+1}}{(\Delta x)^2}.$$

For the concentration in x_{j+1} we use one-side differencing for the second derivate of the concentration. We build a second degree Lagrange polynomial to represent the concentration (in the time t^{n+1}, see [38]) in the interface and in two more grid points. The standard is to use x_{j+1} and x_{j+2}, but if the distance between the interface and the gridpoint x_{j+1} is very small then we observe numerical errors in the implementation. That distance (that we denote by $r_1\Delta x$) is determined by the level set function (at time t^{n+1})

$$r_1\Delta x = |x_{j+1} - x_I| = -\phi_{j+1}^{n+1} = |\phi_{j+1}^{n+1}|.$$

We have used for the numerical experiments the criterion $r_1 < 1/3$ to say the distance $|x_I - x_{j+1}|$ is small. In the case that this distance is too small we will use the interface, x_{j+2} and x_{j+3} to build the interpolation polynomial.

Hence, if $r_1 \geq 1/3$ the polynomial used is

$$\begin{aligned} P(x) &= \frac{c_{sol}}{c_{part}} \frac{(x - x_{j+1})(x - x_{j+2})}{r_1(1 + r_1)(\Delta x)^2} - c_{j+1}^{n+1} \frac{(x - x_I)(x - x_{j+2})}{r_1(\Delta x)^2} + \\ &\quad + c_{j+2}^{n+1} \frac{(x - x_I)(x - x_{j+1})}{(1 + r_1)(\Delta x)^2}, \end{aligned} \tag{6.8}$$

otherwise we will use

$$P(x) = \frac{c_{sol}}{c_{part}}\frac{(x-x_{j+2})(x-x_{j+3})}{(1+r_1)(2+r_1)(\Delta x)^2} - c_{j+2}^{n+1}\frac{(x-x_I)(x-x_{j+3})}{(1+r_1)(\Delta x)^2} + \\ + c_{j+3}^{n+1}\frac{(x-x_I)(x-x_{j+2})}{(2+r_1)(\Delta x)^2}, \tag{6.9}$$

where in both cases x_I represents the position of the moving interface at time t^n. Then, the diffusion equation in x_{j+1} reduces to

$$\frac{c_{j+1}^{n+1}-c_{j+1}^{n}}{\Delta t} = P''(x_{j+1}). \tag{6.10}$$

For $r_1 \geq 1/3$ we obtain

$$\frac{c_{j+1}^{n+1}-c_{j+1}^{n}}{\Delta t} = \frac{c_{sol}}{c_{part}}\frac{2}{r_1(1+r_1)(\Delta x)^2} - c_{j+2}^{n+1}\frac{2}{r_1(\Delta x)^2} + \\ + c_{j+3}^{n+1}\frac{2}{(1+r_1)(\Delta x)^2},$$

and for $r_1 < 1/3$

$$\frac{c_{j+1}^{n+1}-c_{j+1}^{n}}{\Delta t} = \frac{c_{sol}}{c_{part}}\frac{2}{(1+r_1)(2+r_1)(\Delta x)^2} - c_{j+2}^{n+1}\frac{2}{(1+r_1)(\Delta x)^2} + \\ + c_{j+3}^{n+1}\frac{2}{(2+r_1)(\Delta x)^2}.$$

These equations together with the condition of no-flux through the fixed boundary (2.14), which is discretized as

$$\frac{c_{M+1}^{n+1}-c_{M}^{n+1}}{\Delta x} = 0,$$

lead to a linear system of $M+1$ equations and $M+1$ unknowns, which we can express in compact form as $\mathbf{A}\mathbf{c}^{n+1} = \mathbf{b}$, where

$$\mathbf{A} = \begin{pmatrix} 1 & & & & & & & \\ & \ddots & & & & & & \\ & & 1 & & & & & \\ & & & a_{j+1,j+1} & a_{j+1,j+2} & a_{j+1,j+3} & & \\ & & & -\alpha & 1+2\alpha & -\alpha & & \\ & & & & \ddots & \ddots & \ddots & \\ & & & & -\alpha & 1+2\alpha & -\alpha & \\ & & & & & -1 & 1 & \end{pmatrix}, \quad \mathbf{b} = \begin{pmatrix} 1 \\ \vdots \\ 1 \\ b_{j+1} \\ c_{j+2}^{n} \\ \vdots \\ c_{M}^{n} \\ 0 \end{pmatrix},$$

with $\alpha = \frac{\Delta t}{(\Delta x)^2}$, and the elements of the $j+1^{th}$ row of $\mathbf{A}$ depend on the distance r_1 as explained above, as well as b_{j+1} through (6.10). Anyway, the resultant matrix $\mathbf{A}$ is not singular and hence, the linear system of equations has a unique solution. At this point we must note some points of numerical importance. The structure of $\mathbf{A}$ is always the same, only the values in the $j+1^{th}$ row, and if the interface changes the interval $[x_j, x_{j+1})$ where it is placed into the interval $[x_{j-1}, x_j)$ then the resultant matrix $\mathbf{A}$ will be the presented here with the $j+1^{th}$ row moved up and left one position, whereas if the interval is changed into $[x_{j+1}, x_{j+2})$ then we have to move the $j+1^{th}$ row down and right. Finally, we must explain that in the dissolution case, when the interface

moves from $[x_j, x_{j+1})$ to $[x_{j-1}, x_j)$, then we must correct the concentration of the node x_j before solving the diffusion equation for the new time step because that concentration is not continuous with the distribution in the Aluminium matrix for other nodes (due to the jump in the concentration through the interface). We do this correction using the polynomial P evaluated in the node x_j.

This is an implicit scheme to approximate the concentration. It has first order of convergence in time and second order of convergence in space. Moreover, it has no problems of stability (it is unconditionally stable).

6.3.2 Discretization of the velocity extension

The velocity for the interface given by equation (2.15) is discretized using the interpolation polynomial described before

$$v_I^{n+1} = \frac{c_{part}}{c_{part} - c_{sol}} P'(x_I),$$

where v_I^{n+1} denotes the velocity of the interface at time t^{n+1}. Then, we use the advection equation (6.6) to extend this velocity onto the whole domain. We assign $v_j^{n+1} = v_I^{n+1}$ and $v_{j+1}^{n+1} = v_I^{n+1}$, and for the remainder gridpoints we use (6.6), using the zero initialization as introduced in Section 6.2.1 for the first iteration, see Figure 6.2. This leads to

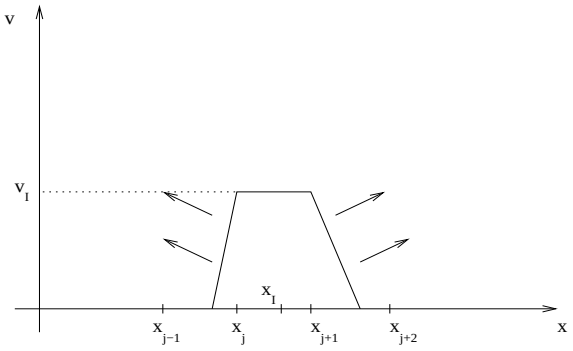

Figure 6.2: Extension of the interface velocity. The interface lies between x_j and x_{j+1}.

- From x_1 to x_{j-1}, we have $S_i(\phi\phi_x) < 0$, then we discretize (6.6) as

$$\frac{v_i^{(new)} - v_i^{(old)}}{\Delta\tau_{ext}} - \frac{v_i^{(old)} - v_{i-1}^{(old)}}{\Delta x} = 0,$$

- and from x_{j+2} to x_{M+1}, $S_i(\phi\phi_x) > 0$, then we use

$$\frac{v_i^{(new)} - v_i^{(old)}}{\Delta\tau_{ext}} + \frac{v_{i+1}^{(old)} - v_i^{(old)}}{\Delta x} = 0.$$

The idea is to use this scheme until we reach the steady state (that is, in the limit $\tau_{ext} \to \infty$). For the one dimensional problem the solution is therefore the constant velocity (the interface velocity). However, for more space dimensions the result is not constant but a smooth function. Note that in more space dimensions the advection is applied in more directions, as it is shown in [26] and [38]. Since reaching the steady state exactly is impossible a stopping criterion should be used. One can be to interrupt the time stepping if

$$\sum_{i=1}^{M+1} |v_i^{(new)} - v_i^{(old)}| < TOL,$$

where the tolerance TOL is a given parameter, for instance 10^{-6}, and the superscripts (new) and (old) denote the velocity at consecutive time-steps in the integration in the fictitious time.

This is a first order convergent scheme (both in time and space), and the CFL condition requires that $\frac{\Delta\tau_{ext}}{\Delta x} \leq 1$ to preserve stability.

6.3.3 Discretization of updating of the level set function

Equation (6.5) for the level set function is a non-linear wave equation with a non-constant speed. Hence, we can use the discretization

$$\frac{\phi_i^{n+1} - \phi_i^n}{\Delta t} + \left(\max(v_i^n, 0) D_i^- \phi^n + \min(v_i^n, 0) D_i^+ \phi^n \right) = 0,$$

where

$$D_i^- \phi^n = \frac{\phi_i^n - \phi_{i-1}^n}{\Delta x},$$

$$D_i^+ \phi^n = \frac{\phi_{i+1}^n - \phi_i^n}{\Delta x}.$$

With this scheme we use the proper upwind direction for the discretization of the space derivative. When $v_i^n < 0$ then the solution propagates through the characteristics with negative slope, then we use the forward scheme. However, when $v_i^n > 0$, then the solution spreads through the characteristics with positive slope and the backward scheme is used.

Since it is an explicit scheme, we have to impose the CFL condition to hold on stability, that is we should impose $\frac{\Delta t}{\Delta x} \max |v(x,t)| \leq 1$. This scheme is first order convergence in time and space. However, we can get higher order space schemes using ENO constructions (described in [44]), and higher order time schemes through Runge-Kutta (described in [36]) or TVD-Runge-Kutta (described in [46]) for time discretizations. For more information about Runge-Kutta schemes, total variation diminishing solution (TVD) and TVD-Runge-Kutta schemes we refer to [44] and [49].

6.3.4 Discretization of the reinitialization of ϕ

The auxiliary equation we use to correct the values of the level set function ϕ

$$\phi_\tau = S(\phi_0)(1 - |\phi_x|), \tag{6.11}$$

could present numerical difficulties. To avoid them we change the sharp sign function S by a more smooth function S_ϵ given by

$$S_\epsilon(\phi_0) = \frac{\phi_0}{\sqrt{\phi_0^2 + \epsilon^2}},$$

where ϵ is a parameter properly chosen for smoothing purposes when ϕ_0 is close to zero. To discretize (6.11) we follow the work presented in [39], the idea is to transform equation (6.11) into a general form of the wave equation and then use a proper scheme.

Putting in order the terms of (6.11) we find

$$\phi_\tau + S_\epsilon(\phi_0)|\phi_x| = S_\epsilon(\phi_0),$$

or equivalently

$$\phi_\tau + S_\epsilon(\phi_0)\frac{\phi_x}{|\phi_x|}\phi_x = S_\epsilon(\phi_0), \tag{6.12}$$

that is a case of non-linear wave equation again. We note that this equation can also be written as $\phi_\tau + S_\epsilon(\phi_0)[\sqrt{\phi^2}]_x = S_\epsilon(\phi_0)$. Equation (6.12) falls into the class of the so-called Hamilton-Jacobi equations. We will show that the equation can be written as a hyperbolic conservation law. Then, we propose for equation (6.12) a discretization in conservative form, e.g. a Finite Volume style discretization.

Hyperbolic conservation laws

Let us assume that we have a general Hamilton-Jacobi equation

$$U_\tau + G(U_x) = 0,$$

for a certain function U. Assuming that U has continuous second order cross-derivatives (then $U_{x\tau} = U_{\tau x}$), we can write this equation as a hyperbolic conservation law

$$u_\tau + \big[G(u)\big]_x = 0,$$

only by defining $u := U_x$ and by differentiating with respect to x. Moreover, integration of the last equation over the domain $[a, b]$ leads to

$$\frac{d}{d\tau}\int_a^b u(x,\tau)dx = G(u(a,\tau)) - G(u(b,\tau)).$$

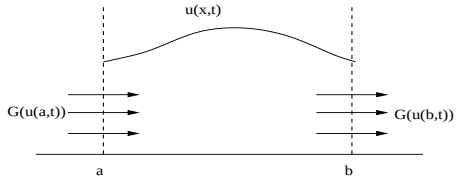

Figure 6.3: Flux G of u into the interval $[a, b]$.

This is a conservation condition for u. This says that the change of u between a and b is equal to the difference of the fluxes $G(u)$ on the boundaries of the interval, see Figure 6.3. Then, a scheme is said in conservation form if there exists a numerical flux function $g(u_{i-1}, u_i), g(u_i, u_{i+1})$ that approximates $G(u_{i-1/2}), G(u_{i+1/2})$ such that

$$\frac{u_i^{n+1} - u_i^n}{\Delta\tau} = -\frac{G(u_{i+1/2}^n) - G(u_{i-1/2}^n)}{\Delta x} \approx -\frac{g(u_i^n, u_{i+1}^n) - g(u_{i-1}^n, u_i^n)}{\Delta x}.$$

Implicitly, the last condition is subject to the consistence requirement $g(u, u) = G(u)$. When $G(u) = \sqrt{u^2}$ Sethian [36] introduces the scheme given by

$$g_{LS}(u_1, u_2) = \big[\max(u_1, 0)^2 + \min(u_2, 0)^2\big]^{1/2},$$

that is what we apply for equation (6.12). Then, we have

$$\frac{\phi_i^{n+1}-\phi_i^n}{\Delta\tau}+\max(S_\epsilon(\phi_i^0),0)\sqrt{\max(D_i^-\phi^n,0)^2+\min(D_i^+\phi^n,0)^2}$$
$$+\min(S_\epsilon(\phi_i^0),0)\sqrt{\max(D_i^+\phi^n,0)^2+\min(D_i^-\phi^n,0)^2}=S_\epsilon(\phi_i^0).$$

This is a first order scheme both in time and space. The order of convergence can be increased using higher order schemes. In most of the existing literature ENO schemes are used to improve the accuracy. The stability of this scheme is characterized by the CFL condition $\frac{\Delta\tau}{\Delta x}\leq 1$.

As we have said in the introduction of the reinitialization process, we are interested in the steady state of this equation. Therefore we have to choose a stopping criterion for this procedure. The simplest one is stopping the loop when $1-|\phi_x^N|$ is small enough for all the grid points. However, this can take a long time and new calculations for the spatial derivative of ϕ. Since it is important to keep ϕ as a distance function (only) in the vicinity of the interface, then we can relax the last criterion by considering only the interface neighboring nodes. Exactly, we only use that ϕ is a distance function when we construct the interpolation polynomial P, and we only use the distance between the interface and the next node (in the right side) x_{j+1}. Hence it might be enough to maintain ϕ a distance function for this node. This is also used in [39] although with another motivation, since there a smoothing of the interface region has been used in that paper.

Chapter 7

Phase Field Method

The Phase Field method is an implicit method that uses a parameter called phase field function to characterize the domain. The Phase Field method does not consider a sharp interface. That means that an interface region of given thickness ε is considered, where the phase transitions occur. However, the interface between phases is captured as a certain level set of the phase field function. In the limit as the interface thickness ε approaches zero, a sharp interface is obtained. The Phase Field method has been deeply studied in the literature. We refer to [50, 51, 52, 53, 54, 55, 56]. The main idea in the Phase Field method is to couple the governing equation of the physical problem (in our case the heat equation) with a certain equation obtained from a Helmholtz free energy functional of the phase field function.

One of the drawbacks of the Phase Field method is the appearance of new parameters which are difficult to control. These parameters depend on the free energy functional chosen (compare for instance [51] or [54] with [53]) and have to be related with the macroscopic properties of the problem. Moreover, comparing the Phase Field method with the classical Stefan problem requires an asymptotic analysis in which the limit in some parameters has to be done in a particular way, as [57] shows.

7.1 The phase field model

The phase field method is based on the use of a function ϕ with values in $[-1, 1]$ that characterizes the domain. For instance, conside a certain domain where solidification takes place. We will have an interface separating the solid and the liquid region. In this case the phase field function is

$$\phi(x,t) = \begin{cases} 1 & \text{if } x \text{ is in the liquid region at time } t \\ 0 & \text{if } x \text{ is on the interface at time } t \\ -1 & \text{if } x \text{ is in the solid region at time } t \end{cases},$$

with $-1 < \phi < 1$ in the interfacial region, and two coupled partial differential equations that describe the evolution of the system are

$$\begin{cases} \alpha\xi^2 \dfrac{\partial \phi}{\partial t} = -\dfrac{\delta \mathcal{F}}{\delta \phi}, \\ \dfrac{\partial u}{\partial t} + \dfrac{L}{2}\dfrac{\partial \phi}{\partial t} = K\Delta u, \end{cases} \tag{7.1}$$

where ξ is a parameter of the model that is related with the width of the interfacial region as we will see further, α is a relaxation time for the model, K and L are the diffusivity and latent heat of the problem studied. $\mathcal{F}$ denotes a free energy functional that is built as a function of ϕ as well as the thermodynamical variables of the problem, in this case the temperature u. Further, $\frac{\delta \mathcal{F}}{\delta \phi}$ denotes the variational derivative of $\mathcal{F}$ with respect to ϕ. The kinetic equation for ϕ is achieved

imposing that $\mathcal{F}$ decreases in time.

There exist many models for this functional in the literature, although the most used are the Caginalp potential and the Kobayashi potential, which are specifically compared in [53]. In both cases the free energy functional can be expressed as

$$\mathcal{F}(\phi, u) = \int_\Omega \big[\frac{1}{2}\xi^2(\nabla\phi)^2 + f(\phi, u)\big]\, dx,$$

where the function f is called free energy density and establishes the differences between models. For the Caginalp potential

$$f(\phi, u) = \frac{1}{8a}(\phi^2 - 1)^2 - 2u\phi, \tag{7.2}$$

that consists of a double well-potential, measured by a parameter a, and a term coupling ϕ and u. From the physical background of the problem we know that there are two stable states: the liquid state and the solid state. Hence, the function should reflect this property and have two local minimum for $\phi = \pm 1$ and therefore the parameter a must be chosen such that

$$\frac{\partial f}{\partial \phi} = \frac{1}{2a}(\phi^3 - \phi) - 2u,$$

has three distinct roots as near as possible of $\phi = 0, \pm 1$. Hence, a has to be small. The third root near to zero is demanded because the interfacial region corresponds to the transitional states between two equilibrium estates.

The Kobayashi potential is a fourth-degree polynomial with two fixed minima at $\phi = \pm 1$ given by the integral

$$f(\phi, u) = W \int_{-1}^{\phi} (1 - p)(1 + p)(\beta(u) - p)dp, \tag{7.3}$$

where W is a constant and β is a monotonic increasing function of the temperature such that $|\beta(u)| < 1$ and $\beta(0) = 0$. There are different choices for β, as for instance in [52] where a linear expression for it is used.

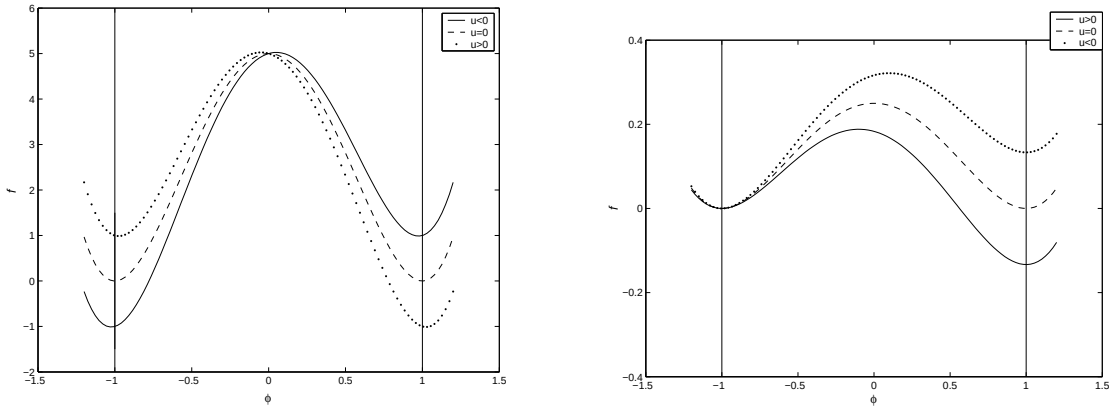

(a) Caginalp free energy density

(b) Kobayashi free energy density

Figure 7.1: Different free energy densities for the phase field model

In Figure 7.1(a) we can see the Caginalp potential and in Figure 7.1(b) the Kobayashi potential for different temperature values. In both cases we can observe that for temperatures below zero the stable state corresponds to $\phi = -1$ (that is, solid state), for temperatures above zero the stable state corresponds to $\phi = 1$ (liquid state) and for zero temperature either $\phi = -1$ and $\phi = 1$ are stable states (that is, solid and liquid states are stable). The main difference between this two potentials comes from their construction: the Kobayashi potential has two minima for $\phi = \pm 1$. However the Caginalp potential has also two minima, but they do not correspond exactly with the values $\phi = \pm 1$. This is due to the parameter a. Nonetheless, these values are close to the expected, and the smaller a is, the closer values to ± 1 we got.

Other thermodynamically-consistent forms for the free energy functional $\mathcal{F}$ as well as phase field models like equations (7.1) have been investigated in [58].

In [59] the existence and uniqueness of solution for the system (7.1) (using the Caginalp potential) under rather general conditions is proved. In [55] existence and uniqueness of solution for an anisotropic phase-field model is also studied. In the present paper, the Caginalp potential is considered, hence this model will be described in more detail, and the model parameters and asymptotic analysis will be considered. The width of the interfacial region ε is given in this case by

$$\varepsilon = \xi \alpha^{1/2},$$

and the governing equations are

$$\begin{cases} \alpha \xi^2 \dfrac{\partial \phi}{\partial t} = \xi^2 \dfrac{\partial^2 \phi}{\partial x^2} - \dfrac{1}{2a}\left(\phi^3 - \phi\right) + 2u, \\ \dfrac{\partial u}{\partial t} + \dfrac{L}{2}\dfrac{\partial \phi}{\partial t} = K \dfrac{\partial^2 u}{\partial x^2}, \end{cases} \tag{7.4}$$

where we have reduced the equations to the one dimensional problem because of the numerical solution of this will be presented below.

7.2 Asymptotic analysis

The main idea of the asymptotic analysis of the phase field equations is to build two extensions (the outer extension, that will show the properties of the solution of the phase field equations far away from the interface, and the inner extension, in which the behavior of the solution near the interface is obtained) that are coupled by some matching conditions that will be presented below.

It has to be pointed out that Caginalp in [57] established the asymptotic limit of the phase field equations to the various kinds of Stefan problems. Hence, in the present paper only a summary of the procedure is presented.

We only consider the limit to a classical Stefan problem. Hence, as in [57], the limit in the parameters α, ξ and a will be taken such that α is fixed, $a, \xi \to 0$ and $\xi a^{-1/2} = \varepsilon a^{-1} \to 0$. There is a certain flexibility in the selection of the parameters ξ and a, hence we could let $c_0^2 = \xi / a$, that is a positive number, and make $\xi \to 0$. Under these conditions Caginalp [57] found that the phase field model is equivalent to the Stefan problem

$$\left|\begin{array}{l} \dfrac{\partial u}{\partial t} = K\dfrac{\partial^2 u}{\partial x^2}, \\ L\dfrac{ds}{dt}(t) = K\big(\dfrac{\partial u}{\partial x}(s(t),t)|_{x\uparrow s(t)} - \dfrac{\partial u}{\partial x}(s(t),t)|_{x\downarrow s(t)}\big), \\ u(s(t),t) = 0. \end{array}\right. \tag{7.5}$$

7.2.1 Outer extension

Multiplying the phase field equation of (7.4) by ξ and defining $\bar{\epsilon}^2 = \xi$, we rewrite the system as

$$\begin{cases} \alpha\bar{\epsilon}^6\dfrac{\partial\phi}{\partial t} = \bar{\epsilon}^6\dfrac{\partial^2\phi}{\partial x^2} - \dfrac{c_0^2}{2}\big(\phi^3-\phi\big) + 2\bar{\epsilon}^2 u, \\ \dfrac{\partial u}{\partial t} + \dfrac{L}{2}\dfrac{\partial\phi}{\partial t} = K\dfrac{\partial^2 u}{\partial x^2}. \end{cases} \tag{7.6}$$

On the other hand, we can expand the variables in the original coordinates as

$$u(x,t;\bar{\epsilon}) = u_0(x,t) + \bar{\epsilon}u_1(x,t) + \bar{\epsilon}^2u_2(x,t) + \dots \quad , \tag{7.7}$$

$$\phi(x,t;\bar{\epsilon}) = \phi_0(x,t) + \bar{\epsilon}\phi_1(x,t) + \bar{\epsilon}^2\phi_2(x,t) + \dots \quad . \tag{7.8}$$

Introducing them in (7.6) and equaling terms of the powers of $\bar{\epsilon}$ we find

- $\mathcal{O}(1)$:

$$\begin{cases} -\dfrac{c_0^2}{2}\big(\phi_0^3-\phi_0\big) = 0, \\ \dfrac{\partial u_0}{\partial t} + \dfrac{L}{2}\dfrac{\partial\phi_0}{\partial t} = K\dfrac{\partial^2 u_0}{\partial x^2}, \end{cases}$$

  where the first equation has solutions ±1 and 0, and hence the second equation reduces to the heat equation. This means that far from the interface region (i.e. in the solid or liquid region) the solution of (7.4) is ruled by the heat equation.

7.2.2 Inner expansion

Now we consider the function $r(x,t)$ that measures the signed distance (positive in the direction of positive ϕ) from the interface of the point x at time t, that is, if we denote by $s(t)$ the position of the interface at time t and assume that initially the liquid was on the right of the interface, it follows $r(x,t) = x - s(t)$. With the help of this function we define the 'stretched out' variable

$$z = \frac{r(x,t)}{\bar{\epsilon}^3} = \frac{x-s(t)}{\bar{\epsilon}^3}, \tag{7.9}$$

and the new variables

$$\bar{u}(z,t;\bar{\epsilon}) = u(x,t;\bar{\epsilon}), \tag{7.10}$$

$$\bar{\phi}(z,t;\bar{\epsilon}) = \phi(x,t;\bar{\epsilon}). \tag{7.11}$$

Then, the system (7.6) is transformed into

$$\begin{cases} \alpha\bar{\epsilon}^6\dfrac{\partial\bar{\phi}}{\partial t} - \alpha\bar{\epsilon}^3 s'\dfrac{\partial\bar{\phi}}{\partial z} = \dfrac{\partial^2\bar{\phi}}{\partial z^2} - \dfrac{c_0^2}{2}\bar{\phi}(\bar{\phi}^2-1) + 2\bar{\epsilon}^2 u, \\ \bar{\epsilon}^6(\dfrac{\partial\bar{u}}{\partial t} + \dfrac{L}{2}\dfrac{\partial\bar{\phi}}{\partial t}) - \bar{\epsilon}^3 s'(\dfrac{\partial\bar{u}}{\partial z} + \dfrac{L}{2}\dfrac{\partial\bar{\phi}}{\partial z}) = K\dfrac{\partial^2\bar{u}}{\partial z^2}, \end{cases} \tag{7.12}$$

where s' denotes the derivative of the interface position, that is the interface velocity. Repeating the previous procedure we use the expansions

$$\bar{u}(z,t;\bar{\epsilon}) = \bar{u}_0(z,t) + \bar{\epsilon}\bar{u}_1(z,t) + \bar{\epsilon}^2\bar{u}_2(z,t) + \cdots \quad , \tag{7.13}$$

$$\bar{\phi}(z,t;\bar{\epsilon}) = \bar{\phi}_0(z,t) + \bar{\epsilon}\bar{\phi}_1(z,t) + \bar{\epsilon}^2\bar{\phi}_2(z,t) + \cdots \quad , \tag{7.14}$$

from where we find the systems:

- $\mathcal{O}(1)$:

$$\begin{cases} \dfrac{\partial^2\bar{\phi}_0}{\partial z^2} - \dfrac{c_0^2}{2}\bar{\phi}_0(\bar{\phi}_0^2-1) = 0, \\ K\dfrac{\partial^2\bar{u}_0}{\partial z^2} = 0. \end{cases}$$

  From the second equation it follows that $\bar{u}_0 = a(t)z + b(t)$ is a linear function, but by the matching conditions (which will be explained below) we find that $a(t) = 0$, therefore $\bar{u}_0(z,t) = b(t)$. For the first equation we have to point out that $\bar{\phi}_0(0,t) = 0$ because of the definition of the phase field function ϕ. We know that with this last condition and the corresponding matching $\lim_{z\to\pm\infty}\phi(z,t) = \pm 1$ conditions there exist a unique solution that is

$$\bar{\phi}_0(z,t) = \tanh(\frac{c_0}{2}z).$$

The idea is to repeat this procedure for all powers of $\bar{\epsilon}$ and to extract properties of the solution of the phase field equations near (and likewise far away with the outer expansion) the interface. To get the latent heat equation (the Stefan condition for the solidification problem) we have to analyze the $\mathcal{O}(\bar{\epsilon}^3)$ system since the term $\frac{L}{2}s'$ term arises as an $\bar{\epsilon}^3$ in the system (7.12). It is done in [57], hence we do not enter into detail and refer to [57] for more detail.

7.2.3 Matching conditions for layer of thickness $\bar{\epsilon}^3$

We will use the phase field function to explain the procedure. So it is suitable to remember the outer expansion (7.8) and the inner expansion (7.14) of this function. We also consider the next expansion of the function $s(t)$

$$s(t;\bar{\epsilon}) = s_0(t) + \bar{\epsilon}s_1(t) + \bar{\epsilon}^2 s_2(t) + \cdots \quad . \tag{7.15}$$

Then, using (7.9) and (7.15)we find the next relation

$$\begin{aligned} \bar{\phi}(z,t;\bar{\epsilon}) &= \phi(x,t;\bar{\epsilon}) = \phi(s(t;\bar{\epsilon}) + \bar{\epsilon}^3 z, t;\bar{\epsilon}) = \\ &= \phi(s_0(t) + \bar{\epsilon}s_1(t) + \bar{\epsilon}^2 s_2(t) + \cdots + \bar{\epsilon}^3 z, t;\bar{\epsilon}) \ . \end{aligned}$$

Here we can use the Taylor expansion of ϕ in the neighborhood of $s_0(t) + \bar{\epsilon}^3 z$ to get

$$
\begin{aligned}
&\phi(s_0(t)+\bar{\epsilon}s_1(t)+\bar{\epsilon}^2 s_2(t)+\cdots+\bar{\epsilon}^3 z,t;\bar{\epsilon}) = \\
&= \phi_0(s_0(t)+\bar{\epsilon}s_1(t)+\bar{\epsilon}^2 s_2(t)+\cdots+\bar{\epsilon}^3 z,t) + \\
&+\bar{\epsilon}\phi_1(s_0(t)+\bar{\epsilon}s_1(t)+\bar{\epsilon}^2 s_2(t)+\cdots+\bar{\epsilon}^3 z,t)+\cdots \\
&= \phi_0(s_0(t)+\bar{\epsilon}^3 z,t) + \big(\bar{\epsilon}s_1(t)+\bar{\epsilon}^2 s_2(t)+\dots\big)\frac{\partial\phi_0}{\partial x}(s_0(t)+\bar{\epsilon}^3 z,t) + \\
&+\frac{(\bar{\epsilon}s_1(t)+\bar{\epsilon}^2 s_2(t)+\dots)^2}{2!}\frac{\partial^2\phi_0}{\partial x^2}(s_0(t)+\bar{\epsilon}^3 z,t)+\cdots \\
&+\bar{\epsilon}\Big[\phi_1(s_0(t)+\bar{\epsilon}^3 z) + \big(\bar{\epsilon}s_1(t)+\bar{\epsilon}^2 s_2(t)+\dots\big)\frac{\partial\phi_1}{\partial x}(s_0(t)+\bar{\epsilon}^3 z) + \\
&+\frac{\big(\bar{\epsilon}s_1(t)+\bar{\epsilon}^2 s_2(t)+\dots\big)^2}{2!}\frac{\partial^2\phi_1}{\partial x^2}(s_0(t)+\bar{\epsilon}^3 z)+\cdots\Big]+\cdots\ . \qquad (7.16)
\end{aligned}
$$

The matching conditions are found by taking the limit $z \to \pm\infty$ and $\bar{\epsilon} \to \pm 0$ on the powers of $\bar{\epsilon}$ terms in equations (7.14) and (7.16) respectively. For instance:

- $\mathcal{O}(1)$:

$$\lim_{z\to\pm\infty} \bar{\phi}_0(z,t) = \lim_{\bar{\epsilon}\to\pm 0} \phi_0(s_0(t)+\bar{\epsilon}^3 z,t),$$

- $\mathcal{O}(\bar{\epsilon})$:

$$\lim_{z\to\pm\infty} \bar{\phi}_1(z,t) = \lim_{\bar{\epsilon}\to\pm 0} \big[s_1(t)\frac{\partial\phi_0}{\partial x}(s_0(t)+\bar{\epsilon}^3 z,t) + \phi_1(s_0(t)+\bar{\epsilon}^3 z,t)\big],$$

and so on.

7.3 Numerical solution

The system of equations (7.4) can be solved by various procedures. In [60], [54] and [31] finite difference schemes are considered for the corresponding phase field equations. We also considered this kind of scheme, using a coarse mesh for the temperature and a fine mesh for the phase field parameter. However, this was quickly abandoned because of its lack of accuracy for our problem, although in the referred articles suitable results have been found. Another option is to use adaptive methods, in which the mesh is updated at each iteration (as in [61]) or after a certain number of iterations (as in [62]).

7.3.1 Moving mesh method

As we introduced before, the phase field function will vary between -1 and 1, being almost constant away from the interface, and with a steep gradient in the vicinity of the interface. In such a case, efficient numerical procedures should incorporate some form of mesh adaptation. In [63] a moving finite difference method has been presented and in [64] and [65] a moving finite element method has been introduced. In both cases the mesh updating was obtained by an equidistribution principle (EP). This is also the case of [61]. Some other references are [66], [62] and [67] (the last two for higher dimensions).

In [68] different types of partial differential equations for defining moving meshes through equidistribution principles are presented. Since this approach is different to the one used in the numerical computations (but however related with the one that we will use) we give a brief summary of it here.

In our numerical approach we chose a monitor function $M(x,t) > 0$ that provides a measure of the computational error in the solution of the physical PDE, and we apply a Equidistribution Principle (EP)

$$\int_0^{x_i(t)} M(\tilde{x},t)d\tilde{x} = \frac{i}{N}\theta(t), \tag{7.17}$$

where $N+1$ is the total number of grid nodes, $x_i(t)$ denotes the position of the i^{th} grid node at time t (with $i = 0,\ldots,N$) and

$$\theta(t) = \int_0^1 M(\tilde{x},t)d\tilde{x}, \tag{7.18}$$

where we choose a domain of computation $x \in [0,1]$. Since in the integral formula (7.17) the grid speed does not appear, it is named Quasi-Static EP (QSEP). In [68] Moving Mesh Partial Differential Equations (MMPDEs) are derived from (7.17), which are equivalent to (7.17), and subsequently a relation between the mesh velocity and the monitor function is established. Next, we will see some examples of these MMPDEs, and for more detail we refer to [68], especially pages 712 to 718. We denote by ζ the computational coordinate and $x = x(\zeta,t)$ the physical coordinate. Further, if $f = f(x,t)$ we denote $\dfrac{\partial f}{\partial \zeta} = \dfrac{\partial f}{\partial x}\dfrac{\partial x}{\partial \zeta}$ and $\dot{f} = \dfrac{df}{dt} = \dfrac{\partial f}{\partial x}\dfrac{\partial x}{\partial t} + \dfrac{\partial f}{\partial t}$.

1. MMPDEs constructed by time differentiation of QSEPs: this kind of PDEs are obtained by differentiation of equation (7.17) with respect to time and the coordinate ζ subsequently, as for instance

$$\frac{\partial}{\partial x}\big(M\dot{x}\big) + \frac{\partial M}{\partial t} = \frac{M\dot{\theta}(t)}{\theta(t)}.$$

2. MMPDEs involving a correction term: in this case the idea is imposing that the mesh satisfies the QSEP at a latter time $t+\tau$ $(0 < \tau \ll 1)$ instead of at t. Then, it yields to

$$\frac{\partial}{\partial \zeta}\Big(M\frac{\partial \dot{x}}{\partial \zeta}\Big) + \frac{\partial}{\partial \zeta}\Big(\frac{\partial M}{\partial \zeta}\dot{x}\Big) = -\frac{\partial}{\partial \zeta}\Big(\frac{\partial M}{\partial t}\frac{\partial x}{\partial \zeta}\Big) - \frac{1}{\tau}\frac{\partial}{\partial \zeta}\Big(M\frac{\partial x}{\partial \zeta}\Big).$$

3. MMPDEs based on attraction and repulsion pseudoforces: it is said that a node attracts others when a measure of the truncation error at this point is larger than average. If the measure is smaller than the average, then the neighboring nodes are repelled.

$$\dot{x} = \frac{1}{\tau}\frac{\partial}{\partial \zeta}\big(M\frac{\partial x}{\partial \zeta}\big),$$

where τ is a positive constant. If one assumes that $M\frac{\partial x}{\partial \zeta}$ is an error indicator, then the last equation moves the nodes where the error is large.

In [68] an analysis for the behavior of the meshes obtained by different MMEDPs was also presented. However, we have chosen to use the EP (7.17) directly since due to the nature of our problem we will only have monotonic movement of the interface, and hence the EP will not produce crossing meshes. This is also done in [69].

7.3.2 Equidistribution of the mesh

In our numerical computation we have chosen to use an EP over a monitor function. We also can consider the equation

$$\int_{x_i(t)}^{x_{i+1}(t)} M(\tilde{x},t)d\tilde{x} = \frac{1}{N}\int_0^1 M(\tilde{x},t)d\tilde{x}, \tag{7.19}$$

which is equivalent to (7.17). The quality of the adaptive grid depends on the monitor function used. Hence, we present some choices for M which are appropriate to our problem.

- The scaled solution arc length

$$M(x,t) = \sqrt{1+\sigma\frac{\partial\phi}{\partial x}^2},$$

  where $\sigma > 0$ is a parameter chosen by the user. The time dependence of M is due to the implicit time dependence of ϕ. This was used in [66]. However, this monitor function is not integrable as an elementary function and hence the equidistribution principle (7.17) or (7.19) has to be approximated by a quadrature rule.

Discretization of the EP can be avoided if the monitor function is analytically integrable. Moreover, if the monitor function is chosen carefully then the resulting grid will be smooth automatically. On the other hand, we would like to have a monitor function that is tailored by the profile of the phase field

$$\bar{\phi}_0(x,t) = \tanh\big(\frac{x-s(t)}{2\varepsilon}\big),$$

that is the zeroth-order term in the inner expansion of the phase field (see section 7.2). Taking this into account, we can advise the next monitor functions

1. $M(x,t) = \operatorname{sech}^2\big(\frac{x-s(t)}{2\varepsilon}\big)$.
2. $M(x,t) = \gamma\beta + \operatorname{sech}\big(\frac{x-s(t)}{2\varepsilon}\big)$, $\gamma > 0$ is a parameter chosen by the user and $\beta = \beta(t) = \int_0^1 \operatorname{sech}\big(\frac{x-s(t)}{2\varepsilon}\big)dx$.

To see more examples of adequate monitor functions and more detail about these introduced here we refer to [69]. In our numerical study we have used the last monitor function. Hence, we present this here with some detail. The EP (7.17) yields the equation

$$\gamma\beta x_i(t) + 2\varepsilon\Big[\sin^{-1}\big(\tanh(\frac{x_i(t)-s(t)}{2\varepsilon})\big) - \sin^{-1}\big(\tanh(\frac{-s(t)}{2\varepsilon})\big)\Big] = \frac{i\beta(\gamma+1)}{N}, \tag{7.20}$$

for $i = 0,\ldots,N$. We must note that the parameter γ should be such that the grid nodes $x_0(t) = 0$ and $x_N(t) = 1$ for all time t. Since the monitor function is a continuous function of the interface position $s(t)$, therefore, the mesh generated by equation (7.20) will also be continuous as a function of the interface position. The term $\gamma\beta$ in the monitor function is needed to avoid that the monitor function clusters all the grid points within the interfacial region, which would be inappropriate. The parameter γ also allows some flexibility in the number of grid nodes placed within the interfacial region. In this case we have approximately $\frac{\gamma N}{1+\gamma}$ nodes inside the interfacial region and approximately $\frac{N}{1+\gamma}$ outside. In our experiments we have chosen $\gamma = 1$ that allows high resolution in the interface and also sufficient nodes away from the interface.

In Figure 7.2(a) we can observe the monitor function for different positions of the interface: the left curve corresponds with a position of the interface 0.2, the central curve with 0.4 and the right curve with 0.6. For the same positions of the interface we can see in Figure 7.2(b) the nodes distribution (–o– for the position of the interface 0.2,–□– for 0.4 and –x– for 0.6).

7.3.3 Discretizing the equations

Before treating the discretizations in more detail, it is convenient to transform system (7.4) into the Lagrangian form

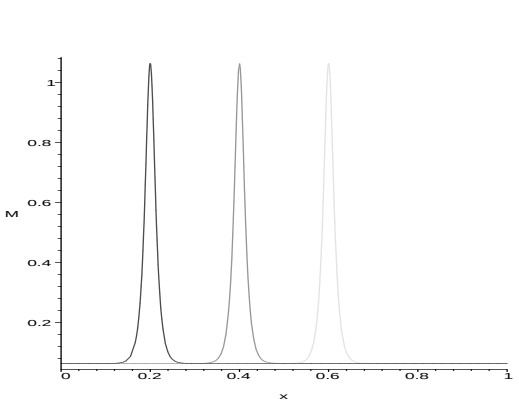

(a) Monitor function for different positions of the interface for $\gamma = 1$

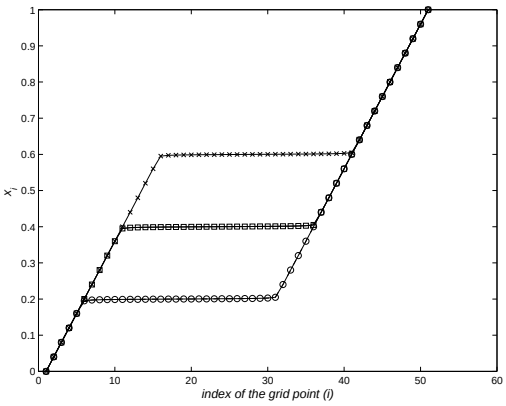

(b) Mesh distribution for different positions of the interface

Figure 7.2: Mesh and monitor function as a function of the interface position

$$\begin{cases} \alpha\xi^2\Big(\dfrac{\partial\phi}{\partial t} - \dfrac{dx}{dt}\dfrac{\partial\phi}{\partial x}\Big) = \xi^2\dfrac{\partial^2\phi}{\partial x^2} - \dfrac{1}{2a}\big(\phi^3 - \phi\big) + 2u, \\ \dfrac{\partial u}{\partial t} - \dfrac{dx}{dt}\dfrac{\partial u}{\partial x} + \dfrac{L}{2}\Big(\dfrac{\partial\phi}{\partial t} - \dfrac{dx}{dt}\dfrac{\partial\phi}{\partial x}\Big) = K\dfrac{\partial^2 u}{\partial x^2}, \end{cases} \tag{7.21}$$

where $\frac{dx}{dt}$ denotes the velocity of the mesh. The numerical approach for system (7.21) consists on the decoupling of the equations. First, the phase field is solved using the temperature values at the previous time, and subsequently the equation of the temperature is solved using the phase field values calculated just before.

In this subsection we will present the discretization of the equations (7.21) as introduced before. We denote by $\mathbf{u}^n = (u_0^1, \ldots, u_N^n)^T$, $\boldsymbol{\phi}^n = (\phi_0^1, \ldots, \phi_N^n)^T$, $\mathbf{x}^n = (x_0^1, \ldots, x_N^n)^T$ the values of the temperature, phase field and grid nodes distribution at time t^n, $\Delta t^n = t^n - t^{n-1}$, and $h_i^n = x_i^n - x_{i-1}^n$ for $i = 1, \ldots, N$, where N denotes the number of space intervals we are going to use. At this moment we present an adaptive time stepping technique, and we will see some sufficient conditions on Δt^n for ensuring the existence of the solution of the resulting systems of equations. However we have seen in practice that this condition is too restrictive, and that larger values for Δt^n are allowed without stability problems. The semi-implicit discretization that we use is

$$\begin{aligned} &\alpha\xi^2\Big(\frac{\phi_i^{n+1} - \phi_i^n}{\Delta t^{n+1}} - \frac{x_i^{n+1} - x_i^n}{\Delta t^{n+1}}\frac{\phi_{i+1}^n - \phi_{i-1}^n}{h_{i+1}^n + h_i^n}\Big) = \\ &= \frac{2\xi^2}{h_{i+1}^{n+1} + h_i^{n+1}}\Big(\frac{\phi_{i+1}^{n+1} - \phi_i^{n+1}}{h_{i+1}^{n+1}} - \frac{\phi_i^{n+1} - \phi_{i-1}^{n+1}}{h_i^{n+1}}\Big) - \frac{1}{2a}\big[\big(\phi_i^{n+1}\big)^3 - \phi_i^{n+1}\big] + 2u_i^n, \end{aligned} \tag{7.22}$$

$$\begin{aligned} &\frac{u_i^{n+1} - u_i^n}{\Delta t^{n+1}} - \frac{x_i^{n+1} - x_i^n}{\Delta t^{n+1}}\frac{u_{i+1}^n - u_{i-1}^n}{h_{i+1}^n + h_i^n} + \frac{L}{2}\Big(\frac{\phi_i^{n+1} - \phi_i^n}{\Delta t^{n+1}} - \frac{x_i^{n+1} - x_i^n}{\Delta t^{n+1}}\frac{\phi_{i+1}^n - \phi_{i-1}^n}{h_{i+1}^n + h_i^n}\Big) = \\ &= \frac{2K}{h_{i+1}^{n+1} + h_i^{n+1}}\Big(\frac{u_{i+1}^{n+1} - u_i^{n+1}}{h_{i+1}^{n+1}} - \frac{u_i^{n+1} - u_{i-1}^{n+1}}{h_i^{n+1}}\Big). \end{aligned} \tag{7.23}$$

Note that the convection-like terms in both equations are discretized by explicit central differences, whereas the rest are treated implicitly.

System for the phase field

The discretization (7.22) may be written in a compact form by the following non-linear system of equations

$$\begin{pmatrix} 1 & 0 & 0 & \cdots & 0 \\ -b_1 & a_1 & -c_1 & \cdots & 0 \\ \vdots & \ddots & \ddots & \ddots & \vdots \\ 0 & \cdots & -b_{N-1} & a_{N-1} & -c_{N-1} \\ 0 & \cdots & 0 & 0 & 1 \end{pmatrix} \begin{pmatrix} \phi_0^{n+1} \\ \phi_1^{n+1} \\ \vdots \\ \phi_{N-1}^{n+1} \\ \phi_N^{n+1} \end{pmatrix} + \frac{1}{2a} \begin{pmatrix} 0 \\ \left(\phi_1^{n+1}\right)^3 \\ \vdots \\ \left(\phi_{N-1}^{n+1}\right)^3 \\ 0 \end{pmatrix} = \begin{pmatrix} -1 \\ g_1 \\ \vdots \\ g_{N-1} \\ 1 \end{pmatrix}, \tag{7.24}$$

where Dirichlet boundary conditions have been used for the extreme grid nodes (which correspond to the subscripts 0 and N), and

$$a_i = \frac{\alpha\xi^2}{\Delta t^{n+1}} + \frac{2\xi^2}{h_{i+1}^{n+1} h_i^{n+1}} - \frac{1}{2a},$$

$$b_i = \frac{2\xi^2}{h_{i+1}^{n+1} + h_i^{n+1}} \frac{1}{h_i^{n+1}},$$

$$c_i = \frac{2\xi^2}{h_{i+1}^{n+1} + h_i^{n+1}} \frac{1}{h_{i+1}^{n+1}},$$

and finally

$$g_i = \frac{\alpha\xi^2}{\Delta t^{n+1}} \phi_i^n + \alpha\xi^2 \frac{x_i^{n+1} - x_i^n}{\Delta t^{n+1}} \frac{\phi_{i+1}^n - \phi_{i-1}^n}{h_{i+1}^n + h_i^n} + 2u_i^n,$$

for $i = 1, \ldots, N$. Finally, we remark under which conditions the system (7.24) has a unique solution. If we write the last system as

$$A\boldsymbol{\phi}^{n+1} + \mathbf{f}(\boldsymbol{\phi}^{n+1}) = \mathbf{g}, \tag{7.25}$$

Theorem 13.1.3 of [70] (page 434) proves that if the matrix A is an M-matrix and $\tilde{\mathbf{f}} : \mathbb{R}^n \to \mathbb{R}^n$ given by $\tilde{\mathbf{f}}(\boldsymbol{\phi}^{n+1}) = \mathbf{f}(\boldsymbol{\phi}^{n+1}) - \mathbf{g}$ is a continuous, diagonal and isotone mapping then the system (7.25) has a unique solution. The mapping $\tilde{\mathbf{f}}$ is obviously continuous and isotone (isotone means that $\tilde{\mathbf{f}}(\mathbf{x}) \geq \tilde{\mathbf{f}}(\mathbf{y})$ if $\mathbf{x} \geq \mathbf{y}$, i.e. $x_i \geq y_i$ for all $i = 1 \ldots n$, and it is true because the function $h(x) = x^3$ is monotonously increasing). That the mapping $\tilde{\mathbf{f}}$ is diagonal means that $\tilde{f}_i$ only depends on the i^{th} component of $\boldsymbol{\phi}^{n+1}$, and that is also the case. Therefore, the unique problem that remains to show is that A is an M-matrix. We have that the off-diagonal terms of A are negative. Hence, if A is strictly diagonal dominant it follows that A is an M-matrix and hence existence and uniqueness of solution for (7.25). Imposing the strictly dominance to A gives a condition on the time stepping as follows:

$$\begin{aligned} a_i > |b_i| + |c_i| \iff & \frac{\alpha\xi^2}{\Delta t^{n+1}} + \frac{2\xi^2}{h_{i+1}^{n+1} h_i^{n+1}} - \frac{1}{2a} > \frac{2\xi^2}{h_{i+1}^{n+1} h_i^{n+1}} \iff \\ & \iff \frac{\alpha\xi^2}{\Delta t^{n+1}} - \frac{1}{2a} > 0 \iff \Delta t^{n+1} < 2\alpha\varepsilon^2 \end{aligned} \tag{7.26}$$

that allows us to use a fixed time stepping, as we have done in our experiments. In [61] the authors impose that the diagonal terms of A are positive (which is a weaker condition than we use, but

that also ensures that A is an M-matrix). This yields the criterium

$$\Delta t^{n+1} < \min\left\{ \frac{2\alpha\varepsilon^2 h_i^{n+1} h_{i+1}^{n+1}}{h_i^{n+1} h_{i+1}^{n+1} - 4\varepsilon^2} \mid i = 1 \dots N-1, \quad h_i^{n+1} h_{i+1}^{n+1} - 4\varepsilon^2 > 0 \right\}. \tag{7.27}$$

The numerical computations have shown that the difference between (7.26) and (7.27) is around a factor 10 in favor of (7.27) (that is, the time step given by (7.27) is approximately 10 times the one given by (7.26)), but both are prohibitive small for numerical use. It has been also verified by the numerical simulations that larger time steps do not produce instabilities or a wrong solution for the system (7.25).

System for the temperature equation

On the other hand, the discretization (7.23) leads to the following system of equations:

$$\begin{pmatrix} 1 & 0 & 0 & \cdots & 0 \\ -e_1 & d_1 & -f_1 & \cdots & 0 \\ \vdots & \ddots & \ddots & \ddots & \vdots \\ 0 & \cdots & -e_{N-1} & d_{N-1} & -f_{N-1} \\ 0 & \cdots & 0 & 0 & 1 \end{pmatrix} \begin{pmatrix} u_0^{n+1} \\ u_1^{n+1} \\ \vdots \\ u_{N-1}^{n+1} \\ u_N^{n+1} \end{pmatrix} = \begin{pmatrix} h_0 \\ h_1 \\ \vdots \\ h_{N-1} \\ h_N \end{pmatrix}, \tag{7.28}$$

where Dirichlet conditions have been prescribed in the boundary nodes, and

$$d_i = 1 + \frac{2K\Delta t^{n+1}}{h_i^{n+1} h_{i+1}^{n+1}},$$

$$e_i = \frac{2K\Delta t^{n+1}}{(h_i^{n+1} + h_{i+1}^{n+1}) h_i^{n+1}},$$

$$f_i = \frac{2K\Delta t^{n+1}}{(h_i^{n+1} + h_{i+1}^{n+1}) h_{i+1}^{n+1}},$$

$$h_i = u_i^n + \left(x_i^{n+1} - x_i^n\right) \frac{u_{i+1}^n - u_{i-1}^n}{h_{i+1}^n + h_i^n} - \frac{L}{2}\left[\phi_i^{n+1} - \phi_i^n - \left(x_i^{n+1} - x_i^n\right) \frac{\phi_{i+1}^n - \phi_{i-1}^n}{h_{i+1}^n + h_i^n}\right],$$

for $i = 1, \dots, N-1$ (where equation (7.23) has been multiplied by Δt^{n+1}), and h_0, h_N are the corresponding values for the temperature in the boundary nodes. These depend on the problem we want to solve. To see an example we refer to [61].

We can write (7.28) in a more compact form: $B\mathbf{u}^{n+1} = \mathbf{h}$. Then, we can observe that the off-diagonal elements of B are negative, and the diagonal elements of B are positive. Further, B is diagonally dominant. Therefore B is an M-matrix, B^{-1} exists and then the last system of equations has a unique solution.

7.4 The complete algorithm

In this section we present the algorithm to solve the system of equations (7.4). We use the notation used in this report. We present it as pseudo-code, hence new variables appear which are important in the programming process. In practice we will solve the nonlinear system of equations (7.25) by the Newton-Raphson procedure, hence a prescribed tolerance Tol_N will be necessary. For computing the mesh distribution (7.20) we will use the bisection method, and hence another tolerance Tol_g will be used. We will use the LU decomposition of the matrix B in the linear system of equations for the temperature to solve (7.28). We have used in our test a fixed time step Δt, as

difference of the presented in [61] where adaptive time stepping were used. Let us assume that we know all the variables at time t^n, that is, we know $\mathbf{u}^n$ the approximation of the temperature at time t^n, $\boldsymbol{\phi}^n$ the approximation of the phase field at time t^n, s^n the approximation of the interface interface position at time t^n and $\mathbf{x}^n$ the grid distribution at time t^n. Then, to approximate the solution at time t^{n+1} we follow the next algorithm.

1. Predict a position of the interface for the new time:

$$x^{(*)} = 2s^{n-1} - s^{n-2}. \tag{7.29}$$

2. Compute the mesh distribution for this position of the interface $x^{(*)}$ (solve equation (7.20)). Call it $\mathbf{x}^{(*)}$.

3. Calculate $\boldsymbol{\phi}^{(*)}$ for the last mesh distribution (using $\mathbf{u}^n$, $\mathbf{x}^n$, $\mathbf{x}^{(*)}$ and $\boldsymbol{\phi}^n$, see system (7.24)).

4. Calculate z the zero of $\boldsymbol{\phi}^{(*)}$ by linear interpolation.

   (a) If $|z - x^{(*)}| > Tol_g$ then: $x^{(*)} = z$ and go to 2.

   (b) Otherwise $\mathbf{x}^{n+1} = \mathbf{x}^{(*)}$, $s^{n+1} = z$ and $\boldsymbol{\phi}^{n+1} = \boldsymbol{\phi}^{(*)}$.

5. Calculate $\mathbf{u}^{n+1}$ with (7.28) using the data $\boldsymbol{\phi}^n$, $\boldsymbol{\phi}^{n+1}$, $\mathbf{x}^n$, $\mathbf{x}^{n+1}$ and $\mathbf{u}^n$.

Remarks:

- The prediction of the interface position established in part 1 comes from the formula used by Mackenzie and Robertson in [61]

$$x^{(*)} = s^{n-1} + \Delta t^{n+1}\Big(\frac{s^{n-1} - s^{n-2}}{\Delta t^n}\Big),$$

  if we take $\Delta t^{n+1} = \Delta t^n$.

- The initial iteration of the algorithm is given by the initial data of the problem. However (7.29) is not defined for the first time step. In that case, we take $x^{(*)}$ as the zero of $\boldsymbol{\phi}^0$ by linear interpolation.

- In our numerical experiments we have observed that accurate results are obtained if the correction of the interface (i.e. step 4a) is excluded. This means that the initial prediction of the interface position is good enough to make the phase field function computed from it accurate.

Chapter 8

Numerical experiments

In this section we present some results for the three numerical methods studied in detail in the present paper: moving grid, level set and phase field methods. We will separate this chapter into two parts. In the first part we will solve the one-phase problem corresponding to particle dissolution (i.e. growth). We call it one-phase problem because on one side of the interface the concentration is constant whereas in the other part diffusion takes place. This problem is the studied along this report. In the second part of this chapter we will present the numerical results for the two-phases problem (that is, the problem that arises when we consider the heat equation on both sides of the interface). We consider this problem because we have found some difficulties in the phase field method for the one-phase problems, but these difficulties disappear if we consider the two-phases problem. We will discuss this later in more detail. In the numerical experiments we will compare the interface movement with the known similarity solutions for each type of problem, the concentration or temperature profiles at different times and the estimation of the mass of the system for the one-phase problem.

8.1 Concentration problem

In this section we will compare the numerical results of the moving grid and level set methods for the dissolution problem in its non-dimensional formulation given by (2.10)-(2.15). The data set used in the experiments are:

- $c_{part} = 1$ the concentration inside the particle,
- $c_{sol} = 0.01$ the concentration at the interface,
- $c_0 = 0.001$ the initial concentration in the alloy,
- $s_0 = 0.1$ the initial position of the interface,

for the case of particle dissolution, and

- $c_{part} = 1$ the concentration inside the particle,
- $c_{sol} = 0.01$ the concentration at the interface,
- $c_0 = 0.05$ the initial concentration in the alloy,
- $s_0 = 0.1$ the initial position of the interface,

for the case of growth. As we mentioned above, the space domain is $[0, 1]$ and the effect of the diffusivity constant has been avoided by a change of variable.

In Figure 8.1 we present the numerical results obtained with Moving Grid Method (using the Implicit Euler scheme for time-discretization and the central differences scheme for space-discretizations) for various time-steps (dt) and grid-sizes (M). These results are compared with the similarity solution (we refer to section 2.6), and a good agreement between the numerical results and the similarity solution is observed for small values of t. This is expected since for the similarity solution an infinite domain is considered whereas for our problem the domain is finite. Another feature that can be observed for the movement of the interface is that a steady state is reached in time, that is the position of the interface becomes stable (does not change) if we allow t be large. The error of the discretization that we have used for the movement of the interface is $\mathcal{O}(\Delta t + \Delta x^2)$, therefore we have chosen time-steps and grid-sizes such that $\frac{\Delta t}{\Delta x^2} = M^2 \Delta t$ is constant to verify the convergence of the results.

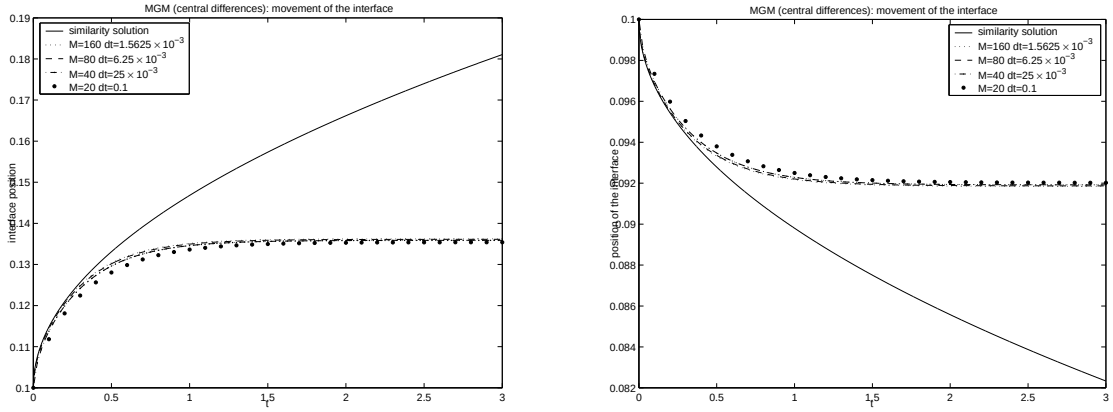

(a) Particle growth

(b) Particle dissolution

Figure 8.1: Moving Grid Method for the one-phase problem.

In Table 8.1 the computed masses with the Moving Grid Method for the various time-steps and grid-sizes used above are presented. We use the trapezoidal quadrature rule to approximate the mass of the system from the discrete concentration values. We can observe the convergence to the initial mass when we refine the time-step and the grid-size.

M	Δt	Growth	Dissolution
		0.145	0.1009
160	1.5625×10^{-3}	0.14487459	0.10092469
80	6.25×10^{-3}	0.14475315	0.10094959
40	25×10^{-3}	0.14451425	0.10099960
20	0.1	0.14404609	0.10110010

Table 8.1: Computed mass with Moving Grid Method

In Figure 8.2 the numerical results obtained with the Level Set Method are presented for various time-steps (dt) and grid-sizes (M). The interface velocity was extended onto the whole domain by advection (see chapter 6), and the upwind discretization was used for the transport equation of the level set function. Therefore, the interface position is approached with an error of $\mathcal{O}(\Delta t + \Delta x)$. We have chosen time-steps and grid-sizes such that $\frac{\Delta t}{\Delta x} = M \Delta t$ is constant for the convergence analysis. Again a good agreement with the similarity solution is observed.

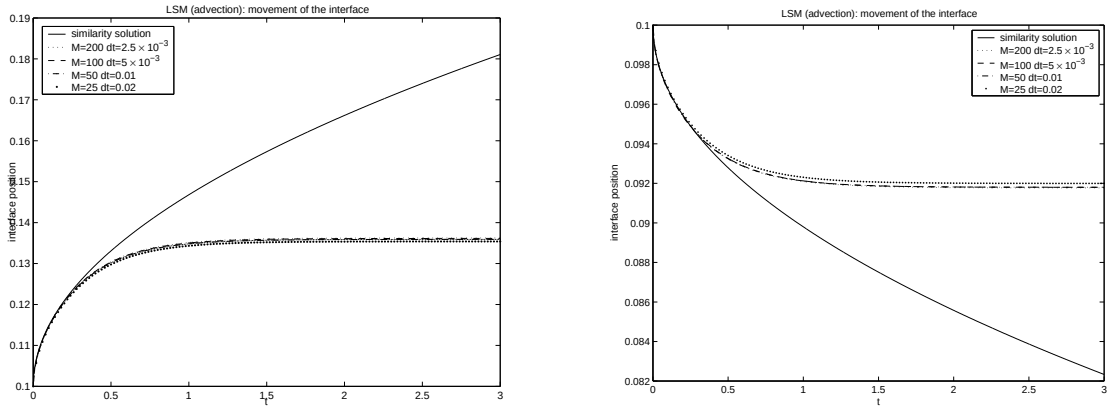

(a) Particle growth

(b) Particle dissolution

Figure 8.2: Level Set Method for the one-phase problem.

In Table 8.2 various values of the computed mass using the results of the level set method for the dissolution case are presented. The trapezoidal quadrature rule is used to approximate the mass of the system. As before, convergence to the initial value of the mass is observed. We also present the computed position of the interface for the final time $t = 3$ and the equilibrium position of the interface (that is, the position of the interface in the steady state). Convergence is also observed for the position of the interface.

M	dt	Mass	Interface position
		0.1009	0.09181818
100	0.001	0.10090310	0.09182208
80	1.25×10^{-3}	0.10090864	0.09182766
60	1.666×10^{-3}	0.10092056	0.09183968
40	2.5×10^{-3}	0.10095406	0.09187346

Table 8.2: Mass and interface position with Level Set Method for dissolution

8.2 Temperature problem

In this section we will consider a solidification problem. The governing equations of the test problem we use for the numerical experiments are

$$\frac{\partial u}{\partial t}(x,t) = \frac{\partial}{\partial x}\big[K(x,t)\frac{\partial u}{\partial x}\big](x,t), \quad 0 < x < s(t) \text{ or } s(t) < x < 1, \quad t \in [0, t_{end}],$$

$$u(x,0) = \begin{cases} u_{sol} & \text{if } 0 \le x < s(0) \\ 0 & \text{if } x = s(0) \\ u_{liq} & \text{if } s(0) < x \le 1 \end{cases},$$

$$L\frac{ds}{dt}(t) = K_{sol}\frac{\partial u}{\partial x}(s(t),t)|_{x\uparrow s(t)} - K_{liq}\frac{\partial u}{\partial x}(s(t),t)|_{x\downarrow s(t)}, \ t \in [0, t_{end}],$$

$$\frac{\partial u}{\partial x}(x,t) = 0, \quad \text{if } x = 0, 1, \ t \in [0, t_{end}],$$

where the function K denotes the thermal diffusivity, which is constant in each phase but with different values, and L denotes the latent heat. Here we have prescribed homogeneous Neumann boundary conditions, but in some cases we will change these conditions.

First we want to show the behavior of the phase field model for the solidification problem with a continuous initial distribution of the temperature. We use the similarity solution of this problem for a semi-infinite domain $[0, \infty)$. In this case the movement of the interface is given by (see [69])

$$s(t) = \beta\sqrt{t + t_0},$$

where t_0 denotes an starting-time, and β is the solution of

$$\beta = \frac{2}{\sqrt{\pi}} e^{\frac{-\beta^2}{4}} \Big[\frac{u_{liq}}{1 - \text{erf}(\beta/2)} - \frac{u_{sol}}{\text{erf}(\beta/2)} \Big].$$

We also know the exact solution for the temperature, that is

$$u^{(s)}(x,t) = \begin{cases} u_{sol} \frac{\text{erf}(\beta/2) - \text{erf}(x/(2\sqrt{t+t_0}))}{\text{erf}(\beta/2)}, & \text{if } 0 \le x \le s(t), \\ u_{liq} \frac{\text{erf}(\beta/2) - \text{erf}(x/(2\sqrt{t+t_0}))}{1 - \text{erf}(\beta/2)}, & \text{if } x > s(t). \end{cases},$$

The data set used for this example is the same as that used by Mackenzie and Robertson [69]. That is, $t_0 = 0.15$, $u_{sol} = -0.085$, $u_{liq} = -0.015$ (we note that here u_{liq} does not correspond with the temperature of a liquid, but we have preferred to maintain the notation presented at the beginning of this section). We use as initial temperature $u(x,0) = u^{(s)}(x,0)$ and phase field function $\phi(x,0) = \tanh\left(\frac{x - s(0)}{2\epsilon}\right)$. The boundary conditions that we use for this particular problem are (see system (7.24)):

$$\phi(0,t) = -1, \quad \phi(1,t) = 1, \quad \forall t > 0,$$

$$u(0,t) = u_{sol}, \quad u(1,t) = u^{(s)}(1,t), \quad \forall t > 0.$$

We have introduced a light simplification to the work presented in [69]. In this paper the authors consider the next boundary conditions for the phase field function

$$\phi(0,t) = \min_{\phi \approx -1} f(\phi, u_{sol}),$$

$$\phi(1,t) = \min_{\phi \approx 1} f(\phi, u^{(s)}(1,t)),$$

where $\min_{\phi \approx -1} f(\phi, u)$ denotes the value of ϕ closest to -1 that gives the minimum for f. Respectively for $\min_{\phi \approx 1} f(\phi, u)$. This corresponds with the philosophy of the phase field method. The first condition says that at $x = 0$ the solid state is the equilibrium state. However, we have observed that these minima are very close to $-1, 1$ respectively, and hence we avoid the work of looking for the minima at each time step. We must remark that this numerical simplification is also related with the set of parameters of the phase field model. In particular with a, since how we have already seen the smaller a is, the closer these minima are to ± 1. In Figure 8.3(a) we present the numerical movement of the interface with the phase field method compared with the similarity solution. We also present the numerical solution if we avoid the correction of the interface position in the phase field algorithm. We can see that the differences are negligible. In Figure 8.3(b) the temperature profiles at the initial and final time $t = 1$ are presented. Again the differences between the phase field algorithm with the correction of the interface and without it are small. We have used the same parameters for the phase field method as Mackenzie and Robertson

[69]. These parameters are: $a = 0.0625$, $\xi = 0.002$ and $\alpha = 1$. Therefore $\varepsilon = \xi a^{1/2} = 0.0005$. We have chosen $N = 50$ mesh intervals, $\gamma = 1$ for the equidistribution principle and the diffusivity equal to $K = 1$ in both phases. Hereafter, we will use the phase field method avoiding the part of the correction of the interface position.

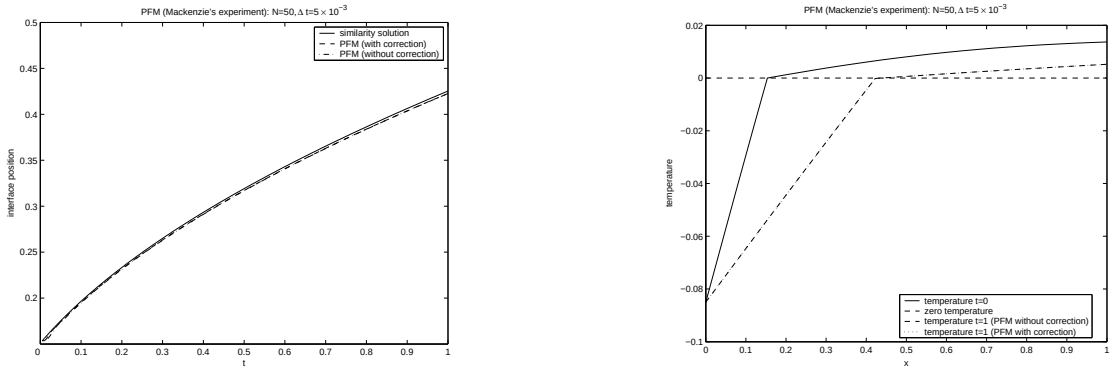

(a) Movement of the interface

(b) Temperature profiles

Figure 8.3: Solidification problem - Mackenzie's experiment with phase field method

After this first experiment we want to apply the phase field model to the particle dissolution/growth problem. We might think that our concentration problem reduces from the solidification problem with one of the diffusivity constants equals to zero (or in a first approach very small). Therefore, to simulate the one-phase problem we use one of the diffusivities (the diffusivity in the solid phase) very small $K_{sol} = 5 \times 10^{-3}$. We should remark that from the asymptotic analysis of the phase field method we need that the temperature at the interface has to be zero. Therefore, if we want to apply the phase field method to our dissolution (or growth) problem we have to shift the concentrations down to make $c(s(t), t) = 0$. Next, we consider initial temperature distributions as the initial concentrations sketched in Figures 2.4, 2.5, shifted down properly as mentioned before. This explains the *temperature* profiles that we present below (Figure 8.4(b)). In Figure 8.4 we see the results obtained with the phase field method for the case of initial distribution that in the one-phase problem would produce *growth*. We see in 8.4(a) that the computed interface movement shows agreement with the similarity solution in the early times, as we should expect. We also observe that at the very early times our phase field method produce wiggles, but they disappear fast. These instabilities can be also observed in Figure 8.3(a). We want to remark that these instabilities can be caused by the discretization used in the convective terms of the phase field equations (central differences, see section 7.3). At the present stage we are not interested on the improvement of the numerical solution but on checking the applicability of the method to our problem. Therefore, better discretizations were not considered.

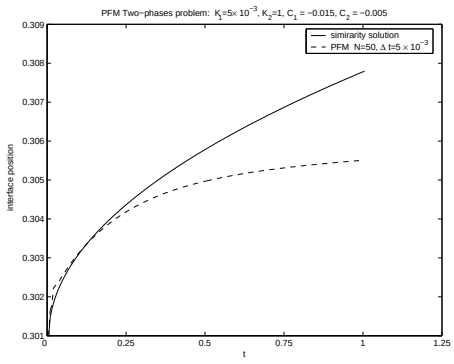

(a) Movement of the interface

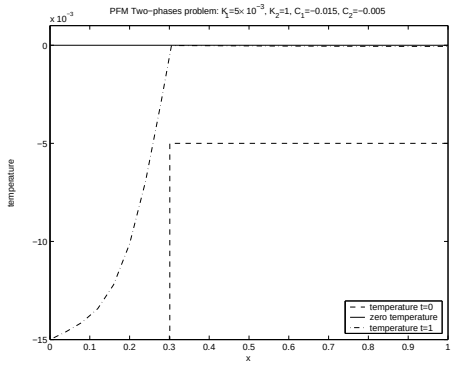

(b) Temperature profiles

Figure 8.4: Phase Field Method - Growth

The case of *particle dissolution* was also considered. First this one-phase problem is approached by the solidification problem (with $K_{sol} = 5 \times 10^{-3}$) and then the phase field method is used to solve this last problem numerically. The results are presented in Figure 8.5. The above conclusions are also valid here.

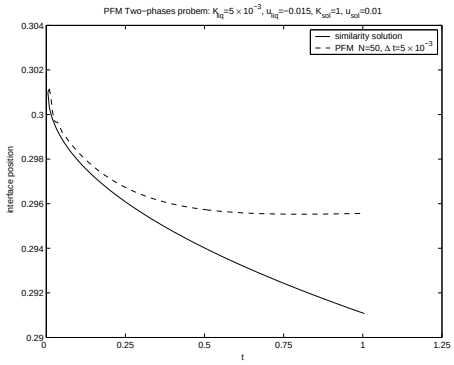

(a) Movement of the interface

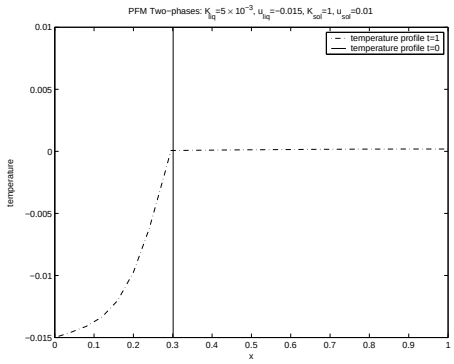

(b) Temperature profiles

Figure 8.5: Phase Field Method - Dissolution

Next, we present the numerical results obtained with Moving Grid Method, Level Set Method and Phase Field Method for the *dissolution* like problem. The final time considered is $t = 1$. The number of grid intervals are $M_{sol} = 50, M_{liq} = 200$ for the solid-phase and liquid-phase respectively for the moving grid method, $M = 100$ for the level set method and $M = 50$ for the phase field method. In Figure 8.6(a) we present the computed interface movement for each numerical method and the similarity solution. In Figure 8.6(b) we present the initial temperature and the final temperature for the moving grid, level set and phase field methods. We have to remark that the problem that we solve uses Dirichlet boundary condition on the left boundary ($u(0,t) = -0.015$) and homogeneous Neumann boundary condition on the right boundary ($\frac{\partial u}{\partial x}(1,t) = 0$). We see that all these methods are appropriate to solve the solidification problem. The differences between the numerical estimation for the movement of the interface can be due to the fact that the discretizations used for each method have distinct orders of convergence ($\mathcal{O}(\Delta t + \Delta x^2)$ for the moving grid

method, $\mathcal{O}(\Delta t + \Delta x)$ for the level set method and in the phase field method the interface position is obtained by linear interpolation of the phase field function. Also we have to remember that both moving grid methods and level set method deal with a sharp interface problem whereas the phase field method considers an interfacial region of thickness $\varepsilon = \xi a^{1/2} > 0$.

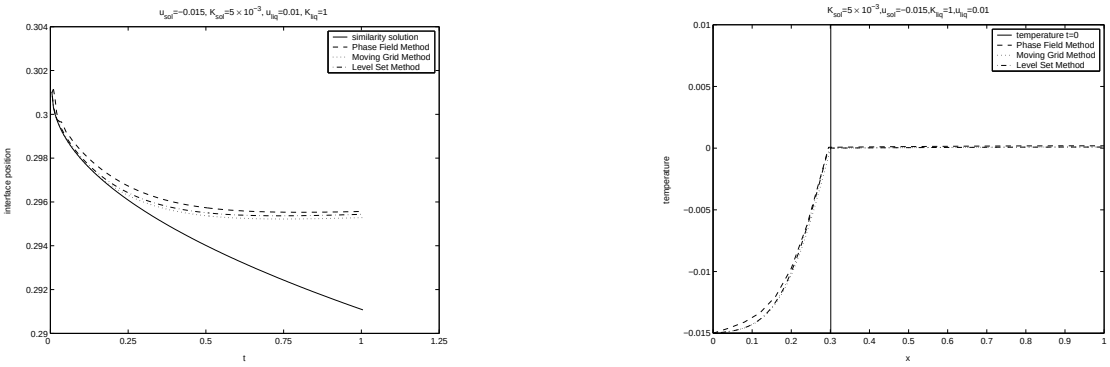

(a) Movement of the interface

(b) Temperature profiles

Figure 8.6: Dissolution problem: comparison of the methods.

Chapter 9

Conclusions

In the present work we have studied in detail various numerical methods to solve the dissolution/growth of a particle in an Aluminium alloy in one dimension. Finally, after some numerical tests we conclude the following:

- The fixed finite-difference grid method is very similar to the level set method and it is reasonable to think that the level set method approaches the interface in a more convenient way (sidebranches and fingers).
- The variable time-stepping method and the method of lines are not a good choice because its difficult applicability for higher dimensional problems.
- The front-fixing method can be generalized to higher dimensional problems with easy geometries without difficulties. However, this method is not applicable when the geometries considered are not simple (merging interfaces, fingers, ...).
- The enthalpy method is not easy to generalize to the concentration problem.
- The variational inequalities method is not applicable for problems in which the concentration on the interface is not a constant.
- The moving grid method is applicable for higher dimensional problems. The interpolation of the concentration to the new grid becomes expensive for higher dimensions. It has been already studied in detail for two-dimensional problems. Three-dimensional problems appear more difficult to work with.
- The level set method is easily generalized to higher dimensional problems. The topological changes (breaking of the interface) are handled in a easy way. It is generalized to the two-phases problem (solidification) fast, and shows convergence to the one-phase problem (that is, make one of the diffusivities to go to zero).
- The phase field model is an appropriate method for two-phases problems, but it has not been possible to reproduce for a one-phase problem. It is very sensitive to the the numerical solution method. The parameters are difficult to determine from the physical background of the problem and play an important role in the numerical solution of the problem.

Considering these conclusions we will focus in the near future on the level set method for two-dimensional problems. The Gibbs-Thomson effect will be introduced to determine the interface velocity. The existing results for this kind of problems with the moving grid method will be used to compare with level set.

Chapter 10

Appendix

10.1 Curvature

The curvature plays an important role in the physical background of the precipitate growing problem, to determine the concentration at the particle/solvent interface through the Gibbs-Thomson effect. For that reason we will give a summary about it in two and three dimensional spaces.

Curves in the 2D space

Let a plane curve be given by $\vec{r}(u)$. The tangent vector to the curve is given by

$$\vec{\tau} = \frac{\frac{d\vec{r}}{du}}{\left|\frac{d\vec{r}}{du}\right|}.$$

The curvature measures the rate at which any nonstraight curve tends to depart from its tangent, that means

$$\kappa = \left|\frac{d\phi}{ds}\right|,$$

where ϕ denotes the tangential angle and s denotes the arc length (that is the length along a curve). Using the tangent vector the curvature is given by

$$\kappa = \frac{\left|\frac{d\vec{r}}{du} \times \frac{d^2\vec{r}}{du^2}\right|}{\left|\frac{d\vec{r}}{du}\right|^3}. \tag{10.1}$$

From that point of view the curvature is always positive. But it can be defined with a sign if we take into account the orientation of the curve. That means that for a clockwise curve the curvature is always negative and for a counter clockwise curve the curvature is always positive. It is easily extended to our problem if we take positive curvature if the interface is concave toward the solute particle. Otherwise the curvature is positive. For more information about the curvature in planar curves (definition, sign and different formulas) we refer to [71], Chapter 17, and to [72], Chapter 1. However, because of its importance in the growing particle here we give some expressions. For the relation between the sign and the orientation of the curve, we refer to Figure 2.7 in Section 2.7.3.

On the planar case, for the parameterization given by $(x(u), y(u))$, the curvature κ is

$$\kappa = \frac{|x'y'' - x''y'|}{(x'^2 + y'^2)^{\frac{3}{2}}} \tag{10.2}$$

where x', x'' denote the first and the second derivate of x respectively, and the same for y', y''. If the curve is given implicitly by $g(x, y) = 0$, then the curvature is determined by

$$\kappa = \frac{g_{xx}g_y^2 - 2g_{xy}g_xg_y + g_{yy}g_x^2}{(g_x^2+g_y^2)^{\frac{3}{2}}}, \tag{10.3}$$

where the lower index denotes a partial derivate with respect to the corresponding variable. To finish, if the curve is parameterized in polar coordinates then the curvature is given by

$$\kappa = \frac{r^2 + 2r_\theta^2 - rr_{\theta\theta}}{(r^2+r_\theta^2)^{\frac{3}{2}}}. \tag{10.4}$$

Surfaces in the 3D space

For surfaces in the three dimensional space we define the mean curvature as the average of the principal curvatures κ_1, κ_2, that is

$$\kappa = \frac{1}{2}\big(\kappa_1 + \kappa_2\big) = \frac{1}{2}\tilde{\kappa} \tag{10.5}$$

where the principal curvatures are the maximum and the minimum respectively of the normal curvature. In one point P of the surface there exist a flat pencil of tangents. Each tangent determines a normal plane. The section of the surface and the normal plane determines a plane curve called normal section, and the curvature of that curve is the so called normal curvature in the tangent direction we have chosen. Therefore κ_1 is the maximum of the normal curvatures in the point P in all directions, and κ_2 is the minimum of those quantities. For more information about these concepts we refer to [71], Chapter 19, and [72], Chapter 14.

In our study of the stability we only need the value of the sum of the principal curvatures $\tilde{\kappa}$. Below we give some expressions for it. If the surface is given implicitly by $g(x,y,z) = 0$ then $\tilde{\kappa}$ is

$$\begin{aligned}\tilde{\kappa} = \frac{g_{xx}(g_y^2+g_z^2) + g_{yy}(g_x^2+g_z^2) + g_{zz}(g_x^2+g_y^2)}{(g_x^2+g_y^2+g_z^2)^{\frac{3}{2}}} - \\ - 2\frac{g_xg_yg_{xy} + g_xg_zg_{xz} + g_yg_zg_{yz}}{(g_x^2+g_y^2+g_z^2)^{\frac{3}{2}}},\end{aligned} \tag{10.6}$$

and if the surface is parameterized by $z = h(x,y)$ yields

$$\tilde{\kappa} = \frac{(1+h_y^2)h_{xx} - 2h_xh_yh_{xy} + (1+h_x^2)h_{yy}}{(1+h_x^2+h_y^2)^{\frac{3}{2}}}. \tag{10.7}$$

If the surface is in the last form but with a small deviation from the flatness (it means $z(x,y)$ is almost constant) then we can express it as $\tilde{\kappa} = -\nabla^2 h$.

10.2 Legendre equations

The Legendre polynomials are polynomial solutions to the so-called Legendre differential equation

$$(1-x^2)\frac{d^2y}{dx^2} - 2x\frac{dy}{dx} + n(n+1)y = 0, \tag{10.8}$$

where n is a non-negative integer. These solutions are polynomials of degree n and can be given in different ways, although the most used is the recurrence relation

$$\begin{gathered}P_0(x) = 1, \quad P_1(x) = x, \\ (n+1)P_{n+1}(x) - (2n+1)xP_n(x) + nP_{n-1}(x) = 0.\end{gathered}$$

The Legendre associated functions are the solutions of the Legendre associated differential equation

$$(1-x^2)\frac{d^2y}{dx^2} - 2x\frac{dy}{dx} + \big(n(n+1) - \frac{m^2}{1-x^2}\big)y = 0, \tag{10.9}$$

where m is a nonnegative integer given. If $m = 0$ it reduces to the Legendre differential equation (10.8). By direct substitution it can be shown that if y is a solution of (10.8), then the function given by

$$(1-x^2)^{m/2}\frac{d^m y}{dx^m}(x)$$

is a solution of (10.9). The function given by

$$\bar{P}_{nm}(x) = (1-x^2)^{m/2}\frac{d^m P_n}{dx^m}(x), \tag{10.10}$$

is called the associated Legendre function of degree n and order m of first kind, where $P_n(x)$ is the Legendre polynomial of degree n. As we said before it is a solution of the Legendre associated differential equation (10.9). For more information about Legendre functions we refer to [1] page 308.

10.3 Laplace equation. Spherical harmonics

We are interested in the diffusion-controlled growing process of a spherical particle in an infinite cell. The diffusion speed is assumed to be so large that a steady-state is reached instantaneously. Further, we assume the interface to move sufficiently slowly such that the influence of the interface motion on the diffusion field can be neglected. Hence if we solve the Laplace equation for an instant of time, holding fixed the domain, we get nearly the same results that for our moving boundary problem in that time. Therefore, we seek solutions of homogeneous Laplace equation:

$$\Delta c(x,y,z) = 0, \tag{10.11}$$

with appropriate boundary conditions. Because of the geometry of the problem we have spherical symmetry and therefore it seems suitable to use spherical co-ordinates, whose relation with the Cartesian co-ordinates is set up in Figure 10.1.

Using spherical co-ordinates for the Laplace equation yields

$$\frac{1}{r}\frac{\partial^2}{\partial r^2}(rc) + \frac{1}{r^2 sin\theta}\frac{\partial}{\partial\theta}\Big(sin\theta\frac{\partial c}{\partial\theta}\Big) + \frac{1}{r^2 sin^2\theta}\frac{\partial^2 c}{\partial\varphi^2} = 0, \tag{10.12}$$

where $c = c(r,\theta,\varphi)$ is the concentration as a function of the spherical co-ordinates. To solve this problem we propose to make a separation of variables. We start separating variables into radial and angular. We look for solutions in the form $c(r,\theta,\varphi) = R(r)Y(\theta,\varphi)$. Then Eq. (10.12) becomes

$$\frac{Y}{r}\frac{d^2}{dr^2}(rR) + \frac{R}{r^2 sin\theta}\frac{\partial}{\partial\theta}\Big(sin\theta\frac{\partial Y}{\partial\theta}\Big) + \frac{R}{r^2 sin^2\theta}\frac{\partial^2 Y}{\partial\varphi^2} = 0 \tag{10.13}$$

and now separating functions and variables we get

$$\frac{1}{Y}\Big[\frac{1}{sin\theta}\frac{\partial}{\partial\theta}\Big(sin\theta\frac{\partial Y}{\partial\theta}\Big) + \frac{1}{sin^2\theta}\frac{\partial^2 Y}{\partial\varphi^2}\Big] = -\lambda = -\frac{r}{R}\frac{d^2}{dr^2}(rR), \tag{10.14}$$

where λ is the so called separation constant. As a consequence of this separation the Laplace equation has been transformed into a partial differential equation and an ordinary differential equation. We will come back to the radial equation later. For the angular equation we separate

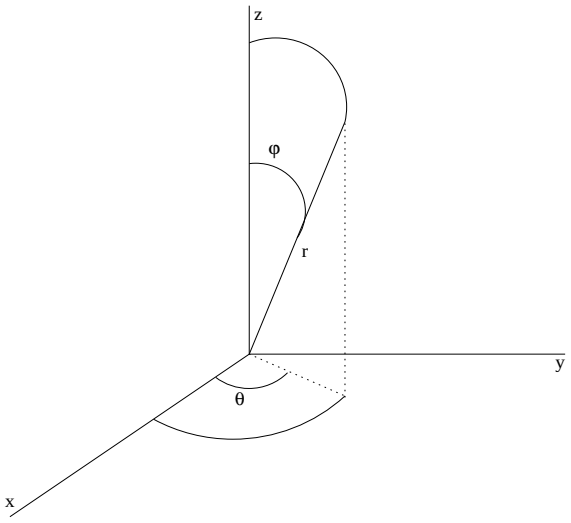

Figure 10.1: The spherical co-ordinates.

variables again and express $Y(\theta,\varphi) = P(\theta)Q(\varphi)$. If we put it into the right side of the Eq. (10.14) then we get

$$\frac{Q}{sin\theta}\frac{d}{d\theta}\Big(sin\theta\frac{dP}{d\theta}\Big) + \frac{P}{sin^2\theta}\frac{d^2Q}{d\varphi^2} = -\lambda PQ \tag{10.15}$$

and putting in order the variables and functions we get the next separation

$$\frac{sin\theta}{P(\theta)}\frac{d}{d\theta}\Big(sin\theta\frac{dP}{d\theta}\Big) + \lambda sin^2\theta = \nu = -\frac{1}{Q(\varphi)}\frac{d^2Q}{d\varphi^2} \tag{10.16}$$

where ν is the separation constant for these equations.

First we solve the equation referred to the azimuthal angle φ. We have

$$\frac{d^2Q}{d\varphi^2} + \nu Q = 0$$

with the boundary conditions $Q(\pi) = Q(-\pi)$ due to the spherical symmetry of the geometry. Analyzing all possibilities we only find non trivial solutions for the eigenvalues $\nu = m^2$ where m is an integer, and the corresponding normalized eigenfunctions are

$$Q_m(\varphi) = \frac{e^{im\varphi}}{\sqrt{2\pi}}. \tag{10.17}$$

Next, we solve the Sturm-Liouville problem associated to the angular variable θ. We have the following equation for P (deduced from (10.16) and note that we know already the possible values of ν from the solution of the equation for the angle φ)

$$\frac{d}{d\theta}\Big(sin\theta\frac{dP}{d\theta}\Big) - \frac{m^2}{sin\theta}P = -\lambda sin\theta P.$$

If we make a change of variable given by $x = cos\theta$ the last equation becomes

$$\frac{d}{dx}\Big[(1-x^2)\frac{dP}{dx}\Big] - \frac{m^2}{1-x^2}P = -\lambda P.$$

The angle $\theta \in [0,\pi)$ then $x \in (-1,1]$. This equation is the Legendre associated differential

equation, and for it the eigenvalues are $\lambda = n(n+1)$ where $n \geq m$ and the corresponding normalized and bounded (when $x \to \pm 1$) eigenfunctions are

$$P_{nm}(\theta) = \sqrt{\frac{(2n+1)(n-m)!}{2(n+m)!}} \bar{P}_{nm}(cos\theta)$$

where the functions $\bar{P}_{mn}$ are the associated Legendre functions of degree n and order m of the first kind. We can find these results in [1] page 315 together with useful information about the Legendre polynomials and the associated functions.

We call the solutions of the angular equation of Laplace equation the spherical harmonic functions, that is, the solutions of the equation

$$\frac{1}{Y}\Big[\frac{1}{sin\theta}\frac{\partial}{\partial\theta}\Big(sin\theta\frac{\partial Y}{\partial\theta}\Big) + \frac{1}{sin^2\theta}\frac{\partial^2 Y}{\partial\varphi^2}\Big] = -\lambda,$$

with $\lambda = n(n+1)$. As we have seen in this section these solutions are in the form

$$Y_{nm}(\theta,\varphi) = \sqrt{\frac{(2n+1)(n-m)!}{2(n+m)!}} \bar{P}_{nm}(cos\theta)\frac{e^{im\varphi}}{\sqrt{2\pi}},$$

where m and n are integer parameters such that $m \leq n$.

Finally, to get explicitly the solution of the Laplace equation we have to solve the radial differential equation, that comes from the left side of the Eq. (10.14), where $\lambda = n(n+1)$,

$$r\frac{d^2}{dr^2}(rR) - n(n+1)R = 0. \tag{10.18}$$

That equation has two linearly independent solutions that are r^n and $r^{-(n+1)}$. Therefore the general solution of that equation is in the form

$$R(r) = Ar^n + \frac{B}{r^{n+1}}. \tag{10.19}$$

To conclude, the explicit expression for a particular solution of the Laplace equation expressed as a function of the spherical coordinates is

$$(Ar^n + \frac{B}{r^{n+1}})\sqrt{\frac{(2n+1)(n-m)!}{2(n+m)!}} \bar{P}_{nm}(cos\theta)\frac{e^{im\varphi}}{\sqrt{2\pi}},$$

where the A and B are determined from the boundary conditions.

Bibliography

[1] D.W. Trim. *Applied partial differential equations*. P.W.S. Kent Publishing Company, Boston, 1990.

[2] C. Vuik. *The Solution of a One-Dimensional Stefan Problem*. CWI-tract 90. CWI, Amsterdam, 1993.

[3] J. Crank. *Free and moving boundary problems*. Clarendon Press, Oxford, 1984.

[4] M.H. Protter and H.F. Weinberger. *Maximum principles in differential equations*. Prenitence-Hall, Englewood Cliffs, 1967.

[5] F.J. Vermolen. *Mathematical models for particle dissolution in extrudable aluminium alloys*. PhD thesis, Delft University of Technology, The Netherlands, 1998.

[6] G.W. Evans. A note on the existence of a solution to a problem of Stefan. *Q. Appl. Math.*, 9:185–193, 1951.

[7] J. Douglas. A uniqueness theorem for the solution of a Stefan problem. *Proc. Amer. Math. Soc.*, 8:402–408, 1957.

[8] D. Kinderlehrer and G. Stampacchia. *An introduction to Variational Inequalities and Their Applications*. Academic Press., New York, 1980.

[9] C. Vuik. An L^2-error estimate for an approximation of the solution of a parabolic variational inequality. *J. Numer. Math.*, 57:453, 1990.

[10] C. Vuik and C. Cuvelier. Numerical solution of an etching problem. *J. Comp. Phys.*, 59:247–263, 1985.

[11] J.M. Hill. *One-dimensional Stefan problems: an introduction*. Longman Scientific & Technical, Harlow, 1987.

[12] Milton Abramowitz and Irene A. Stegun, editors. *Handbook of mathematical functions with formulas, graphs, and mathematical tables*. Dover Publications Inc., New York, 1992. Reprint of the 1972 edition.

[13] C. Vuik, G. Segal, and F.J. Vermolen. A conserving discretization for a Stefan problem with an interface reaction at the free boundary. *Comput. Visual Sci.*, 3:109–114, 2000.

[14] D.A. Porter and K.E. Easterling. *Phase transformations in metalls and alloys*. Chapman & Hall, London, 1992.

[15] A. Schatz. *J. Math. Anal. Appl.*, 28:569–580, 1969.

[16] F.J. Vermolen, C. Vuik, and S. van der Zwaag. Particle dissolution and cross-diffusion in multi-component alloys. *Materials Science and Engineering A*, 347:265–279, 2003.

[17] F.J. Vermolen and C. Vuik. A mathematical model for the dissolution of particles in multi-component alloys. *J. Comp. and Appl. Math.*, 126:233–254, 2000.

[18] C. Vuik F. Vermolen and S. van der Zwaag. Particle dissolution and cross-diffusion in multi-component alloys. *Materials Science and Engineering A*, 347:265–279, 2002.

[19] W.W. Mullins and R.F. Sekerka. Morphological stability of a particle growing by diffusion or heat flow. *J. Appl. Phys.*, 34:323–329, 1963.

[20] F.A. Nichols and W.W. Mullins. Surface-(interface-) and volume-diffusion contributions to morphological changes driven by capillarity. *Transactions of the Metallurgical Society of AIME*, 233:1840–1848, 1965.

[21] W. Shyy, H.S. Udaykumar, M.M. Rao, and R.W. Smith. *Computational fluid dynamics with moving boundaries*. Taylor & Francis, Bristol, 1996.

[22] R.L. Burden and J.D. Faires. *Numerical analysis*. Brooks/Cole, Australia, 2001.

[23] W.E. Schiesser. *The numerical method of lines; integration of partial differential equations*. Academic Press, San Diego, 1991.

[24] C.M. Elliot and J.R. Ockendon. *Weak and Variational Methods for Moving Boundary Problems*. Pitman Publishing inc., Marshfield, Massachusetts, 1982.

[25] R.E. White. An enthalpy formulation of the Stefan problem. *SIAM Journal on Numerical Analysis*, 19:1129–1157, 1982.

[26] W. van Til, C. Vuik, and S. van der Zwaag. An inventory of numerical methods to model solid-solid phase transformations in aluminium alloys. Report, Delft University of Technology, 2000.

[27] J.F. Rodrigues. *Obstacle Problems in Mathematical Physics*. Elsevier Science Publishers B.V., Amsterdam, 1987.

[28] W.D. Murray and F. Landis. Numerical and machine solutions of transient heat-conduction problems involving melting or freezing. *Tasnsactions of the ASME (C)*, 81:106–112, 1959.

[29] G. Segal, C. Vuik, and F. Vermolen. A conserving discretization for the free boundary in a two-dimensional Stefan problem. *Journal of Computational Physics*, 141:1–21, 1998.

[30] P. Pinson. Aluminium alloys: Moving boundary problems - Practical study. Technical report, INSA GMM - Delft University of Technology, Delft University of Technology, 2001.

[31] W. van Til, C. Vuik, and S. van der Zwaag. A mathematical model of the morphological changes in aluminium extrusion alloys during homogenization. Report, Delft University of Technology, 2001.

[32] C. Vuik and F. Vermolen. A mathematical model for the dissolution of particles in multi-component alloys. Technical report, Delft University of Technology, Delft University of Technology, 1999.

[33] F. Vermolen, C. Vuik, and S. van der Zwaag. A mathematical model for the dissolution of stoichiometric particles in multi-component alloys. *Materials Science and Engineering A*, 328:14–25, 2002.

[34] F. Vermolen and C. Vuik. A numerical method to compute the dissolution of second phases in ternary alloys. *Journal of Computational and Applied Mathematics*, 93:123–143, 1998.

[35] S. Osher and J.A. Sethian. Fronts propagating with curvature-dependent speed: Algorithms based on Hamilton-Jacobi formulations. *J. Comput. Phys.*, 79:12, 1988.

[36] J.A. Sethian. *Level set methods and fast marching methods*. Cambridge University Press, New York, 1999.

[37] S. Osher and P. Fedkiw. Level set methods: an overview and some recent results. *J. Comput. Phys.*, 169:463–502, 2001.

[38] S. Chen, B. Merriman, S. Osher, and P. Smereka. A simple level set method for solving Stefan problems. *Journal of Computational Physics*, 135:8–29, 1997.

[39] M. Sussman, P. Smereka, and S. Osher. A level set approach for computing solutions to incompressible two-phase flow. *J. Comput. Phys.*, 114:146–159, 1994.

[40] D. Enright, R. Fedkiw, J. Ferziger, and I. Mitchell. A hybrid particle level set method for improved interface captured. *J. Comput. Phys.*, 183:83–116, 2002.

[41] S.P. van der Pijl, A. Segal, and C. Vuik. A mass conserving level set (mcls) method for modeling of multi-phase flows. Report 03-03, Delft University of Technology, Department of Applied Mathematical Analysis, Delft, 2003.

[42] T.J. Barth and J.A. Sethian. Numerical schemes for the Hamilton-Jacobi and level set equations on triangulated domains. *J. Comput. Phys.*, 145:1–40, 1998.

[43] M. Quecedo and M. Pastor. Application of the level set method to the finite element solution of two-phase flows. *Int. J. Numer. Meth. Engng*, 50:645–663, 2001.

[44] R. J. LeVeque. *Numerical methods for conservation laws*. Birkhauser Verlag, Berlin, 1994.

[45] R. J. LeVeque. *Finite volume methods for hyperbolic problems*. Cambridge University Press, Cambridge, 2002.

[46] C.W. Shu and S. Osher. Efficient implementation for essential non oscillatory shock-capturing schemes, II. *J. Comput. Phys.*, 77:439, 1988.

[47] Y.-T. Kim, N. Goldenfeld, and J. Dantzig. Computation of dentritic microstructures using a level set method. *Physical Review E*, 62:2471–2474, 2000.

[48] Y.C. Chang, T.Y. Hou, B. Merriman, and S. Osher. A Level Set Formulation of Eulerian Interface Capturing Methods for Incompressible Fluid Flows. *Journal of Computational Physics*, 124:449–464, 1996.

[49] P. Wesseling. *Principles of computational fluid dynamics*. Springer, Berlin, 1991.

[50] G. Caginalp and P. Fife. Phase-field methods for interfacial boundaries. *Physical Review B*, 33:7792–7794, 1986.

[51] T. Suzuki, M. Ode, S. G. Kim, and W.T. Kim. Phase-field model of dentritic growth. *Journal of Crystal Growth*, 237:125–131, 2002.

[52] A.A. Wheeler, W.J. Boettinger, and G.B. McFadden. Phase-field model for isothermal phase transitions in binary alloys. *Physical Review A*, 45:7424–7439, 1992.

[53] M. Fabbri and V. R. Voller. The Phase-Field Method in the Sharp-Interface Limit: a comparision between model potentials. *Journal of Computational Physics*, 130:256–265, 1997.

[54] D.I. Popov, L.L. Regel, and W.R. Wilcox. One-dimensional phase-field model for binary alloys. *Journal of Crystal Growth*, 212:574–583, 2000.

[55] M. Beneš. Anisotropic phase-field model with focused latent-heat release. In *Free boundary problems: theory and applications, II (Chiba, 1999)*, volume 14 of *GAKUTO Internat. Ser. Math. Sci. Appl.*, pages 18–30. Gakkōtosho, Tokyo, 2000.

[56] H. Emmerich. *The Diffuse Interface Approach in Materials Science*. Springer, Berlin, 2003.

[57] G. Caginalp. Stefan and Hele-Shaw type models as asymptotics of the phase-field equations. *Physical Review A*, 39:5887–5896, 1989.

[58] S.-L. Wang, R.F. Sekerka, A.A. Wheeler, B.T. Murray, S.R. Coriell, R.J. Braun, and G.B. McFadden. Thermodynamically-consistent phase-field models for solidification. *Physica D*, 69:189–200, 1993.

[59] G. Caginalp. An analysis of a phase field model of a free boundary. *Arch. Rat. Mech. Anal.*, 92:205–245, 1986.

[60] G. Caginalp and J.T. Lin. A numerical analysis of an Anisotropic Phase Field Model. *IMA J. Appl. Math.*, 39:51–66, 1987.

[61] J.A. Mackenzie and M.L. Robertson. A Moving Mesh Method for the solution of the One-Dimensional Phase-Field Eequations. *J. of Comp. Phys.*, 181:526–544, 2002.

[62] N. Provatas, N. Goldenfeld, and J. Dantzig. Adaptive Mesh Refinement Computation of Solidification Microstructures Using Dynamic Data Structures. *J. Comp. Phys.*, 148:265–290, 1999.

[63] E.A. Dorfi and L.O'c Drury. Simple adaptive grids for 1-D initial value problems. *J. of Comp. Phys.*, 69:175–195, 1987.

[64] K. Miller and R.N. Miller. Moving finite elements I. *SIAM J. Numer. Anal.*, 18:1019–1032, 1981.

[65] K. Miller. Moving finite elements II. *SIAM J. Numer. Anal.*, 18:1033 – 1057, 1981.

[66] J.F. McCarthy. One-dimensional phase field models with adaptive grids. *Trans. ASME*, 120:956, 1998.

[67] A. Schmidt. Computational of three dimensional dendrites with finite elements. *J. Comput. Phys.*, 125:293, 1996.

[68] W. Huang, Y. Ren, and R.D. Russell. Moving Mesh Partial Differential Equations (MMPDES) based on the equidistribution principle. *SIAM J. Numer. Anal.*, 31:709–730, 1994.

[69] J.A. Mackenzie and M.L. Robertson. The Numerical Solution of One-Dimensional Phase Change Problems Using an Adaptive Moving Mesh Method. *J. of Comp. Phys.*, 161:537–557, 2000.

[70] J.M. Ortega and W.C. Rheinboldt. *Iterative solutions of nonlinear equations in several variables*. Academic Press., San Diego, 1970.

[71] H.S.M. Coxeter. *Introduction to Geometry*. John Wiley & Sons, Inc., New York, 1989.

[72] A. Gray. *Modern Differential Geometry of Curves and Surfaces*. CRC Press, Inc., Florida, 1993.